# MODERN DESIGN OF CLASSICAL CONTROLLERS

A Dissertation

by

IVÁN DE JESÚS DÍAZ RODRÍGUEZ

Submitted to the Office of Graduate and Professional Studies of
Texas A&M University
in partial fulfillment of the requirements for the degree of

DOCTOR OF PHILOSOPHY

| | |
|---|---|
| Chair of Committee, | Shankar P. Bhattacharyya |
| Committee Members, | Jean-Francois Chamberland |
| | Pilwon Hur |
| | Aniruddha Datta |
| Head of Department, | Miroslav M. Begovic |

May 2017

Major Subject: Electrical Engineering

ABSTRACT

Classical controller design emphasizes simple low-order controllers. These classical controllers include Proportional-Integral (PI), Proportional-Integral-Derivative (PID), and First Order. In modern control theory, it is customary to design high-order controllers based on models, even for simple plants. However, it was shown that such controllers are invariably fragile, and this led to a renewal of interest in classical design methods. In the present research, a modern approach to the design of classical controllers (by introducing a complete stabilizing set in the space of the design parameters) is described. When classical specifications such as gain margin, phase margin, bandwidth, and time-delay tolerance are imposed, the achievable performance can be easily determined graphically. The objective of this research is to determine the controller gains, contained in the stabilizing set, which satisfy desired performance specifications such as crossover frequency and closed-loop stability margins. The design procedure starts with the calculation of the stabilizing set using recent methods. Then, a simple parametrization produces ellipses and straight lines (for PI controller design) and cylinders and planes (for PID controller design) in the space of controller gains. Each set of ellipses/cylinders and straight lines/planes represents constant magnitude and constant phase loci for the controller. The main result is that the crossing points, which are the intersection of ellipses/cylinders and straight lines/planes, are selected such that they are contained in the stabilizing set of controllers. They provide the controller gains that we need to satisfy our desired robust performance, seen as desired gain margin, phase margin, gain crossover frequency, and time-delay tolerance in our system. Then, using these crossing points contained in the stabilizing set, a new plot with information about the achievable

performance in terms of gain margin, phase margin, and gain crossover frequency is constructed. Each point of this achievable performance can be used to retrieve the controller's gains, which are contained in the stabilizing set. This result provides the possibility to analyze the system's achievable performance by exploring the stabilizing set and considering different desired configurations in the performance capabilities for the system using a PI or PID controller. This expands our possibilities when designing controllers by considering different classical controller's configurations. This research considers the discrete-time and continuous-time linear time invariant systems and cases including First Order with time-delay in the system, and the extension to the controller design for multivariable systems. Finally, the design procedure is illustrated with different examples and real applications for all such cases.

# DEDICATION

I dedicate this dissertation work to my beloved parents and family for their continuous support and encouragement.

# ACKNOWLEDGEMENTS

Firstly, I would like to express my sincere gratitude to my advisor Prof. Shankar P. Bhattacharyya for his continuous support of my Ph.D. program and his advice to improve my research skills, for his patience, motivation, and knowledge. His guidance helped me all the time during my research and writing of research papers.

Besides my advisor, I would like to thank the rest of my dissertation committee: Prof. Pilwon Hur, Prof. Aniruddha Datta, and Prof. Jean-Francois Chamberland, for their insightful comments and encouragement, but also for being part of my committee members.

Last but not the least, I would like to thank my family for supporting me all the time. Also, I have a special thank to Alicia for her patience and support during my Ph.D. Finally, I thank all my friends that I met during my Ph.D. program who helped me during my time in College Station.

# CONTRIBUTORS AND FUNDING SOURCES

## Contributors

This work was supervised by a dissertation committee consisting of Professor Shankar P. Bhattacharyya, Professor Aniruddha Datta, and Professor Jean-Francois Chamberland of the Department of Electrical and Computer Engineering and Professor Pilwon Hur of the Department of Mechanical Engineering.

All work for the dissertation was completed by the student, under the advisement of Professor Shankar P. Bhattacharyya of the Department of Electrical and Computer Engineering and in part collaboration with Sangjin Han of the Department of Electrical and Computer Engineering.

## Fundings

This work was made possible by Consejo Nacional de Ciencia y Tecnología (CONACYT) and Consejo Tamaulipeco de Ciencia y Tecnología (COTACYT) for the financial support granted by the scholarship number 308935.

Graduate study was supported in part by a dissertation fellowship from the Office of Graduate and Professional Studies in Texas A&M University.

TABLE OF CONTENTS

Page

LIST OF FIGURES

FIGURE Page

# LIST OF TABLES

TABLE Page

# 1. INTRODUCTION

In control theory, there are two main approaches: Modern and Classical. Modern control theory deals with state space representation and with the possibility of multi-input and multi-output (MIMO) systems. It can handle more sophisticated design problems. However, it is customary to develop high-order controllers based on models, even for simple plants. In [7], it shows that such controllers are invariably fragile, and this led to a renewal of interest in classical controllers and conventional design methods. In classical control theory, the design emphasizes simple, low-order controllers. It plays an important role in real-world applications. Specifically, in industrial applications, new advances in technology make possible the adaptation of automatic production processes. Therefore, controller design has a great impact on the efficiency of production processes. For this reason, it is crucial to develop new controller design approaches for classical controllers.

## 1.1 Review of PI/PID Controller Design Approaches

The Proportional-Integral-Derivative (PID) and Proportional-Integral (PI) controller are the most widely used traditional controllers in the control industry and are universally accessible in motion control, process control, power electronics, hydraulics, pneumatics, and manufacturing (see references [8–11]). In fact, in process control, more than 95% of the control loops are of PID type, most loops are PI control, see [1]. Their popularity is because of their simple structure, easy implementation, and straightforward maintenance. Also, they provide a satisfactory performance with a cost/benefits ratio that's hard for other types of controllers to match.

### *1.1.1 PID Controller Actions*

The PID controller is the name given to a controller which scheme consists of the addition of three control actions (see Fig 1.1). These actions are an action proportional to the control error, a control action proportional to the integral of the error, and a control action proportional to the first derivative of the control error (see [12]).

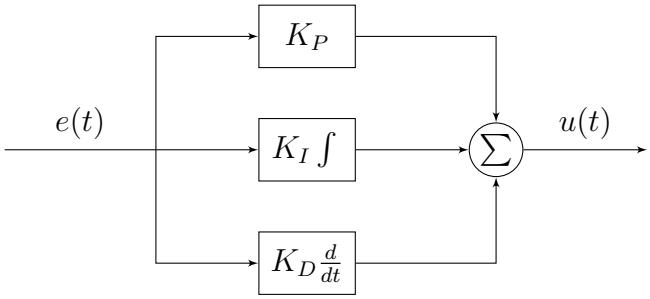


Figure 1.1: PID Controller Block Diagram

- **Proportional controller**. The proportional action deals with the present values of the error signal; it is proportional to the size of the process error signal increasing the control variable when the error signal increases. When using only a P control, we notice that increasing the proportional gain $K_P$ will speed up the time response. However, it is possible that steady state error will occur. This can be seen as

$$u = u_0 + K_P e \tag{1.1}$$

where $u$ is the control signal, $u_0$ is the control signal when there is no control error, $K_P$ is the proportional gain, and $e$ is the control process error. Using

(1.1), the error signal is

$$e = \frac{u - u_0}{K_P} \tag{1.2}$$

Given (1.2), the steady state error is zero if and only if $K_P$ is very large or the control signal $u = u_0$, see [13].

- **Integral controller**. The integral action is used to reduce the steady-state error to zero. When using an integral gain, increasing the value of $K_I$ can give a broad range of response types in addition to the elimination of the offset in the reference response. The control signal is

$$u = K_I \int e dt \tag{1.3}$$

The integral of the control error is proportional to the area under the control error curve. The control signal $u$ will continuously change depending on if the error signal is positive or negative. If the control signal $u$ is constant, then the error signal must be identically zero, see [14].

- **Derivative controller**. The derivative action is used to improve the closed-loop stability. It deals with the possible future values of the error signal based on its current rate of change, anticipating the incorrect trend of the control error, see [1, 15]. The control signal is

$$u = K_D \frac{d}{dt} e dt \tag{1.4}$$

The derivative part is proportional to the predicted error. However, in practice, the derivative is taken from the process variable, see [15].

### *1.1.2 PID Controller Representations*

Today's PID controller structures are based on parallel and series types, see [15].

- **Parallel type**: this controller type has the following control law

$$u = K_c \left( e + \frac{1}{T_i} \int e dt + T_d \frac{de}{dt} \right) \tag{1.5}$$

  where $K_P = K_c$ is the proportional gain, $T_i$ is the integral time of the controller with $K_I = \frac{K_c}{T_i}$, and $T_d$ is the derivative time of the controller with $K_D = K_c T_d$. This representation is known as *ideal*, see [15].

- **Series type**: this controller type has the following control law

$$\begin{aligned} e_1 &= e + T_d \frac{de}{dt}, \\ u &= K_c \left( e_1 + \frac{1}{T_i} \int e dt \right) \end{aligned} \tag{1.6}$$

  In this case, the integral and derivative part are not independent.

### *1.1.3 Classical PID Controller Design Tuning*

Due to the popularity of classical controllers in industry and their widespread use, many approaches for their design and implementation exist. Over the years, researchers have developed new PI/PID tuning methods for the design of these controller configurations. The classical methods found in the literature can be classified as follows (see [1, 12, 16–18]):

- **Trial and Error Method**: this method is applied when there is no a systematic approach to follow when designing the controller. The method is based

on experience about the effects of adjusting the individual $K_P, K_I, K_D$ gains trying to get a better time response in terms of speed and closed-loop stability. The effects of increasing each gain separately are represented in the following table 1.1 (see [15])

Table 1.1: Effects of Adjusting Individual PID Gains on the System

| **Parameter** | **Steady state error** | **Speed** | **Stability** |
|---|---|---|---|
| $K_P$ | reduces | increases | decreases |
| $K_I$ | eliminates | reduces | increases |
| $K_D$ | no effect | increases | increases |

The advantage of this method is that it does not require any mathematical model or mathematical derivation. However, it requires some experience to adequately adjust the controller gains to satisfy a desired performance in terms of speed and stability.

- **The Ziegler-Nichols step response method**: this PID tuning method was developed between 1941 and 1942 at Taylor Instrument company, see [19]. Since that time, this method has been extensively used in his original form and with some variations, see [1]. The method is based on the step response of the open-loop stable system, see Fig. 1.2. The procedure is the following (see [1, 15, 19])

  1. Calculate the step response of the open-loop system.
  2. Draw a tangent line with the maximum slope possible from the step response, see Fig 1.2.

3. Calculate $L$, which is the distance from the intersection of the slope and vertical axis to the starting point of the step response.
4. Calculate $A$, which is the distance from the intersection of the slope and the vertical axis to the horizontal axis.
5. Compute the PID gains from the following formulas

$$\begin{aligned} K_P &= \frac{1.2}{A} \\ K_I &= \frac{0.6}{AL} \\ K_D &= \frac{0.6L}{A} \end{aligned} \tag{1.7}$$

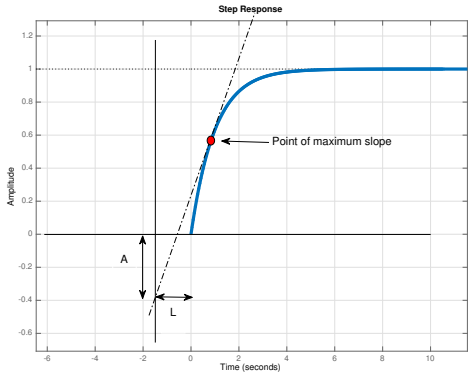


Figure 1.2: Ziegler-Nichols Step Response Method

- **The Ziegler-Nichols frequency response method**: this PID tuning method considers a proportional controller attached to the system in a closed-loop configuration. The objective is to find the ultimate frequency where the phase of the process is $-180^o$. That is the ultimate gain where the system reaches the stability boundary. The tuning procedure is the following (see [1, 15, 19])

1. Connect a proportional controller to the system in a closed-loop configuration.

2. Slowly increase the proportional gain until the output starts oscillating. This gain is called ultimate gain $K_u$.

3. Measure the period of the oscillation in the output. This period is called ultimate period $T_u$.

4. Compute the PID gains from the following formulas

$$\begin{aligned} K_P &= 0.6K_u \\ K_I &= \frac{1.2K_u}{T_u} \\ K_D &= 0.075K_uT_u \end{aligned} \tag{1.8}$$

This tuning method is capable of finding the PID controller gains for the system. However, it requires some experience and skill because the system is taken to its limits of instability and it becomes very close to getting it damaged.

- **Relay PID Tuning Method**: This PID tuning method was developed by K. Åström and T. Hägglund as an alternative to the Ziegler-Nichols frequency response PID tuning method. This method is very similar, but instead of increasing a proportional gain until the system's output oscillates, a relay is used to generate an oscillation in the output, see Fig 1.3 and Fig 1.4. The relay connected to the system generates a square signal with certain amplitude and frequency. Then, a signal in the output approximated to a sinusoid, is generated. The tuning procedure is the following (see [1, 15, 19, 20]):

  1. The system should be working at the operating point.

2. Set the amplitude of the square signal in the relay.

3. Calculate the ultimate period $T_u$, see Fig. 1.4

4. Calculate the controller parameters $K_P$, $K_I$, and $K_D$ using the Ziegler-Nichols table using $K_u = K_e$, where $K_e = A_u/A_e$. Where $A_u = 4A/\pi$ and $A_e = E$ with $E$ being the amplitude of the oscillations in the control error signal.

The advantage of this method is that it doesn't require to force the system close to instability. Therefore, it keeps the system safer not being close to instability and the possibility of damage. Also, this relay method can be automated since the output oscillation amplitude is proportional to the amplitude of the relay signal.

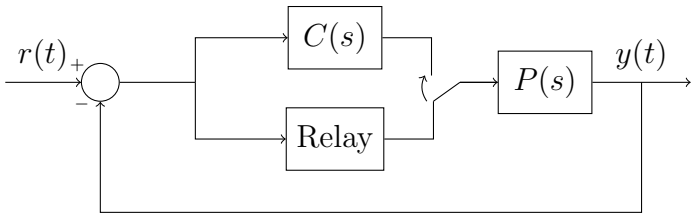


Figure 1.3: FOPTD Unity Feedback Block Diagram With a Relay

- **The Cohen-Coon Method**: This is an open-loop PID tuning method which follows the same procedure as the Ziegler-Nichols step response method, see [15]. In Fig. 1.5, it shows a step response of the open-loop system where the parameters $K_P$, $L$, and $T$ can be determined. The gain $K_P$ is determined by taking the ratio between the amplitude increment of the output and the

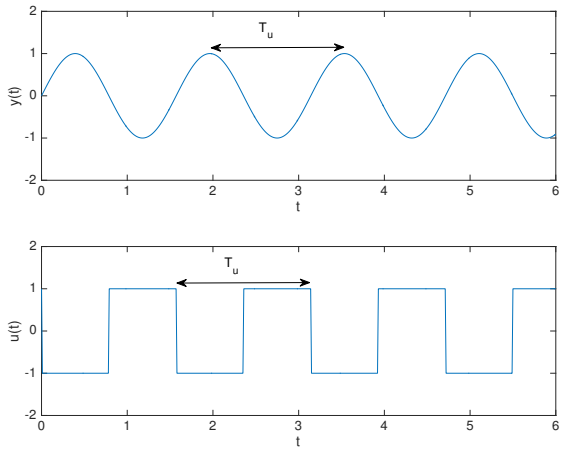


Figure 1.4: Output Oscillating and Relay Signals

increase in the control signal. That is

$$K_P = \frac{\Delta y}{\Delta u} \tag{1.9}$$

The variables $L$ and $T$ are the time where the system's output reacts after the step is introduced as a control input and the time of the step response of the intersection of the maximum slope and the set point. Then, considering the PID controller parallel type, the Cohen-Coon method includes the following formulas to calculate the PID gains

$$\begin{aligned} K_c &= \frac{1}{K_P}\left(0.25 + \frac{1.35T}{L}\right) \\ T_i &= \frac{2.5 + \frac{0.46L}{T}}{1 + \frac{0.61L}{T}}L \\ T_d &= \frac{0.37}{1 + \frac{0.19L}{T}}L \end{aligned} \tag{1.10}$$

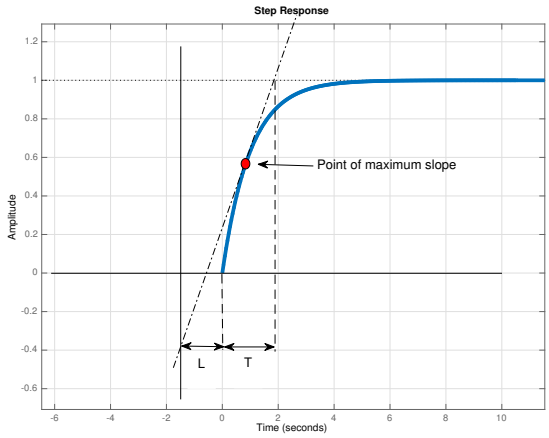


Figure 1.5: Cohen-Coon Method

### *1.1.4 Modern PID Controller Design Tuning*

After the appearance of the classical PID controller tuning techniques, the complexity of the systems and performance demands from the controller designer made necessary the development of new tuning design techniques. Over the years, many good results were developed toward PID tuning methods for more performance specific requirements and to deal with complex systems. Some of the called modern approaches are the following

- **Internal Model Control design**

  This controller approach considers stable systems. Consider the closed-loop system block diagram presented in Fig. 1.6. Where $\hat{G}(s)$ is an approximation of the system $G(s)$, $G_F(s)$ is a low pass filter, and $\hat{G}^+(s)$ is the inverse of $\hat{G}(s)$. Then, the controller design objective is to cancel the poles and zeros from the original system $G(s)$ by connecting in parallel with $\hat{G}(s)$, see [21] and [22]. This approach is called internal model control because the controller contains

a model of the system internally, see [1]. The purpose of $G_F(s)$ is to make the system less sensitive to modeling errors. The controller $C(s)$ is given by

$$C(s) = \frac{G_F(s)\hat{G}^+(s)}{1 - G_F(s)\hat{G}^+(s)\hat{G}(s)} \tag{1.11}$$

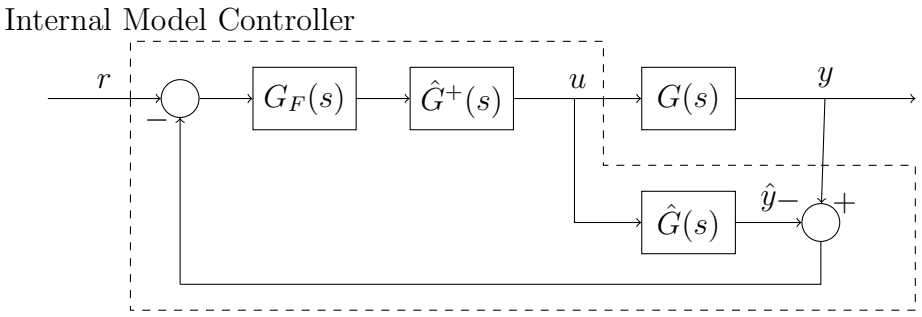


Figure 1.6: Closed-Loop System Block Diagram with Internal Model Controller

There is a particular case where this approach considers PI and PID controllers, see [1] and [23]. For the case of first order plus time delay systems, we have that

$$P(s) = \frac{K}{1 + sT}e^{-sL} \tag{1.12}$$

$$\hat{G}^+(s) = \frac{1 + sT}{K} \tag{1.13}$$

$$G_F(s) = \frac{1}{1 + sT_f} \tag{1.14}$$

Then, by a first order Pad approximation for the time delay

$$e^{-sL} \approx \frac{1 - sL/2}{1 + sL/2} \tag{1.15}$$

we have the controller of the PID form

$$C(s) = \frac{(1+sL/2)(1+sT)}{Ks(L+T_f+sT_fL/2)} \approx \frac{(1+sL/2)(1+sT)}{Ks(L+T_f)} = \frac{K_d s^2 + K_p + K_i}{s} \tag{1.16}$$

Where

$$K_d = \frac{LT}{2K(L+T_f)} \tag{1.17}$$

$$K_p = \frac{(L+2T)}{2K(L+T_f)} \tag{1.18}$$

$$K_i = \frac{1}{K(L+T_f)} \tag{1.19}$$

In [24–29] different methods are presented considering IMC approach.

- **Pole Placement Design**

  Pole placement is a controller design method, based on knowledge of the system's transfer function, where the objective is to determine the closed-loop poles locations on the complex plane by setting the controller gains. It is known that the system's closed-loop pole locations determine the behavior of the system. Therefore, the designer can apply this method to place the locations of the poles for a desirable behavior of the closed-loop system.

  PI and PID controllers can be used for pole placement design as long as the transfer function system is of the first or second order. For higher order systems, one way to use PI or PID controller is to approximate the system's transfer function by a first or second order transfer function.

For the first order case, the system can be described by

$$P(s) = \frac{K}{1 + Ts} \tag{1.20}$$

where $K$ is the system's gain and $T$ is the time constant. Using a PI controller

$$C(s) = K_c \left(1 + \frac{1}{T_i s}\right) \tag{1.21}$$

where $K_c$ is the controller gain and $T_i$ the integral time. The closed-loop transfer function is

$$G(s) = \frac{C(s)P(s)}{1 + C(s)P(s)} \tag{1.22}$$

The characteristic equation becomes of second order

$$\delta(s) = s^2 + \left(\frac{1 + KK_c}{T}\right) s + \left(\frac{KK_c}{TT_i}\right) \tag{1.23}$$

A second order characteristic equation can be represented in terms of the relative damping $\zeta$ and the natural frequency $\omega_n$ as

$$\delta(s) = s^2 + 2\zeta\omega_n s + \omega_n^2 \tag{1.24}$$

where the parameters $\zeta$ and $\omega_n$ determine the time response of the second order system, see [30].

Combining (1.23) and (1.24) we have that

$$K_c = \frac{2\zeta\omega_n T - 1}{K} \tag{1.25}$$

$$T_i = \frac{2\zeta\omega_n T - 1}{\omega_n^2 T} \tag{1.26}$$

For the second order case, the system can be described by

$$P(s) = \frac{K}{(1 + T_1 s)(1 + T_2 s)} \tag{1.27}$$

Using a PID controller

$$C(s) = \frac{K_c \left(1 + T_i s + T_i T_d s^2\right)}{T_i s} \tag{1.28}$$

The characteristic equation becomes of third order

$$\delta(s) = s^3 + \left(\frac{1}{T_i} + \frac{1}{T_2} + \frac{K K_c T_d}{T_1 T_2}\right) s^2 + \left(\frac{1}{T_1 T_2} + \frac{K K_c}{T_1 T_2}\right) s + \frac{K K_c}{T_1 T_2 T_i} \tag{1.29}$$

A third order characteristic equation can also be represented in terms of the relative damping $\zeta$ and the natural frequency $\omega_n$ as

$$\delta(s) = (s + \alpha\omega_n)(s^2 + 2\zeta\omega_n s + \omega_n^2) \tag{1.30}$$

Combining (1.29) and (1.30) we have that

$$K_c = \frac{T_1 T_2 \omega_n^2 (1 + 2\alpha\zeta) - 1}{K} \tag{1.31}$$

$$T_i = \frac{T_1 T_2 \omega_n^2 (1 + 2\alpha\zeta) - 1}{T_1 T_2 \alpha \omega_n^3} \tag{1.32}$$

$$T_d = \frac{T_1 T_2 \omega_n (\alpha + 2\zeta) - T_1 - T_2}{T_1 T_2 \omega_n^2 (1 + 2\alpha\zeta) - 1} \tag{1.33}$$

- **Dominant Pole Placement Design**

  This controller design approach follows the same idea of the previous pole placement design. However, this method is focused on higher order systems. The objective is to select a pair of dominant poles, which have more influence on the behavior of the system time response, see [31].

  For PI and PID controllers design for dominant pole placement, there is an approach developed by Cohen-Coon for first order plus time delay systems as equation (1.12), see [1] and [23]. The main design is the rejection of load disturbances with a position of the dominant poles that give a quarter amplitude decay ratio. For PID controllers, two complex dominant poles and one real are placed to satisfy the quarter amplitude decay ratio in the time response. The following table presents some formulas to calculate the PI and PID controller gains.

Table 1.2: Cohen-Coon Formulas for Dominant Pole Placement Controller Design

| **Controller** | $K_c$ | $T_i$ | $T_d$ |
|---|---|---|---|
| PI | $\frac{0.9}{a}\left(1 + \frac{0.92\tau}{1-\tau}\right)$ | $\frac{3.3-3.0\tau}{1+1.2\tau}L$ | |
| PID | $\frac{1.35}{a}\left(1 + \frac{0.18\tau}{1-\tau}\right)$ | $\frac{2.5-2.0\tau}{1-0.39\tau}L$ | $\frac{0.37-0.37\tau}{1-0.81\tau}L$ |

where

$$a = \frac{KL}{T} \tag{1.34}$$

$$\tau = \frac{L}{(L+T)} \tag{1.35}$$

In [32–36], dominant pole placement controller designs are presented for PID controllers.

- **Time domain optimization methods**

  In the time domain optimization methods, the controller gains are calculated based on numerical optimization methods where an objective function is specified, see [23]. For PID controllers, an objective function is defined by the form

$$J(\theta) = \int_0^\infty t|e(\theta,t)|dt \tag{1.36}$$

$$J(\theta) = \int_0^\infty |e(\theta,t)|dt \tag{1.37}$$

$$J(\theta) = \int_0^\infty e(\theta,t)^2 dt \tag{1.38}$$

  where $\theta$ represents a vector with the PID gains and $e(\theta,t)$ is the error signal of the control system. The objective function in (1.36) is called Integral Time-Weighted Absolute Error (ITAE), this function integrates the absolute error multiplied by time as a weight. The objective function (1.37) is called Integral Absolute Error (IAE), this function integrates the absolute error without weights. The objective function (1.38) is called Integral Square Error (ISE), which only integrates the square error.

The parameters of the controller are obtained after minimizing a selected objective function to obtain a better performance of the closed-loop system.

- **Gain and Phase Margin Design**

  Gain and phase margin determine how stable is the system. These margins are calculated from the open-loop system to determine how robust is the closed-loop system. The gain margin is the amount of additional gain necessary to make the system unstable and the phase margin the amount of additional phase necessary to make the system unstable. These margins are considered classical control designs associated with the frequency response of the system, see [30]. The gain and phase margins can be obtained from the Nyquist plot, see Fig 1.7.

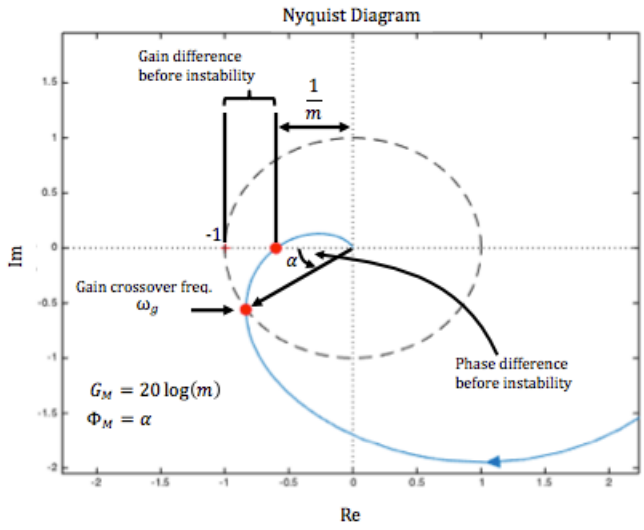


Figure 1.7: Gain and Phase Margins From Nyquist Plot

where $m$ represents the gain margin, $\alpha$ is the phase margin, and $\omega_g$ the gain crossover frequency. Over the time, there has been a research interest develop-

ing new controller design approaches to achieve certain gain and phase margin for the closed-loop system. However, the problem to achieve an exact gain and phase margin becomes difficult because the non-linearity and solvability of the problem, see [15]. There is a great number of research papers with different approaches for PI and PID to achieve certain gain and phase margins. For example, in [24, 37–48] different approaches for PI/PID controller design considering first order or second order plus time delay processes are presented. There are also different controller design approaches for PI and PID trying to achieve gain and phase margin. For example, in [29, 49, 50] surveys of PID controller designs are shown. In [24–29] different methods are presented considering IMC. In [28, 29, 42, 45, 47, 51] optimization approaches are presented. In [38, 41, 48, 52, 53] unstable processes are considered for the design of PI/PID controllers. In [17, 26, 54, 55] controller design methods applying system identification are presented. In [38, 43, 48, 56–58] the proposed methods apply an arctangent approximation to achieve a controller design. In [39, 46, 52, 53, 59–62] some graphical methods are applied to find a controller gains. In [8, 46, 54, 59, 63, 64] different methods are presented to calculate the controller gains.

- **Adaptive Control Design**

  In the adaptive controller design, the controller gains are continuously adjusting on the changes in the system or the presence of some perturbations. There are two types of adaptive control based on direct and indirect methods, see [1], [65–68]. In the direct approach, the information from the closed-loop system is used directly to change the controller gains. In the indirect approach, a recursive parameter estimation is used to update the process model, see Fig

1.8. These types of adaptive controller techniques are widely used for PID controllers. For example in [69–74] different approaches are presented for PID controller design considering adaptive control techniques.

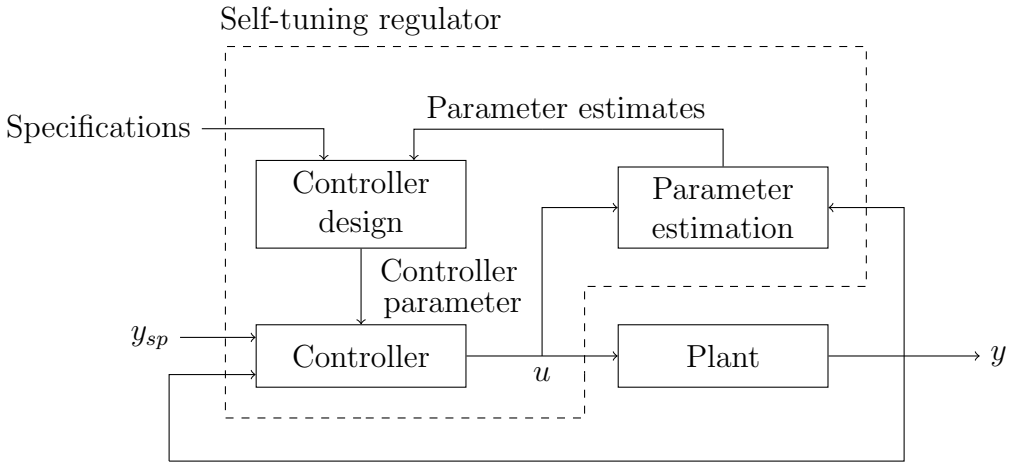


Figure 1.8: Block Diagram of an Indirect Adaptive Controller From [1]

## 1.2 Dissertation Objective

The main objective of this dissertation is to present alternative approaches for controller design of low-order classical controllers (PI, PID, and First Order controllers) based on simultaneous achievement of the design specifications most often required in applications. These are a) gain margin, b) phase margin, c) gain crossover frequency, and d) time-delay tolerance.

### Particular Objectives

- Present a Discrete-Time PI and PID controller design approach to satisfy a desired gain margin, phase margin, gain crossover frequency, and time-delay

tolerance simultaneously from a constructed gain and phase margin achievable performance set. Also, provide a computational tool to analyze the stabilizing set looking for capabilities and achievable performances for a given but arbitrary single-input and single-output systems.

- Describe a Continuous-Time First Order, PI, and PID controller design approach for delay and delay-free systems to satisfy a desired gain margin, phase margin, gain crossover frequency, and time-delay tolerance simultaneously from a constructed gain and phase achievable performance set. Also, provide a computational tool to analyze the stabilizing set looking for capabilities and achievable performances for a given but arbitrary single-input and single-output systems.

- Introduce a new approach for the design of continuous-time controllers for Multivariable systems to satisfy a desired gain margin, phase margin, gain crossover frequency, and time-delay tolerance.

## 1.3 Organization of the Dissertation

The dissertation content is as follows:

- In Section 2, a review of the computation of the stabilizing set for discrete and continuous First-Order, PI, and PID controller cases is presented.

- In Section 3, constant magnitude and constant phase loci representation for First Order, PI, and PID controllers for delay and delay-free discrete and continuous time systems are presented.

- In Section 4, the achievable robust performance for the controller design of

discrete-time PI/PID, continuous-time PI/PID, and First-Order controllers are presented for delay-free and first order plus time-delay systems is presented.

- In Section 5 the results are extended for controller design based on achievable performance for Multivariable systems.
- In Section 6, the final conclusions, discussions, and future research are given.

## 1.4 References

For more information and details about the classical PID controller design tuning approached presented in this section see [1,12,16–18]. For the modern PID controller design tuning approaches, the reader can find more information in [1, 1, 8, 17, 21–24, 24–26, 26–47, 47–53, 53–74].

# 2. COMPUTATION OF THE STABILIZING SET

In this section, the procedure to compute the stabilizing sets for First Order, PI, and PID controllers for a LTI system is reviewed. The derivations for the stabilizing sets are presented in [14]. Finding the stabilizing sets for the different controller configurations is the first step in the controller design procedure presented in the following sections; these stabilizing sets are used to analyze and explore them to select the controller gains that will satisfy the desired conditions, leading to a robust performance in our system in terms of prescribed gain and phase margins.

## 2.1 Introduction

In control theory, the first consideration, when designing a controller for a given system, is that the controller guarantees the stability property. For this reason, we can find many approaches in the literature dealing with this important property of stability. For example, in [75], an approach to compute all stabilizing PID controllers for an arbitrary plant is presented. The result is an extension of the YJBK characterization restricted to PID. In [76], a new approach for the designing of digital PID controllers for a given LTI plant is presented. In this result, the Chebyshev polynomials are used to represent the discrete-time transfer function and the PID gains are obtained by solving sets of linear inequalities. In [77], a computation of the PID controllers that stabilize a digital control systems is presented. In this result, a bilinear transformation is used to determine the PID gains.

In [78] is shown that the PID and First Order controllers stabilizing regions can be computed for a finite dimensional LTI plant considering the frequency response

(Nyquist/Bode) data $P(j\omega)$ for $\omega \in [0, \infty)$ without the need of an mathematical model. In [79] is considered the problem of stabilizing a discrete-time LTI system by a First Order discrete-time controller. The stabilizing set of controllers is determined using the Chebyshev representation of the characteristic equation on the unit circle.

In the following sections, a summary of the computation of the stabilizing set for PI, and PID controllers for discrete-time and First Order, PI, and PID controllers for continuous-time will be presented. It is assumed that there exist a controller that stabilizes the plant for all cases.

## 2.2 Discrete-Time Controllers

For the case of Discrete-Time controllers, the Chebyshev polynomials of the first and second kind will be used (see [80]). The objective is to parametrize the controller such that the stabilizing set can be calculated by solving a set of linear inequalities.

### *2.2.1 PI Controllers*

Consider the control system in Fig 2.1 with a LTI system with a rational and proper plant

$$P(z) := \frac{N(z)}{D(z)} \tag{2.1}$$

with $D(z) = n$ and $N(z) \leq n$ degrees. The PI controller is

$$C(z) = \frac{K_0 + K_1 z}{z - 1} \tag{2.2}$$

The procedure to compute the PI stabilizing set is the following:

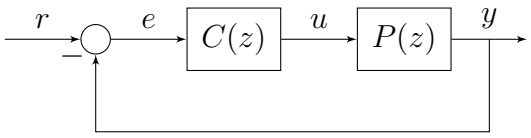


Figure 2.1: Unity Feedback Discrete-Time Control System

1. Represent the polynomials $N(z)$ and $D(z)$ from (2.1) as

$$D(e^{j\theta}) := T_D(\nu) + j\sqrt{1-\nu^2}U_D(\nu) \tag{2.3}$$

$$N(e^{j\theta}) := T_N(\nu) + j\sqrt{1-\nu^2}U_N(\nu) \tag{2.4}$$

where

$$N(z) = a_n z^n + a_{n-1}z^{n-1} + \cdots + a_1 z + a_0 \tag{2.5}$$

$$D(z) = b_n z^n + b_{n-1}z^{n-1} + \cdots + b_1 z + b_0 \tag{2.6}$$

with $a_0, a_1, \cdots, a_n$ and $b_0, b_1, \cdots, b_n$ real, evaluated on the unit circle.

$$\begin{aligned} T_N(\nu) &= a_n t_n(\nu) + a_{n-1}t_{n-1}(\nu) + \cdots + a_1 t_1(\nu) + a_0 \\ U_N(\nu) &= a_n u_n(\nu) + a_{n-1}u_{n-1}(\nu) + \cdots + a_1 u_1(\nu) \\ T_D(\nu) &= b_n t_n(\nu) + b_{n-1}t_{n-1}(\nu) + \cdots + b_1 t_1(\nu) + b_0 \\ U_D(\nu) &= b_n u_n(\nu) + b_{n-1}u_{n-1}(\nu) + \cdots + b_1 u_1(\nu) \end{aligned} \tag{2.7}$$

and

$$t_k(\nu) = \cos k\theta \qquad \text{and} \qquad u_k(\nu) = \frac{\sin k\theta}{\sin\theta}, \quad k = 1, 2, 3, ..., n \tag{2.8}$$

are the Chebyshev polynomials of the first and second kind. With

$$\nu := -\cos\theta \qquad \text{and} \qquad z = e^{j}\theta = -\nu + j\sqrt{1-\nu^2} \tag{2.9}$$

The generalized Chebyshev polynomials are presented in Table 2.1. Where $u_k(\nu)$ and $t_k(\nu)$ are obtained recursively as

$$u_k(\nu) = -\frac{1}{k}\frac{d[t_k(\nu)]}{d\nu} \tag{2.10}$$

$$t_{k+1}(\nu) = -\nu t_k(\nu) - (1-\nu^2)u_k(\nu) \tag{2.11}$$

Table 2.1: Chebyshev Polynomials of the First and Second Kind

| $k$ | $t_k(\nu)$ | $u_k(\nu)$ |
|---|---|---|
| 1 | $-\nu$ | 1 |
| 2 | $(2\nu^2-1)$ | $-2\nu$ |
| 3 | $(-4\nu^3+3\nu)$ | $(4\nu^2-1)$ |
| 4 | $(8\nu^4-8\nu^2+1)$ | $(-8\nu^3+4\nu)$ |
| 5 | $(-16\nu^5+20\nu^3-5\nu)$ | $(16\nu^4-12\nu^2+1)$ |
| $\vdots$ | $\vdots$ | $\vdots$ |

2. Calculate the characteristic polynomial from the closed-loop system in Fig. 2.1

$$\delta(z) = (z-1)D(z) + (K_0 + K_1 z)N(z). \tag{2.12}$$

3. Obtain

$$\delta(z)N(z^{-1}) = (z-1)D(z)N(z^{-1}) + (K_0 + K_1 z)N(z)N(z^{-1}) \tag{2.13}$$

4. Use the Chebyshev representations to calculate

$$\begin{aligned}\delta(z)N(z^{-1})|_{z=e^{j\theta},\nu=-\cos\theta} = &\left(-\nu-1+j\sqrt{1-\nu^2}\right)\left(P_1(\nu)+j\sqrt{1-\nu^2}P_2(\nu)\right)\\ &+jK_1\sqrt{1-\nu^2}P_3(\nu)-K_1\nu P_3(\nu)+K_0P_3(\nu)\end{aligned} \tag{2.14}$$

where

$$\begin{aligned}P_1(\nu) &= T_D(\nu)T_N(\nu)+(1-\nu^2)U_D(\nu)U_N(\nu)\\ P_2(\nu) &= T_N(\nu)U_D(\nu)-U_N(\nu)T_D(\nu)\\ P_3(\nu) &= T_N^2(\nu)+(1-\nu^2)U_N^2(\nu)\end{aligned} \tag{2.15}$$

and $T_N(\nu)$, $T_D(\nu)$, $U_N(\nu)$, and $U_D(\nu)$ are calculated as (2.7). Letting $N_r(z)$ denote the reverse polynomial of $N(z)$,

$$\begin{aligned}\delta(z)N(z^{-1})|_{z=e^{j\theta},\nu=-\cos\theta} &= \frac{\delta(z)N_r(z)}{z^l}\Big|_{z=e^{j\theta},\nu=-\cos\theta}\\ &= T(\nu,K_0,K_1)+\sqrt{1-\nu^2}U(\nu,K_1)\end{aligned} \tag{2.16}$$

where

$$\begin{aligned}T(\nu,K_0,K_1) &= -(\nu+1)P_1(\nu)-(1-\nu^2)P_2(\nu)-(K_1\nu-K_0)P_3(\nu)\\ U(\nu,K_1) &= P_1(\nu)-(\nu+1)P_2(\nu)+K_1P_3(\nu).\end{aligned} \tag{2.17}$$

5. Fixing a specific value of $K_1$, we can calculate the zeros of $t_i$ of $U(\nu,K_1)$ which

are real distinct of odd multiplicity for $\nu \in (-1, +1)$:

$$-1 < t_1 < t_2 < \cdots < t_k < +1. \tag{2.18}$$

6. For fixed $K_1$, calculate the set of strings, using the roots $t_j$ obtained in the previous step, for the real part $T(\nu, K_0, K_1)$, for stability, using

$$i_\delta + i_{N_r} - l = \frac{1}{2} Sgn\left[U^{(p)}(-1)\right]\Big(Sgn[T(-1, K_0, K_1)] + 2\sum_{j=1}^{k}(-1)^j Sgn[T(t_j, K_0, K_1)] + (-1)^{k+1} Sgn[T(+1, K_0, K_1)]\Big). \tag{2.19}$$

   where $i_\delta$, $i_{N_r}$, are the number of zeros inside the unit circle for $\delta(z)$ and $N_r(z)$, respectively (The sum of $i_\delta + i_{N_r} - l$ is the number required for stability). For fixed $K_1$, this leads to linear inequalities in $K_0$.

7. Sweep over the $K_1$ range for which a right number of real roots $t_k$ exist in $(-1, 1)$ for $U(\nu, K_1) = 0$.

### *2.2.2 PID Controllers*

Consider the control system in Fig 2.1 with a LTI system with a rational and proper plant

$$P(z) := \frac{N(z)}{D(z)} \tag{2.20}$$

with $D(z) = n$ and $N(z) \leq n$ degrees. The PID controller is

$$C(z) = \frac{K_0 + K_1 z + K_2 z^2}{z(z-1)} \tag{2.21}$$

The procedure to compute the PID stabilizing set is the following:

1. Calculate the characteristic polynomial from the closed-loop system in Fig. 2.1

$$\delta(z) = z(z-1)D(z) + (K_0 + K_1 z + K_2 z^2)N(z). \tag{2.22}$$

2. Obtain

$$z^{-1}\delta(z)N(z^{-1}) = (z-1)D(z)N(z^{-1}) + (K_0 z^{-1} + K_1 + K_2 z)N(z)N(z^{-1}) \tag{2.23}$$

3. Use the Chebyshev representations to calculate

$$\begin{aligned} z^{-1}\delta(z)N(z^{-1}) = &-(\nu+1)P_1(\nu) - (1-\nu^2)P_2(\nu) - [(K_0+K_2]\nu - K_1]P_3(\nu) \\ &+ j\sqrt{1-\nu^2}[-(\nu+1)P_2(\nu) + P_1(\nu) + (K_2 - K_0)P_3(\nu)] \end{aligned} \tag{2.24}$$

where

$$\begin{aligned} P_1(\nu) &= T_D(\nu)T_N(\nu) + (1-\nu^2)U_D(\nu)U_N(\nu) \\ P_2(\nu) &= T_N(\nu)U_D(\nu) - U_N(\nu)T_D(\nu) \\ P_3(\nu) &= T_N^2(\nu) + (1-\nu^2)U_N^2(\nu) \end{aligned} \tag{2.25}$$

and $T_N(\nu)$, $T_D(\nu)$, $U_N(\nu)$, and $U_D(\nu)$ are calculated as (2.7). Now, let $K_3 :=$

$K_2 - K_0$. Rewriting, we have

$$\begin{aligned} z^{-1}\delta(z)N(z^{-1}) &= -(\nu+1)P_1(\nu) - (1-\nu^2)P_2 - [(2K_2 - K_3)\nu) - K_1]P_3(\nu) \\ &+ j\sqrt{1-\nu^2}[-(\nu+1)P_2(\nu) + P_1(\nu) + K_3P_3(\nu)] \\ &= T(\nu, K_1, K_2, K_3) + j\sqrt{1-\nu^2}U(\nu, K_3). \end{aligned} \tag{2.26}$$

4. Fixing a specific value of $K_3$, we can calculate the zeros of $t_i$ of $U(\nu, K_3)$ which are real distinct of odd multiplicity for $\nu \in (-1, +1)$:

$$-1 < t_1 < t_2 < \cdots < t_k < +1. \tag{2.27}$$

5. For fixed $K_3$, calculate the set of strings, using the roots $t_j$ obtained in the previous step, of sign patterns for the real part $T(\nu, K_1, K_2, K_3)$, corresponding to stability, using

$$\begin{aligned} i_\delta + i_{N_r} - (l+1) = \frac{1}{2}Sgn\left[U^{(p)}(-1)\right]\Big(Sgn[T(-1, K_1, K_2, K_3)] \\ +2\sum_{j=1}^{k}(-1)^j Sgn[T(t_j, K_1, K_2, K_3)] + (-1)^{k+1}Sgn[T(+1, K_1, K_2, K_3)]\Big). \end{aligned} \tag{2.28}$$

where $i_\delta$, $i_{N_r}$, are the number of zeros inside the unit circle for $\delta(z)$ and $N_r(z)$, respectively (The sum of $i_\delta + i_{N_r} - l + 1$ is the number required for stability). For fixed $K_3$, this leads to linear inequalities in $(K_1, K_2)$.

6. Sweep over the $K_3$ range for which a right number of real roots $t_k$ exist in $(-1, 1)$ for $U(\nu, K_3) = 0$.

## 2.3 Continuous-Time Controllers

For the case of Continuous-Time controllers, an even-odd decomposition will be used. The objective is to parametrize the controller such we can compute the stabilizing set by solving a set of linear inequalities.

### *2.3.1 First Order Controllers*

Consider the system configuration in Fig 2.2 with a linear time invariant system

$$P(s) := \frac{N(s)}{D(s)} \tag{2.29}$$

and a First Order controller

$$C(s) := \frac{x_1 s + x_2}{s + x_3} \tag{2.30}$$

The procedure to compute the stabilizing set is the following:

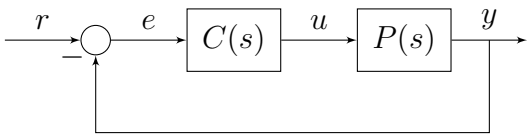


Figure 2.2: Unity Feedback Continuous-Time Control System

1. Represent the polynomials $N(s)$ and $D(s)$ from (2.29) in a even-odd decompo-

sition as

$$N(s) := N_E(s^2) + sN_O(s^2) \tag{2.31}$$

$$D(s) := D_E(s^2) + sD_O(s^2) \tag{2.32}$$

where $N_E$,$D_E$ represent the even part of $N(s)$ and $D(s)$ respectively. Likewise $N_O$,$D_O$ represent the odd part of $N(s)$ and $D(s)$ respectively.

2. Calculate the characteristic polynomial derived from Fig. 2.2

$$\begin{aligned}\delta(s) = &\left[s^2 D_O(s^2) + x_3 D_E(s^2) + x_2 N_E(s^2) + x_1 s^2 N_O(s^2)\right] \\ &+ s\left[D_E(s^2) + x_3 D_O(s^2) + x_2 N_O(s^2) + x_1 N_E(s^2)\right]\end{aligned} \tag{2.33}$$

3. substitute $s = j\omega$ in the characteristic equation (2.33)

$$\begin{aligned}\delta(j\omega) = &\left[-\omega^2 N_O(-\omega^2)x_1 + N_E(-\omega^2)x_2 + D_E(-\omega^2)x_3 - \omega^2 D_O(-\omega^2)\right] \\ &+ j\omega\left[N_E(-\omega^2)x_1 + N_O(-\omega^2)x_2 + D_O(-\omega^2)x_3 + D_E(-\omega^2)\right]\end{aligned} \tag{2.34}$$

4. Find the stability boundary for complex roots. This boundary is given by setting

$$\delta(j\omega) = 0, \qquad \omega \in (0, +\infty) \tag{2.35}$$

and

$$\delta(0) = 0, \qquad \delta_{n+1} = 0 \tag{2.36}$$

respectively. $\delta_{n+1}$ denotes the leading coefficient of $\delta(s)$. At $\omega = 0$ (2.34) becomes

$$N_E(0)x_2 + D_E(0)x_3 = 0 \tag{2.37}$$

and the condition $\delta_{n+1} = 0$ becomes

$$d_n + x_1 n_n = 0 \tag{2.38}$$

where $d_n$, $n_n$ are the coefficients of $s^n$ in $D(s)$ and $N(s)$ respectively. For a fixed value of $x_3$ and $\omega > 0$ to $\infty$, we have the curve in the $(x_1, x_2)$ plane that represents the stability boundary for the complex roots. The curves are given by

$$\begin{aligned} x_1(\omega) = \frac{1}{|A(\omega)|}(&\left[N_O(-\omega^2)D_E(-\omega^2) - N_E(-\omega^2)D_O(-\omega^2)\right] x_3 \\ &- \omega^2 N_O(-\omega^2)D_O(-\omega^2) - N_E(-\omega^2)D_E(-\omega^2)) \end{aligned} \tag{2.39}$$

$$\begin{aligned} x_2(\omega) = \frac{1}{|A(\omega)|}(&\left[-N_E(-\omega^2)D_E(-\omega^2) - \omega^2 N_O(-\omega^2)D_O(-\omega^2)\right] x_3 \\ &+ \omega^2 N_E(-\omega^2)D_O(-\omega^2) - \omega^2 N_O(-\omega^2)D_E(-\omega^2)) \end{aligned} \tag{2.40}$$

where

$$|A(\omega)| = \omega^2 N_O^2(-\omega^2) + N_E^2(-\omega^2) \tag{2.41}$$

The equations (2.37), (2.38), (2.39), and (2.40) forms different regions for fixed $x_3$, as $\omega$ runs from 0 to $+\infty$. Each region corresponds to a set of characteristic

polynomials with a fixed number of RHP roots.

5. For a fixed $x_3$, pick a point inside every region and calculate the roots of the characteristic equation. Select the regions with no RHP roots. By Sweeping over $x_3$, it is possible to see the stability region in three dimensions for a given plant, if one exists.

### *2.3.2 PI Controllers*

Lets consider the system configuration in Fig 2.2 with a linear time invariant system

$$P(s) := \frac{N(s)}{D(s)} \tag{2.42}$$

and a PI controller of the form

$$C(s) = \frac{K_P s + K_I}{s} \tag{2.43}$$

The procedure to compute the stabilizing set is the following:

1. Calculate the characteristic equation derived from Fig 2.2

$$\delta(s) = sD(s) + (K_P s + K_I)N(s) \tag{2.44}$$

2. form the new polynomial

$$v(s) := \delta(s)N(-s) \tag{2.45}$$

3. Represent the polynomials $v(s)$ from (2.45) in a even-odd decomposition as

$$v(s) = v_{even}(s^2, K_I) + sv_{odd}(s^2, K_P) \tag{2.46}$$

4. Fix $K_P = K_P^*$ and let $0 < \omega_1 < \omega_2 < \cdots < \omega_{l-1}$ be finite frequencies that are real and positive which also are roots of

$$v_{odd}(-\omega^2, K_P) = 0 \tag{2.47}$$

of odd multiplicities. Lets consider $\omega_0 := 0$ and $\omega_l := \infty$.

5. Let

$$j = sgn[v_{odd}(0^+, K_P)] \tag{2.48}$$

Let $deg[D(s)] = n$, $deg[N(s)] = m \leq n$, and let $z^+$ and $z^-$ be the number of zeros in the right half plane and left half plane of the plant, respectively. That is, zeros of $N(s)$. Let $i_0, i_1, \cdots$ equal to $\pm 1$ denote integers such that:
if $n + m$ is even, the signature is:

$$j(i_0 - 2i_1 + 2i_2 + \cdots + (-1)^{l-1}2i_{l-1} + (-1)^l i_l) = n - m + 1 + 2z^+ \tag{2.49}$$

if $n + m$ is odd, the signature is:

$$j(i_0 - 2i_1 + 2i_2 + \cdots + (-1)^{l-1}2i_{l-1}) = n - m + 1 + 2z^+ \tag{2.50}$$

6. Let $I_1$, $I_2$, $I_3, \cdots$ be the distinct strings of $i_0, i_1, \cdots$ that satisfy the signature condition (even or odd part expression). The stabilizing sets in the space of

$(K_P, K_I)$ , for a fixed $K_P = K_P^*$ can be computed by solving the set of linear inequalities

$$v_{even}(-\omega_t^2, K_I) i_t > 0 \tag{2.51}$$

where $i_t$ range over for each of $I_1, I_2, \cdots$

7. For every string $I_j$, it creates a stability region that is convex $S_j(K_P^*)$ and, for a specific value of $K_P^*$, the total stabilizing region is the union of these convex sets

$$S(K_P^*) = \cup_j S_j(K_P^*) \tag{2.52}$$

8. All the stabilizing regions, in the space of controller gains $(K_P, K_I)$, can be computed by sweeping $K_P$ over the real axis and following the steps above.

### *2.3.3 PID Controllers*

Lets consider the system configuration in Fig 2.2 with a linear time invariant system

$$P(s) := \frac{N(s)}{D(s)} \tag{2.53}$$

and a PID controller

$$C(s) = \frac{K_D s^2 + K_P s + K_I}{s} \tag{2.54}$$

The procedure to compute the stabilizing set is the following:

1. Calculate the characteristic equation derived from Fig 2.2

$$\delta(s) = sD(s) + (K_D s^2 + K_P s + K_I)N(s) \tag{2.55}$$

2. form the new polynomial

$$v(s) := \delta(s)N(-s) \tag{2.56}$$

3. Represent the polynomials $v(s)$ from (2.45) in a even-odd decomposition as

$$v(s) = v_{even}(s^2, K_I, K_D) + sv_{odd}(s^2, K_P) \tag{2.57}$$

4. Fix $K_P = K_P^*$ and let $0 < \omega_1 < \omega_2 < \cdots < \omega_{l-1}$ be finite frequencies that are real and positive which also are roots of

$$v_{odd}(-\omega^2, K_P) = 0 \tag{2.58}$$

of odd multiplicities. Lets consider $\omega_0 := 0$ and $\omega_l := \infty$.

5. Write

$$j = sgn[v_{odd}(0^+, K_P)] \tag{2.59}$$

Let $deg[D(s)] = n$, $deg[N(s)] = m \leq n$, and let $z^+$ and $z^-$ be the number of zeros in the right half plane and left half plane of the plant, respectively. that is, zeros of $N(s)$. Let $i_0, i_1, \cdots$ equal to $\pm 1$ denote integers such that:

if $n+m$ is even, the signature is:

$$j(i_0 - 2i_1 + 2i_2 + \cdots + (-1)^{l-1}2i_{l-1} + (-1)^l i_l) = n - m + 1 + 2z^+ \quad (2.60)$$

if $n+m$ is odd, the signature is:

$$j(i_0 - 2i_1 + 2i_2 + \cdots + (-1)^{l-1}2i_{l-1}) = n - m + 1 + 2z^+ \quad (2.61)$$

6. Let $I_1,\ I_2,\ I_3, \cdots$ be different strings of $i_0, i_1, \cdots$ that satisfy the signature condition (even or odd part expression). Then the stabilizing region in the controller gains space $(K_P, K_I, K_D)$, for a specific value of $K_P = K_P^*$ can be computed by solving the set of linear inequalities

$$v_{even}(-\omega_t^2, K_I, K_D) i_t > 0 \quad (2.62)$$

where $i_t$ range over for each of $I_1, I_2, \cdots$

7. For every string $I_j$, it creates a stability region that is convex $S_j(K_P^*)$ and, for a specific value of $K_P^*$, the total stabilizing region is the union of these convex sets

$$S(K_P^*) = \cup_j S_j(K_P^*) \quad (2.63)$$

8. All stabilizing regions, in the space of controller gains $(K_P, K_I, K_D)$, can be computed by sweeping $K_P$ over the real axis and following the steps above.

## 2.4 Time-Delay Case

In this section, the computation of the stabilizing set for Time-Delay systems is presented. The description of the procedures includes continuous-time PI and PID controllers for stable and unstable First Order Systems Plus Time-Delay (FOPTD). The results presented in this section are summarized from [14], [81], and [82].

In real world applications, many processes can be modeled or approximated as FOPTD. Typically, time-delay systems have the characteristic equation

$$\delta(s) = d(s) + e^{-L_1 s} n_1(s) + e^{-L_2 s} n_2(s) + \cdots + e^{-L_m s} n_m(s) \tag{2.64}$$

These type of polynomials are called quasipolynomials. In the computation of the stabilizing set for time-delay systems, it will be considered the following characteristic equation

$$\delta^*(s) = e^{Ls}\delta(s, L) = e^{L_m s} d(s) + e^{L_m - L_1 s} n_1(s) + e^{L_m - L_2 s} n_2(s) + \cdots + n_m(s) \tag{2.65}$$

For stability, two conditions must be satisfied. Given $\delta^*(s)$, we can write

$$\delta^*(j\omega) = \delta_r(\omega) + j\delta_i(\omega) \tag{2.66}$$

where $\delta_r(\omega)$ and $\delta_i(\omega)$ represent the real and imaginary part of $\delta^*(j\omega)$ respectively. $\delta^*(j\omega)$ is stable if and only if

- $\delta_r(\omega)$ and $\delta_i(\omega)$ have only roots that are simple, real and that interlace.
- $\delta_i'(\omega_0)\delta_r(\omega_0) - \delta_i(\omega_0)\delta_r'(\omega_0) > 0$, for some $\omega_0 \in (-\infty, +\infty)$

where $\delta_r'$ and $\delta_i'$ denote the first derivative of $\delta_r(\omega)$ and $\delta_i(\omega)$ respectively.

### *2.4.1 PI Controllers*

Lets consider the system configuration in Fig 2.2 with a linear time invariant system

$$P(s) := \frac{k}{1+Ts}e^{-Ls} \tag{2.67}$$

and a PI controller

$$C(s) = \frac{K_P s + K_I}{s} \tag{2.68}$$

where $k$ is the steady-state gain, $L$ is the time-delay, and $T$ is the time constant.

#### *2.4.1.1 Stable First Order Systems*

For stable First Order systems, the considerations are $T > 0$, $k > 0$, and $L > 0$. The procedure to compute the stabilizing set is the following:

1. For $L = 0$, calculate the characteristic equation

$$\delta(s) = Ts^2 + (kK_P + 1)s + kK_I \tag{2.69}$$

For stability, it is required

$$K_P > -\frac{1}{k}, \quad K_I > 0 \tag{2.70}$$

2. For $L > 0$, calculate the characteristic equation

$$\delta(s) = (kK_I + kK_P)e^{-Ls} + (1 + Ts)s \tag{2.71}$$

Considering $\delta^*(s) = e^{Ls}\delta(s)$ we have

$$\delta^*(s) = (kK_I + kK_P s) + (1 + Ts)se^{Ls} \tag{2.72}$$

3. Calculate

$$\delta^*(j\omega) = \delta_r(\omega) + j\delta_i(j\omega) \tag{2.73}$$

where

$$\delta_r(\omega) = kK_I - \omega\sin(L\omega) - T\omega^2\cos(L\omega) \tag{2.74}$$

$$\delta_i(\omega) = \omega\left[kK_P + \cos(L\omega) - T\omega\sin(L\omega)\right] \tag{2.75}$$

4. Make a change in variable $z = L\omega$ and calculate the new real and imaginary parts of $\delta^*(j\omega)$

$$\delta_r(z) = k\left[K_I - a(z)\right] \tag{2.76}$$

$$\delta_i(z) = \frac{z}{L}\left[kK_P + \cos(z) - \frac{T}{L}z\sin(z)\right] \tag{2.77}$$

where

$$a(z) = \frac{z}{kL}\left[sin(z) + \frac{T}{L}z\cos(z)\right] \tag{2.78}$$

5. Pick a value for $K_P$ and set $j = 1$ in the range

$$-\frac{1}{k} < K_P < \frac{T}{kL}\sqrt{\alpha_1^2 + \frac{L^2}{T^2}} \tag{2.79}$$

where $\alpha_1$ is the solution of

$$\tan(\alpha) = -\frac{T}{L}\alpha \tag{2.80}$$

in the interval $(\frac{\pi}{2}, \pi)$.

6. Find the root $z_j$ from

$$\left[kK_P + \cos(z) - \frac{T}{L} z \sin(z)\right] = 0 \tag{2.81}$$

that is part of $\delta_i(z)$. The roots can be found graphically for the following cases:

- $-\frac{1}{k} < K_P < \frac{1}{k}$: in this case, take the intersection of the functions $\frac{kK_P + \cos(z)}{\sin(z)}$ and $\frac{T}{L}z$.
- $K_P = \frac{1}{k}$: in this case, take the intersection of the functions $kK_P + cos(z)$ and $\frac{T}{L} z \sin(z)$.
- $\frac{1}{k} < K_P < \frac{T}{kL}\sqrt{\alpha_1^2 + \frac{L^2}{T^2}}$, in this case take the intersection of the functions $\frac{kK_P + \cos(z)}{\sin(z)}$ and $\frac{T}{L}z$.

7. Compute the parameters $a_j(z_j)$ using (2.78).

8. If $cos(z_j) > 0$ go to the next step. If not, $j = j + 2$ and go to step 6.

9. Determine the lower and upper bounds for $K_I$ as

$$0 < K_I < \min_{l=1,3,5,\ldots j} \{a_l\} \tag{2.82}$$

10. Go to step 5.

#### *2.4.1.2 Unstable First Order Systems*

For unstable First Order systems, the considerations are $T < 0$, $k > 0$, and $L > 0$. The procedure to compute the stabilizing set is the following:

1. For $L = 0$, calculate the characteristic equation

$$\delta(s) = Ts^2 + (kK_P + 1)s + kK_I \tag{2.83}$$

   For stability, it is required

$$K_P < -\frac{1}{k}, \quad K_I < 0 \tag{2.84}$$

2. For $L > 0$, calculate the characteristic equation

$$\delta(s) = (kK_I + kK_P)e^{-Ls} + (1 + Ts)s \tag{2.85}$$

   Considering $\delta^*(s) = e^{Ls}\delta(s)$ we have

$$\delta^*(s) = (kK_I + kK_P s) + (1 + Ts)se^{Ls} \tag{2.86}$$

3. Calculate

$$\delta^*(j\omega) = \delta_r(\omega) + j\delta_i(j\omega) \tag{2.87}$$

where

$$\delta_r(\omega) = kK_I - \omega\sin(L\omega) - T\omega^2\cos(L\omega) \tag{2.88}$$

$$\delta_i(\omega) = \omega\left[kK_P + \cos(L\omega) - T\omega\sin(L\omega)\right] \tag{2.89}$$

4. Make a change in variable $z = L\omega$ and calculate the new real and imaginary parts of $\delta^*(j\omega)$

$$\delta_r(z) = k\left[K_I - a(z)\right] \tag{2.90}$$

$$\delta_i(z) = \frac{z}{L}\left[kK_P + \cos(z) - \frac{T}{L}z\sin(z)\right] \tag{2.91}$$

where

$$a(z) = \frac{z}{kL}\left[sin(z) + \frac{T}{L}z\cos(z)\right] \tag{2.92}$$

5. Pick a value for $K_P$ and set $j = 1$ in the range

$$\frac{T}{kL}\sqrt{\alpha_1^2 + \frac{L^2}{T^2}} < K_P < -\frac{1}{k} \tag{2.93}$$

where $\alpha_1$ is the solution of

$$\tan(\alpha) = -\frac{T}{L}\alpha \tag{2.94}$$

in the interval $(0, \frac{\pi}{2})$.

6. Find the root $z_j$ from

$$\left[kK_P + \cos(z) - \frac{T}{L} z \sin(z)\right] = 0 \tag{2.95}$$

that is part of $\delta_i(z)$. The roots can be found graphically for the following cases:

- $\frac{1}{k} < K_P < -\frac{1}{k}$: in this case, take the intersection of the functions $\frac{kK_P + \cos(z)}{\sin(z)}$ and $\frac{T}{L} z$.
- $K_P = \frac{1}{k}$: in this case, take the intersection of the functions $kK_P + cos(z)$ and $\frac{T}{L} z \sin(z)$.
- $\frac{T}{kL}\sqrt{\alpha_1^2 + \frac{L^2}{T^2}} < K_P < \frac{1}{k}$, in this case take the intersection of the functions $\frac{kK_P + \cos(z)}{\sin(z)}$ and $\frac{T}{L} z$.

7. Compute the parameters $a_j(z_j)$ using (2.92).

8. If $cos(z_j) > 0$ go to the next step. If not, $j = j + 2$ and go to step 6.

9. Determine the lower and upper bounds for $K_I$ as

$$\max_{l=1,3,5,\ldots j} \{a_l\} < K_I < 0 \tag{2.96}$$

10. Go to step 5.

### *2.4.2 PID Controllers*

Lets consider the system configuration in Fig 2.2 with a linear time invariant system

$$P(s) := \frac{k}{1 + Ts} e^{-Ls} \tag{2.97}$$

and a PID controller of the form

$$C(s) = \frac{K_D s^2 + K_P s + K_I}{s} \tag{2.98}$$

where $k$ is the steady-state gain, $L$ is the time-delay, and $T$ is the time constant.

#### *2.4.2.1 Stable First Order Systems*

For stable First Order systems, the considerations are $T > 0$, $k > 0$, and $L > 0$. The procedure to compute the stabilizing set is the following:

1. For $L = 0$, calculate the characteristic equation

$$\delta(s) = (T + kK_D)s^2 + (kK_P + 1)s + kK_I \tag{2.99}$$

For stability, it is required

$$K_P > -\frac{1}{k}, \quad K_I > 0 \quad , \text{ and} K_D > -\frac{T}{k} \tag{2.100}$$

2. For $L > 0$, calculate the characteristic equation

$$\delta(s) = (kK_I + kK_P s + kK_D s^2)e^{-Ls} + (1 + Ts)s \tag{2.101}$$

Considering $\delta^*(s) = e^{Ls}\delta(s)$ we have

$$\delta^*(s) = (kK_I + kK_P s + kK_D s^2) + (1 + Ts)se^{Ls} \tag{2.102}$$

3. Calculate

$$\delta^*(j\omega) = \delta_r(\omega) + j\delta_i(j\omega) \tag{2.103}$$

where

$$\delta_r(\omega) = kK_I - kK_D\omega^2 - \omega\sin(L\omega) - T\omega^2\cos(L\omega) \tag{2.104}$$

$$\delta_i(\omega) = \omega\left[kK_P + \cos(L\omega) - T\omega\sin(L\omega)\right] \tag{2.105}$$

4. Make a change in variable $z = L\omega$ and calculate the new real and imaginary parts of $\delta^*(j\omega)$

$$\delta_r(z) = kK_I - \frac{kK_D}{L^2}z^2 - \frac{1}{L}z\sin(z) - \frac{T}{L^2}z^2 cos(z) \tag{2.106}$$

$$\delta_i(z) = \frac{z}{L}\left[kK_P + \cos(z) - \frac{T}{L}z\sin(z)\right] \tag{2.107}$$

5. Pick a value for $K_P$ in the range

$$-\frac{1}{k} < K_P < \frac{1}{k}\left[\frac{T}{L}\alpha_1\sin(\alpha_1) - \cos(\alpha_1)\right] \tag{2.108}$$

where $\alpha_1$ is solved from

$$\tan(\alpha) = -\frac{T}{T+L}\alpha \tag{2.109}$$

in the interval $(0, \pi)$.

6. Find the roots $z_1$ and $z_2$ from

$$\left[kK_P + \cos(z) - \frac{T}{L} z \sin(z)\right] = 0 \tag{2.110}$$

that is part of $\delta_i(z)$. The roots can be found graphically for the following cases:

- $-\frac{1}{k} < K_P < \frac{1}{k}$: in this case, take the intersection of the functions $\frac{kK_P + \cos(z)}{\sin(z)}$ and $\frac{T}{L} z$.
- $K_P = \frac{1}{k}$: in this case, take the intersection of the functions $kK_P + cos(z)$ and $\frac{T}{L} z \sin(z)$.
- $\frac{1}{k} < K_P < \frac{T}{kL}\left[\frac{T}{L}\alpha_1 \sin(\alpha_1) - \cos(\alpha_1)\right]$, in this case take the intersection of the functions $\frac{kK_P + \cos(z)}{\sin(z)}$ and $\frac{T}{L} z$.

7. Compute the parameters $m_j(z_j)$ and $b_j(z_j)$ for $j = 1, 2$ where

$$m(z) = \frac{L^2}{z^2} \tag{2.111}$$

$$b(z) = -\frac{L}{kz}\left[\sin(z) + \frac{T}{L} z \cos(z)\right] \tag{2.112}$$

8. Calculate the $(K_I, K_D)$ stabilizing set using Fig. 2.3

9. Go to step 5.

#### *2.4.2.2 Unstable First Order Systems*

For unstable First Order systems, the considerations are $T < 0$, $k > 0$, and $L > 0$. The procedure to compute the stabilizing set is the following:

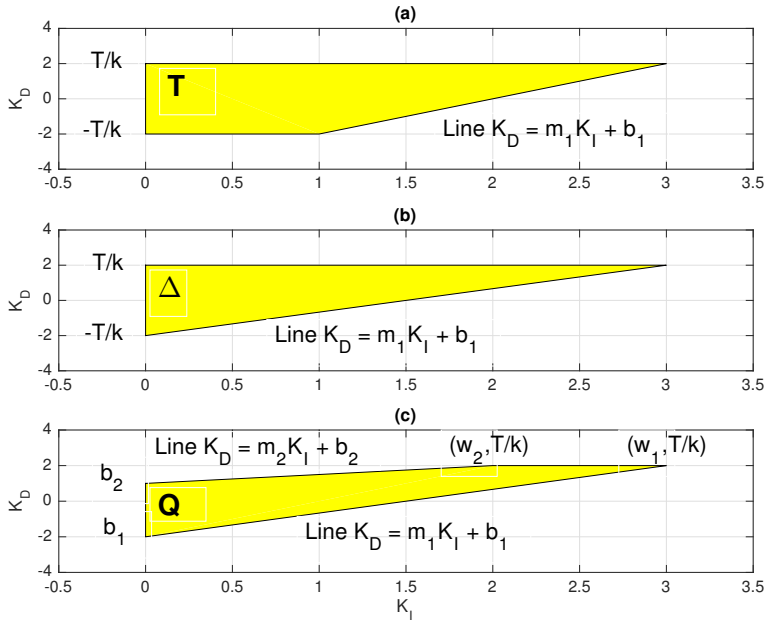


Figure 2.3: Stabilizing Region of $(K_I, K_D)$ for: (a) $-\frac{1}{k} < K_P < \frac{1}{k}$, (b) $K_P = \frac{1}{k}$, (c) $\frac{1}{k} < K_P < \frac{T}{kL}\left[\frac{T}{L}\alpha_1 \sin(\alpha_1) - \cos(\alpha_1)\right]$

1. For $L = 0$, calculate the characteristic equation

$$\delta(s) = (T + kK_D)s^2 + (kK_P + 1)s + kK_I \tag{2.113}$$

For stability, it is required

$$K_P < -\frac{1}{k}, \quad K_I < 0 \quad , \text{ and} K_D < -\frac{T}{k} \tag{2.114}$$

2. For $L > 0$, calculate the characteristic equation

$$\delta(s) = (kK_I + kK_P s + kK_D s^2)e^{-Ls} + (1 + Ts)s \tag{2.115}$$

Considering $\delta^*(s) = e^{Ls}\delta(s)$ we have

$$\delta^*(s) = (kK_I + kK_P s + kK_D s^2) + (1 + Ts)se^{Ls} \tag{2.116}$$

3. Calculate

$$\delta^*(j\omega) = \delta_r(\omega) + j\delta_i(j\omega) \tag{2.117}$$

where

$$\delta_r(\omega) = kK_I - kK_D\omega^2 - \omega\sin(L\omega) - T\omega^2\cos(L\omega) \tag{2.118}$$

$$\delta_i(\omega) = \omega\left[kK_P + \cos(L\omega) - T\omega\sin(L\omega)\right] \tag{2.119}$$

4. Make a change in variable $z = L\omega$ and calculate the new real and imaginary parts of $\delta^*(j\omega)$

$$\delta_r(z) = kK_I - \frac{kK_D}{L^2}z^2 - \frac{1}{L}z\sin(z) - \frac{T}{L^2}z^2 cos(z) \tag{2.120}$$

$$\delta_i(z) = \frac{z}{L}\left[kK_P + \cos(z) - \frac{T}{L}z\sin(z)\right] \tag{2.121}$$

5. For $\left|\frac{T}{L}\right| > 0.5$, pick a value for $K_P$ in the range

$$\frac{1}{k}\left[\frac{T}{L}\alpha_1\sin(\alpha_1) - \cos(\alpha_1)\right] < K_P < -\frac{1}{k} \tag{2.122}$$

where $\alpha_1$ is solved from

$$\tan(\alpha) = -\frac{T}{T+L}\alpha \tag{2.123}$$

in the $(0, \pi)$ interval. For the case $\left|\frac{T}{L}\right| = 1$, $\alpha_1 = \frac{\pi}{2}$.

6. Find the roots $z_1$ and $z_2$ from

$$\left[kK_P + \cos(z) - \frac{T}{L} z \sin(z)\right] = 0 \tag{2.124}$$

that is part of $\delta_i(z)$. The roots can be found graphically for the following cases:

- $\frac{1}{k} < K_P < -\frac{1}{k}$: in this case, take the intersection of the functions $\frac{kK_P + \cos(z)}{\sin(z)}$ and $\frac{T}{L} z$.
- $K_P = \frac{1}{k}$: in this case, take the intersection of the functions $kK_P + cos(z)$ and $\frac{T}{L} z \sin(z)$.
- $\frac{T}{kL}\left[\frac{T}{L}\alpha_1 \sin(\alpha_1) - \cos(\alpha_1)\right] < K_P < \frac{1}{k}$, in this case take the intersection of the functions $\frac{kK_P + \cos(z)}{\sin(z)}$ and $\frac{T}{L} z$.

7. Compute the parameters $m_j(z_j)$ and $b_j(z_j)$ for $j = 1, 2$ where

$$m(z) = \frac{L^2}{z^2} \tag{2.125}$$

$$b(z) = -\frac{L}{kz}\left[\sin(z) + \frac{T}{L} z \cos(z)\right] \tag{2.126}$$

8. Calculate the $(K_I, K_D)$ stabilizing set using Fig. 2.4

9. Go to step 5.

## 2.5 References

The procedures presented in this section are summarized from [14]. Also, more information about these results is available in [78, 79] for the First Order controller

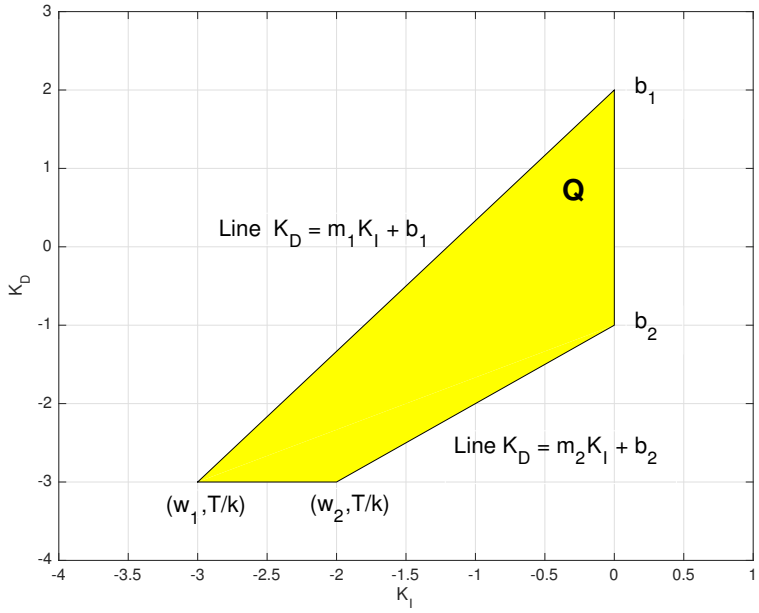


Figure 2.4: Stabilizing Region of $(K_I, K_D)$ for: $\frac{1}{k}\left[\frac{T}{L}\alpha_1 \sin(\alpha_1) - \cos(\alpha_1)\right] < K_P < -\frac{1}{k}$

case, in [76] for the discrete-time PI/PID controller case, in [78] for continuous-time PI/PID controller case, and in [81, 82] for the time-delay case.

# 3. FIRST ORDER, PI, AND PID CONTROLLERS CONSTANT GAIN AND CONSTANT PHASE LOCI*

## 3.1 Introduction

In this section, a parametrization for the First Order, PI, and PID controllers for discrete and continuous-time systems is presented. This parametrization produces ellipses and straight lines (for First Order and PI cases) and cylinder and plane (for PID case) that will be used to find the intersection points, given a prescribed crossover frequency, gain, and phase margins, that are contained in the stabilizing set and that will satisfy our desired robust performance in terms of a specific gain and phase margin.

---

*Part of this section is reprinted with permission from: ©2015 IEEE I. D. Díaz-Rodríguez and S. P. Bhattacharyya, "Modern design of classical controllers: Digital PI controllers," 2015 IEEE International Conference on Industrial Technology (ICIT), Seville, 2015, pp. 2112-2119. doi: 10.1109/ICIT.2015.7125408.

*Part of this section is reprinted with permission from: ©2015 IEEE I. D. Díaz-Rodríguez, V. A. Oliveira and S. P. Bhattacharyya, "Modern design of classical controllers: Digital PID controllers," 2015 IEEE 24th International Symposium on Industrial Electronics (ISIE), Buzios, 2015, pp. 1010-1015. doi: 10.1109/ISIE.2015.7281610.

*Part of this section is reprinted with permission from: ©2015 IEEE I. D. Díaz-Rodríguez, "Modern design of classical controllers: Continuous-time first order controllers," IECON 2015 - 41st Annual Conference of the IEEE Industrial Electronics Society, Yokohama, 2015, pp. 000070-000075. doi: 10.1109/IECON.2015.7392967.

*Part of this section is reprinted with permission from: ©2016 IEEE I. D. Díaz-Rodríguez and S. P. Bhattacharyya, "PI controller design in the achievable gain-phase margin plane," 2016 IEEE 55th Conference on Decision and Control (CDC), Las Vegas, NV, 2016, pp. 4919-4924. doi: 10.1109/CDC.2016.7799021.

*Part of this section is reprinted with permission from: ©2017 Elsevier I. D. Dıaz-Rodrıguez, S. Han, L. H. Keel, and S. P. Bhattacharyya, "Advanced Tuning for Ziegler-Nichols Plants," The 20th World Congress of the International Federation of Automatic Control (IFAC), 9-14 July, Toulouse, France, 2017. (Accepted for publication)

## 3.2 Constant Gain and Constant Phase Loci for Discrete-Time Controllers

For discrete-time controllers, it is possible to parametrize the controller parameters in a geometric form. For the cases of PI, and PID digital controllers, the constant gain and constant phase loci result in ellipses and straight lines.

### *3.2.1 PI Controllers*

Let $P(z)$ and $C(z)$ denote the plant and controller transfer functions. The frequency response of the plant and controller are $P(e^{j\omega T})$, $C(e^{j\omega T})$ respectively where $T$ is the sampling period and $\omega \in \left[0, \frac{2\pi}{T}\right]$. For a PI controller

$$C(z) = \frac{K_0 + K_1 z}{z - 1} \tag{3.1}$$

where $K_0$, $K_1$ are design parameters. Then

$$C(e^{j\omega T}) = \frac{K_0 + K_1 e^{j\omega T}}{e^{j\omega T} - 1} \tag{3.2}$$

Letting $\omega T =: \theta$

$$C(e^{j\theta}) = \frac{K_0 + K_1 e^{j\theta}}{e^{j\theta} - 1} \tag{3.3}$$

Note that,

$$C(e^{j\theta}) = \frac{K_0 e^{-j\frac{\theta}{2}} + K_1 e^{j\frac{\theta}{2}}}{e^{j\frac{\theta}{2}} - e^{-j\frac{\theta}{2}}} = \frac{(K_1 + K_0)\cos\frac{\theta}{2} + j(K_1 - K_0)\sin\frac{\theta}{2}}{2j\sin\frac{\theta}{2}} \tag{3.4}$$

Let

$$L_0 := K_1 + K_0 \tag{3.5}$$

$$L_1 := K_1 - K_0 \tag{3.6}$$

From (3.4), (3.5), and (3.6) we have

$$|C(e^{j\theta})|^2 = \frac{L_0^2}{4\tan^2\frac{\theta}{2}} + \frac{L_1^2}{4} =: M^2 \tag{3.7}$$

$$\angle C(e^{j\theta}) = \arctan\left(\frac{-L_0}{L_1\tan\frac{\theta}{2}}\right) =: \Phi \tag{3.8}$$

Equations (3.7) and (3.8) can be written as

$$\frac{L_0^2}{a^2} + \frac{L_1^2}{b^2} = 1 \tag{3.9}$$

$$L_1 = cL_0 \tag{3.10}$$

where

$$a^2 = 4M^2\tan^2\frac{\theta}{2} \tag{3.11}$$

$$b^2 = 4M^2 \tag{3.12}$$

$$c = -\frac{1}{\tan\Phi\tan\frac{\theta}{2}} \tag{3.13}$$

Thus constant $M$ loci are ellipses and constant phase loci are straight lines in $L_0$, $L_1$ space. The major and minor axes of the ellipse are given by (3.11), (3.12) and $c$ represents the slope of the line. The mapping from $K_0$, $K_1$ to $L_0$, $L_1$ and viceversa

is given by

$$K_0 = \frac{L_0 - L_1}{2} \tag{3.14}$$

$$K_1 = \frac{L_0 + L_1}{2} \tag{3.15}$$

Suppose $\omega_g$ is the prescribed closed-loop gain crossover frequency. Then $M_g := \frac{1}{|P(e^{j\theta_g})|}$ and if $\phi_g^*$ is the desired phase margin in radians, $\Phi_g := \pi + \phi_g^* - \angle P(e^{j\theta_g})$. From (3.9) and (3.10) we obtain the ellipse and straight lines corresponding to $M = M_g$ and $\Phi = \Phi_g$, giving the design point $(K_P^*, K_I^*)$. If these intersection points lie in the stabilizing set $S$, the design is feasible, otherwise the specifications have to be altered.

### *3.2.2 PID Controllers*

Let $P(z)$ and $C(z)$ denote the plant and controller transfer functions. The frequency response of the plant and controller are $P(e^{j\omega T})$, $C(e^{j\omega T})$ respectively where $T$ is the sampling period and $\omega \in \left[0, \frac{2\pi}{T}\right]$. For a PID controller

$$C(z) = \frac{K_0 + K_1 z + K_2 z^2}{z(z-1)} \tag{3.16}$$

where $K_0$, $K_1$, and $K_2$ are design parameters. Then, letting $\omega T =: \theta$

$$C(e^{j\theta}) = \frac{K_0 e^{-j\theta} + K_1 + K_2 e^{j\theta}}{e^{j\theta} - 1} \tag{3.17}$$

Note that,

$$C(e^{j\theta}) = \frac{(K_2 + K_0)\cos\theta + K_1 + j(K_2 - K_0)\sin\theta}{(\cos\theta - 1 + j\sin\theta)} \tag{3.18}$$

Let

$$L_0 := K_2 + K_0, \quad L_1 := K_2 - K_0 \tag{3.19}$$

From (3.18) and (3.19) we have

$$|C(e^{j\theta})|^2 = \frac{\cos^2\theta\left(L_0 + \frac{K_1}{\cos\theta}\right)^2 + \sin^2\theta L_1^2}{(\cos\theta - 1)^2 + (\sin\theta)^2} = \frac{\left(L_0 + \frac{K_1}{\cos\theta}\right)^2}{\left(\frac{\sqrt{\mu}}{\cos\theta}\right)^2} + \frac{L_1^2}{\left(\frac{\sqrt{\mu}}{\sin\theta}\right)^2} =: M^2 \tag{3.20}$$

where $\mu = (\cos\theta - 1)^2 + (\sin\theta)^2$ and

$$\angle C(e^{j\theta}) = \tan^{-1}\left(\frac{L_1\sin\theta}{K_1 + L_0\cos\theta}\right) - \tan^{-1}\left(\frac{\sin\theta}{\cos\theta - 1}\right) \tag{3.21}$$

Using the relationships among the inverse trigonometric functions

$$\tan^{-1}u - \tan^{-1}v = \tan^{-1}\left(\frac{u - v}{1 + uv}\right) \tag{3.22}$$

we have

$$\angle C(e^{j\theta}) = \tan^{-1}\left(\frac{\sin\theta\left(L_1(\cos\theta - 1) - (L_0\cos\theta + K_1)\right)}{(L_0\cos\theta + K_1)(\cos\theta - 1) + L_1\sin^2\theta}\right) =: \Phi. \tag{3.23}$$

Equations (3.20) and (3.23) can be written as

$$\frac{(L_0 + a)^2}{b^2} + \frac{L_1^2}{c^2} = 1, \quad L_1 = dL_0 + e \tag{3.24}$$

where

$$a = \frac{K_1}{\cos\theta}, \quad b^2 = \frac{\mu M^2}{\cos^2\theta}, \quad c^2 = \frac{\mu M^2}{\sin^2\theta} \tag{3.25}$$

$$d = \frac{\sin\theta\cos\theta + \cos\theta\tan\Phi(\cos\theta - 1)}{\sin\theta(\cos\theta - 1) - \sin^2\theta\tan\Phi} \tag{3.26}$$

$$e = \frac{K_1(\cos\theta - 1)\tan\Phi + \sin\theta}{\sin\theta(\cos\theta - 1) - \sin^2\theta\tan\Phi} \tag{3.27}$$

for fixed $K_1$. Thus constant $M$ loci are ellipses and constant phase loci are straight lines in $L_0$, $L_1$ space. The major and minor axes of the ellipse are given by the square root of $b$ and $c$. The slope of the line is represented by $d$ and $e$ determines the point at which the line crosses the $L_1$ axis. The mapping from $K_0$, $K_2$ to $L_0$, $L_1$ and viceversa is given by

$$K_0 = \frac{L_0 - L_1}{2}, \quad K_2 = \frac{L_0 + L_1}{2} \tag{3.28}$$

Suppose $\omega_g$ is the prescribed closed-loop gain crossover frequency. Then $M_g := \frac{1}{|P(e^{j\theta_g})|}$ and if $\phi_g^*$ is the desired phase margin in radians, $\Phi_g := \pi + \phi_g^* - \angle P(e^{j\theta_g})$. From (3.24) we obtain the ellipse and straight lines corresponding to $M = M_g$ and $\Phi = \Phi_g$, giving the design point $(K_P^*, K_I^*, K_D^*)$. If these intersection points lie in the stabilizing set $S$, the design is feasible, otherwise the specifications have to be altered.

## 3.3 Constant Gain and Constant Phase Loci for Continuous-Time Controllers

For continuous-time controllers, it is possible to parametrize the controller parameters in a geometric form. For the cases of First Order, PI, the constant gain and phase loci result in ellipses and straight lines. For the case of PID controllers, the constant gain and constant phase loci result in a cylinder and a plane.

### *3.3.1 First Order Controllers*

Let $P(s)$ and $C(s)$ denote the plant and controller transfer functions. The frequency response of the plant and controller are $P(j\omega)$, $C(j\omega)$ respectively. For the First Order controller

$$C(s) = \frac{x_1 s + x_2}{s + x_3} \tag{3.29}$$

where $x_1$, $x_2$, and $x_3$ are design parameters. Then taking $s = j\omega$

$$C(j\omega) = \left(\frac{x_1(j\omega) + x_2}{j\omega + x_3}\right)\left(\frac{x_3 - j\omega}{x_3 - j\omega}\right) = \frac{(x_1\omega^2 + x_2 x_3) + j\omega(x_1 x_3 - x_2)}{x_3^2 + \omega^2} \tag{3.30}$$

Let

$$L_0 := x_1\omega^2 + x_2 x_3, \quad L_1 := x_1 x_3 - x_2 \tag{3.31}$$

From (3.30) and (3.31) we have

$$|C(j\omega)|^2 = \frac{L_0^2}{(x_3^2 + \omega^2)^2} + \frac{L_1^2}{\left(\frac{x_3^2+\omega^2}{\omega}\right)^2} =: M^2 \tag{3.32}$$

and

$$\angle C(j\omega) = \arctan\left(\frac{\omega L_1}{L_0}\right) =: \Phi \tag{3.33}$$

Equations (3.32) and (3.33) can be written as

$$\frac{L_0^2}{a^2} + \frac{L_1^2}{b^2} = 1, \tag{3.34}$$

$$L_1 = cL_0 \tag{3.35}$$

where

$$a^2 = M^2(x_3^2 + \omega^2)^2, \tag{3.36}$$

$$b^2 = \frac{M^2}{\omega}(x_3^2 + \omega^2)^2, \tag{3.37}$$

$$c = \frac{\tan\Phi}{\omega} \tag{3.38}$$

Thus, for a fixed $x_3$, constant $M$ loci are ellipses and constant phase loci are straight lines in $L_0$, $L_1$ space. The major and minor axes of the ellipse are given by the square root of $a$ and $b$. The slope of the line is represented by $c$. The mapping from $x_1$, $x_2$ to $L_0$, $L_1$ and vice versa is given by

$$x_1 = \frac{L_0 + L_1 x_3}{x_3^2 + \omega^2}, \quad x_2 = \frac{L_0 x_3 - \omega^2 L_1}{x_3^2 + \omega^2} \tag{3.39}$$

Suppose $\omega_g$ is the prescribed closed-loop gain crossover frequency. Then $M_g := \frac{1}{|P(j\omega_g)|}$ and if $\phi_g^*$ is the desired phase margin in radians, $\Phi_g := \pi + \phi_g^* - \angle P(j\omega_g)$. From (3.34) and (3.35) we obtain the ellipse and straight lines corresponding to $M = M_g$ and $\Phi = \Phi_g$, giving the design point $(x_1^*, x_2^*, x_3^*)$. If these intersection points lie in the stabilizing set $S$, the design is feasible, otherwise the specifications have to be altered.

### *3.3.2 PI Controllers*

Let $P(s)$ and $C(s)$ denote the plant and controller transfer functions. The frequency response of the plant and controller are $P(j\omega)$, $C(j\omega)$ respectively where $\omega \in [0, \infty]$. For a PI controller

$$C(s) = \frac{K_P s + K_I}{s} \tag{3.40}$$

where $K_P$ $K_I$ are design parameters. Then taking $s = j\omega$

$$C(j\omega) = \frac{K_P(j\omega) + K_I}{j\omega} \tag{3.41}$$

Then, we have

$$|C(j\omega)|^2 = K_P^2 + \frac{K_I^2}{\omega^2} =: M^2 \tag{3.42}$$

and

$$\angle C(j\omega) = \arctan\left(\frac{-K_I}{\omega K_P}\right) := \Phi \tag{3.43}$$

Equations (3.42) and (3.43) can be written as

$$\frac{(K_P)^2}{a^2} + \frac{(K_I)^2}{b^2} = 1 \tag{3.44}$$

$$K_I = cK_P \tag{3.45}$$

where

$$a^2 = M^2 \tag{3.46}$$

$$b^2 = M^2\omega^2 \tag{3.47}$$

$$c = -\omega \tan \Phi \tag{3.48}$$

Thus constant $M$ loci are ellipses and constant phase loci are straight lines in $K_P$, $K_I$ space. The major and minor axes of the ellipse are given by the square roots of (3.46) and (3.47) (see Fig 3.1). The slope of the line is represented by $c$ (see Fig 3.1). Suppose $\omega_g$ is the prescribed closed-loop gain crossover frequency. Then $M_g := \frac{1}{|P(j\omega_g)|}$ and if $\phi_g^*$ is the desired phase margin in radians, $\Phi_g := \pi + \phi_g^* - \angle P(j\omega_g)$. From (3.42) and (3.43) we obtain the ellipse and straight lines corresponding to $M = M_g$ and $\Phi = \Phi_g$, giving the design point $(K_P^*, K_I^*)$. If these intersection points lie in the stabilizing set $S$, the design is feasible, otherwise the specifications have to be altered.

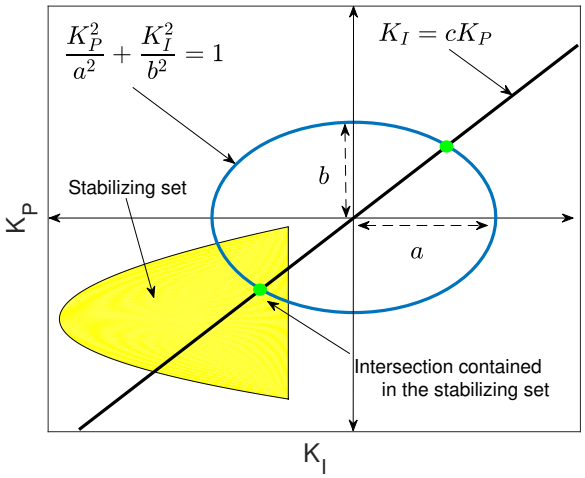


Figure 3.1: Ellipse and Straight Line Intersecting With a Stabilizing Set

### *3.3.3 PID Controllers*

Let $P(s)$ and $C(s)$ denote the plant and controller transfer functions. The frequency response of the plant and controller are $P(j\omega)$, $C(j\omega)$ respectively where $\omega \in [0, \infty]$. For a PID controller

$$C(s) = \frac{K_D s^2 + K_P s + K_I}{s}, \tag{3.49}$$

where $K_P$, $K_I$, and $K_D$ are design parameters. Then for $s = j\omega$

$$C(j\omega) = \frac{K_D(j\omega)^2 + K_P(j\omega) + K_I}{j\omega} \tag{3.50}$$

From (3.50), we have

$$|C(j\omega)|^2 = K_P^2 + \left(K_D\omega - \frac{K_I}{\omega}\right)^2 := M^2 \tag{3.51}$$

and

$$\angle C(j\omega) = \arctan\left(\frac{K_D\omega - \frac{K_I}{\omega}}{K_P}\right) := \Phi \tag{3.52}$$

from (3.51) and (3.52) we have that

$$K_P^2 = M^2 - \left(K_D\omega - \frac{K_I}{\omega}\right)^2 = \frac{\left(K_D\omega - \frac{K_I}{\omega}\right)^2}{\tan^2\Phi}. \tag{3.53}$$

From (3.53) we can have the following expressions

$$K_I = K_D\omega^2 \pm \omega\sqrt{\frac{M^2\tan^2\Phi}{1+\tan^2\Phi}} \tag{3.54}$$

$$K_P = \pm\sqrt{\frac{M^2}{1+\tan^2\Phi}} \tag{3.55}$$

Suppose $\omega_g$ is the prescribed closed-loop gain crossover frequency. Then $M_g = \frac{1}{|P(j\omega_g)|}$. If $\phi_g^*$ is the desired phase margin in radians, $\Phi_g = \pi + \phi_g^* - \angle P(j\omega_g)$. Thus, for equation (3.51) and (3.52), for different values of $K_P$, $K_I$, and $K_D$ we have a cylinder and a plane (see Fig 3.2). For a fixed value of $K_P$ there is a straight line in $(K_I, K_D)$ plane represented in equation (3.55).

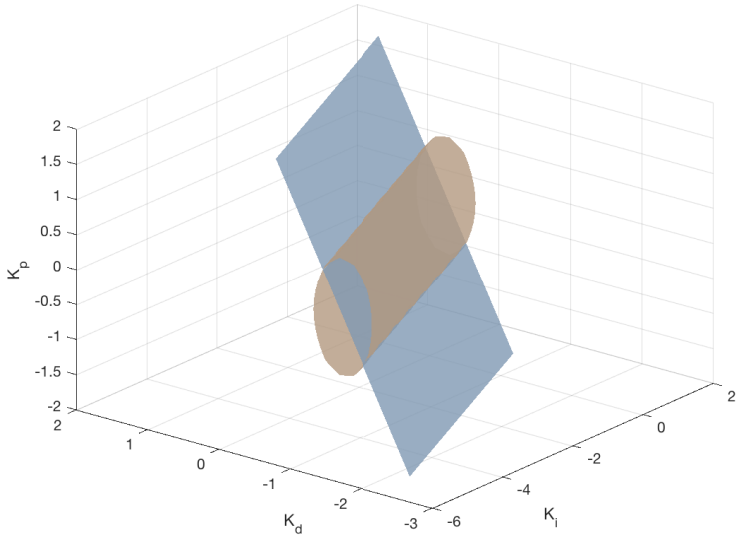


Figure 3.2: Cylinder and Plane Intersecting in the $(K_P, K_I, K_D)$ Space

## 3.4 Constant Gain and Constant Phase Loci for Continuous-Time Systems With Time-Delay

For continuous-time systems with time-delay, it is possible to parametrize the controller parameters in a geometric form. For the cases of PI and PID controllers, the constant gain and phase loci result in ellipses and straight lines.

### *3.4.1 PI Controllers*

Let $G(s)$ and $C(s)$ denote the plant and controller transfer functions. In this case, the plant includes a time-delay, tha is $G(s) = e^{-Ls}P(s)$, where $L > 0$ is the time-delay. The frequency response of the plant and controller are $e^{-Lj\omega}P(j\omega)$, $C(j\omega)$ respectively where $\omega \in [0, \infty]$. For a PI controller

$$C(s) = \frac{K_P s + K_I}{s} \tag{3.56}$$

where $K_P$ and $K_I$ are design parameters. Then taking $s = j\omega$

$$C(j\omega) = \frac{K_P(j\omega) + K_I}{j\omega} \tag{3.57}$$

Then, we have

$$|C(j\omega)|^2 = K_P^2 + \frac{K_I^2}{\omega^2} =: M^2 \tag{3.58}$$

and

$$\angle C(j\omega) = \arctan\left(\frac{-K_I}{\omega K_P}\right) := \Phi \tag{3.59}$$

Equations (3.58) and (3.59) can be written as

$$\frac{(K_P)^2}{a^2} + \frac{(K_I)^2}{b^2} = 1 \tag{3.60}$$

$$K_I = cK_P \tag{3.61}$$

where

$$a^2 = M^2 \tag{3.62}$$

$$b^2 = M^2\omega^2 \tag{3.63}$$

$$c = -\omega \tan \Phi \tag{3.64}$$

Thus constant $M$ loci are ellipses and constant phase loci are straight lines in $K_P$, $K_I$ space. The major and minor axes of the ellipse are given by the square roots of (3.62) and (3.63). The slope of the line is represented by $c$.

Suppose $\omega_g$ is the prescribed closed-loop gain crossover frequency. Then

$$M_g := \frac{1}{|G(e^{j\omega_g})|} = \frac{1}{|e^{-Lj\omega}||P(j\omega)|} \tag{3.65}$$

and by the identity

$$|e^{-x}| = |\cos x - j \sin x| \quad \text{and} \quad \cos^2 x + \sin^2 x = 1 \tag{3.66}$$

Then, (3.65) becomes

$$M_g := \frac{1}{|P(j\omega)|} \tag{3.67}$$

and if $\phi_g^*$ is the desired phase margin in radians,

$$\Phi_g := \pi + \phi_g^* - \angle G(e^{j\omega_g}). \tag{3.68}$$

In this case, we have that

$$\angle G(e^{j\omega_g}) = \angle \left[ e^{-jL\omega} P(e^{j\omega_g}) \right] = -L\omega + \angle P(j\omega) \tag{3.69}$$

Then (3.68) becomes

$$\Phi_g := \pi + \phi_g^* + L\omega - \angle P(j\omega) \tag{3.70}$$

From (3.60) and (3.61) we obtain the ellipse and straight lines corresponding to $M = M_g$ and $\Phi = \Phi_g$, giving the design point ($K_P^*$, $K_I^*$). If these intersection points lie in the stabilizing set $S$, the design is feasible, otherwise the specifications have to be altered.

### *3.4.2 PID Controllers*

Let $G(s)$ and $C(s)$ denote the plant and controller transfer functions. In this case, the plant includes a time-delay, tha is $G(s) = e^{-Ls}P(s)$, where $L > 0$ is the time-delay. The frequency response of the plant and controller are $e^{-Lj\omega}P(j\omega)$, $C(j\omega)$ respectively where $\omega \in [0, \infty]$. For a PID controller

$$C(s) = \frac{K_D s^2 + K_P s + K_I}{s}, \tag{3.71}$$

where $K_P$, $K_I$, and $K_D$ are design parameters. Then for $s = j\omega$

$$C(j\omega) = \frac{K_D(j\omega)^2 + K_P(j\omega) + K_I}{j\omega} \tag{3.72}$$

From (3.72), we have

$$|C(j\omega)|^2 = K_P^2 + \left(K_D\omega - \frac{K_I}{\omega}\right)^2 := M^2 \tag{3.73}$$

and

$$\angle C(j\omega) = \arctan\left(\frac{K_D\omega - \frac{K_I}{\omega}}{K_P}\right) := \Phi \tag{3.74}$$

from (3.73) and (3.74) we have that

$$K_P^2 = M^2 - \left(K_D\omega - \frac{K_I}{\omega}\right)^2 = \frac{\left(K_D\omega - \frac{K_I}{\omega}\right)^2}{\tan^2\Phi}. \tag{3.75}$$

From (3.75) we can have the following expressions

$$K_I = K_D\omega^2 \pm \omega\sqrt{\frac{M^2\tan^2\Phi}{1+\tan^2\Phi}} \tag{3.76}$$

$$K_P = \pm\sqrt{\frac{M^2}{1+\tan^2\Phi}} \tag{3.77}$$

Suppose $\omega_g$ is the prescribed closed-loop gain crossover frequency. Then

$$M_g := \frac{1}{|G(e^{j\omega_g})|} = \frac{1}{|e^{-Lj\omega}||P(j\omega)|} \tag{3.78}$$

and by the identity (3.66), (3.78) becomes

$$M_g := \frac{1}{|P(j\omega)|} \tag{3.79}$$

If $\phi_g^*$ is the desired phase margin in radians,

$$\Phi_g = \pi + \phi_g^* - \angle G(j\omega_g) \tag{3.80}$$

and by (3.69), (3.80) becomes

$$\Phi_g := \pi + \phi_g^* + L\omega - \angle P(j\omega) \tag{3.81}$$

Thus, for equation (3.76) is a straight line in $(K_I, K_D)$ plane for a constant value of $K_P$ represented in equation (3.77).

## 3.5 References

Part of the content of this section have been published in [2,3,5,6,83]. The results presented in this section have been implemented in a MATLAB code to graphically show the ellipses and straight lines for the case of First-Order and PI controllers and to show cylinder and plane for PID controllers. These plots and the stabilizing set will be used in the next sections to find a controller that will satisfy our design conditions.

# 4. ACHIEVABLE ROBUST PERFORMANCE FOR FIRST ORDER, PI, AND PID CONTROLLER DESIGN*

## 4.1 Introduction

In this section, the following is presented. First, the construction steps of the gain-phase margin achievable performance for First-Order, PI, and PID controllers in continuous and discrete-time systems is presented. Second, the procedure to select a simultaneous gain margin, phase margin, and gain crossover frequency specification is shown. Also, the controller design methodology to follow when designing a PI or PID controller achieving a desired gain-phase margin specification. Finally, different examples and a power electronics application are presented to illustrate the main results.

## 4.2 Construction of the Gain-Phase Margin Design Curves

The gain-phase margin design curves represent the actual achievable performance, regarding gain margin (GM), phase margin (PM), and gain crossover frequency ($\omega_g$)

*Part of this section is reprinted with permission from: ©2016 IEEE I. D. Díaz-Rodríguez and S. P. Bhattacharyya, "PI controller design in the achievable gain-phase margin plane," 2016 IEEE 55th Conference on Decision and Control (CDC), Las Vegas, NV, 2016, pp. 4919-4924. doi: 10.1109/CDC.2016.7799021.

*Part of this section is reprinted with permission from: ©2017 Elsevier I. D. Dıaz-Rodrıguez, S. Han, L. H. Keel, and S. P. Bhattacharyya, "Advanced Tuning for Ziegler-Nichols Plants," The 20th World Congress of the International Federation of Automatic Control (IFAC), 9-14 July, Toulouse, France, 2017. (Accepted for publication)

*Part of this section is reprinted with permission from: ©2015 IEEE I. D. Díaz-Rodríguez, "Modern design of classical controllers: Continuous-time first order controllers," IECON 2015 - 41st Annual Conference of the IEEE Industrial Electronics Society, Yokohama, 2015, pp. 000070-000075. doi: 10.1109/IECON.2015.7392967.

*Part of this section is reprinted with permission from: ©2015 IEEE I. D. Díaz-Rodríguez, V. A. Oliveira and S. P. Bhattacharyya, "Modern design of classical controllers: Digital PID controllers," 2015 IEEE 24th International Symposium on Industrial Electronics (ISIE), Buzios, 2015, pp. 1010-1015. doi: 10.1109/ISIE.2015.7281610.

for our system to accomplish with a PI, or PID controller. The procedure to construct these design curves is the following:

1. Set a range of PM $\phi_g^* \in [\phi_g^-, \phi_g^+]$ and gain crossover frequency $\omega_g \in [\omega_g^-, \omega_g^+]$.

2. For fixed values of $\phi_g^*$ and $\omega_g$, plot an ellipse and a straight line following the description in the methodology.

3. If the intersection point of the ellipse and straight line lies outside of the stabilizing set, then this point is rejected and go to step (2).

4. If the intersection of the ellipse and straight line is contained in the stabilizing set, it represents the design point with the PI, or PID controller gains $(K_P^*, K_I^*)$ or $(K_P^*, K_I^*, K_D^*)$ that satisfies the fixed $\phi_g^*$ and $\omega_g$.

5. Given the selected PI or PID controller gains $(K_P^*, K_I^*)$ or $(K_P^*, K_I^*, K_D^*)$, the upper and lower GM of the system are given by

$$GM_{upper} = \frac{K_P^{ub}}{K_P^*} \quad \text{and} \quad GM_{lower} = \frac{K_P^{lb}}{K_P^*} \tag{4.1}$$

   where $K_P^{ub}$ and $K_P^{lb}$ are the controller gains at the upper and lower boundary respectively of the stabilizing set following the straight line intersecting the ellipse.

6. Go to step 2 and repeat for all values of $\phi_g^*$ and $\omega_g$ in the ranges.

## 4.3 Construction of the Time-Delay Tolerance Design Curves

The time-delay tolerance design curves represent the actual achievable performance, regarding the time-delay, phase margin and gain crossover frequency for our

system to accomplish with a PI or PID controller. This set of design curves is an extension of the previous gain-phase design curves because we can use the information calculated before to create this new time-delay tolerance design set. The time-delay tolerance can be calculated as

$$\tau_{max} := \frac{PM}{\omega_g} \tag{4.2}$$

where $PM$ is the phase margin and $\omega_g$ is the gain crossover frequency in radians. Then, taking all the points calculated from the gain-phase margin design set, we can find the values of time-delay tolerance and express the new plot with the x-axis as phase margin and y-axis as time-delay tolerance. Similarly to gain-phase margin design curves, these time-delay tolerance curves are indexed by a fixed value of gain crossover frequency.

## 4.4 Simultaneous Specifications and Retrieval of Controller Gains From the Achievable Performance Set

The designer can select a desired point from the achievable performance Gain-Phase margin set and retrieve the controller gains corresponding to that simultaneous specification of desired GM, PM, and $\omega_g$. The controller gain retrieval process is the following.

(1) Select desired GM, PM, and $\omega_g$ from the achievable gain-margin set.

(2) For the specified point, construct the ellipse and straight line for a PI controller and a cylinder and plane for PID controller by using the selected PM and $\omega_g$ in the constant gain and constant phase loci.

(3) Take the intersection of the ellipse and straight line or cylinder and plane con-

tained in the stabilizing set. This will provide the gains $(K_P^*, K_I^*)$ or $(K_P^*, K_I^*, K_D^*)$.

(4) The controller that satisfies the prescribed margin specifications is $C_{PI}(s) = \frac{K_P^* s + K_I^*}{s}$ or $C_{PID}(s) = \frac{K_D^* s^2 + K_P^* s + K_I^*}{s}$.

For the case of retrieving the controller gains using the time-delay tolerance design curves, the procedure is the same. We can select a point from the time-delay tolerance design curves and use the value of phase margin and gain crossover frequency to compute the ellipse and straight line and find the intersection contained in the stabilizing set.

## 4.5 Controller Design Methodology

The PI or PID Controller design approach to satisfy a simultaneous specification of gain margin, phase margin, and gain crossover frequency for Linear Time-Invariant Single-Input Single-Output systems can be summarized as follows.

A. Computation of the PI or PID Stabilizing set.

B. Parametrization of a constant gain and phase loci.

C. Construction of the gain-phase margin design curves.

D. Selection of simultaneous gain margin, phase margin, and gain crossover frequency design specifications from the achievable performance set.

E. Retrieval of the PI or PID controller gains satisfying the design specifications.

## 4.6 Example 1a. Continuous-Time First Order Controller Design

Consider the system configuration as in Fig 4.1 with an unstable, non-minimum phase plant

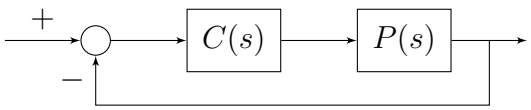


Figure 4.1: Unity Feedback Block Diagram

$$P(s) = \frac{s-2}{s^2+0.6s-0.1}, \qquad C(s) = \frac{x_1 s + x_2}{s + x_3} \tag{4.3}$$

### *4.6.1 Computation of the Stabilizing Set*

For the computation of the stabilizing set, we can refer to section 2.3.1. Considering $P(s)$ in (4.3), we get

$$\begin{aligned} N_E(s^2) &= -2 \\ N_O(s^2) &= 1 \\ D_E(s^2) &= s^2 - 0.1 \\ D_O(s^2) &= 0.6 \end{aligned} \tag{4.4}$$

For the two conditions to be satisfied described in (2.35) and (2.36). For $\omega = 0$ we have

$$-2x_2 - 0.1x_3 = 0 \tag{4.5}$$

Then, there exist a real root boundary at

$$x_2 = -0.05x_3 \tag{4.6}$$

For $\omega > 0$, using (2.39), (2.40), and (2.41) we have

$$\begin{aligned} x_1(\omega) &= \frac{(-\omega^2 - 0.1)x_3 - 2.6\omega^2 - 0.2}{\omega^2 + 4} \\ x_2(\omega) &= \frac{(-2.6\omega^2 - 0.2)x_3 + \omega^4 - 1.1\omega^2}{\omega^2 + 4} \end{aligned} \tag{4.7}$$

The stability region for $x_3 = 1$ and the curves and lines are shown in Fig 4.2. The regions numbered represent invariant root regions. Then, we can pick any value contained in the regions and check the roots. It was found that the region numbered 4 is the stabilizing zone. By sweeping $x_3$ from $-0.4$ to 8, we obtain the following

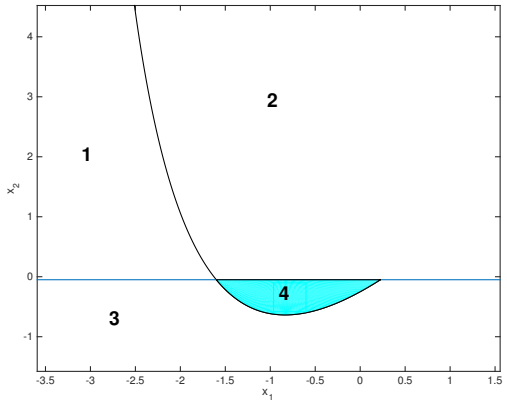


Figure 4.2: Root Invariant Regions for $x_3 = 1$ in Example 1a [2]

three dimensional figure shown in Fig 4.3. Which represents the stabilizing set for our plant $P(s)$ in (4.3).

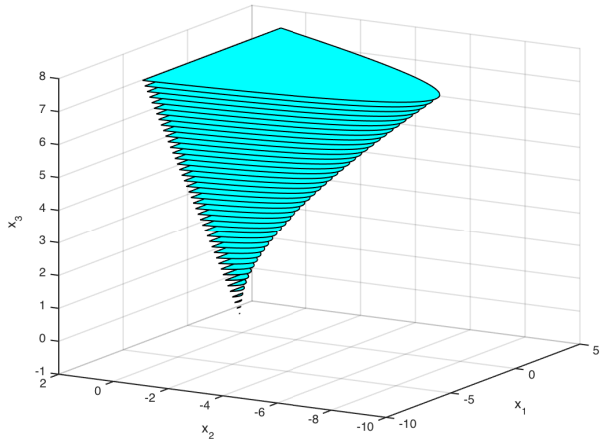


Figure 4.3: Stability Region for $-0.4 \leq x_3 \leq 8$ in Example 1a [2]

### *4.6.2 Construction of the Achievable Gain-Phase Margin Design Curves*

For the construction of the achievable Gain-Phase margin set in this example, the evaluated range of gain crossover frequencies $\omega_g \in [0.1, 2]$ and the range of phase margin $PM \in [1^o, 120^o]$. Using the ellipse and straight line intersection points, we can construct the achievable Gain-Phase margin set presented in Fig. 4.4.

### *4.6.3 Simultaneous Specifications and Retrieval of Controller Gains*

In Fig 4.4, we can see the achievable Gain-Phase margin set of curves indexed by fixed $\omega_g^*$ in different colors. Notice that the curves above the $10^0$ GM represent the upper GM and the curves below $10^0$ GM represent the lower GM. We notice that the maximum PM that we can get is $100^o$ for a $\omega_g = [0.3, 0.4, 0.5]$ rad/sec with a value of upper $GM = [2.68, 2.589, 2.446]$ and lower $GM = [0.9974, 0.9929, 0.9059]$ respectively. Another example of the values of GM and PM that we can get is the point with a PM of $40^o$ with an upper GM of 13.3 and a $\omega_g = 0.2$ rad/sec. However,

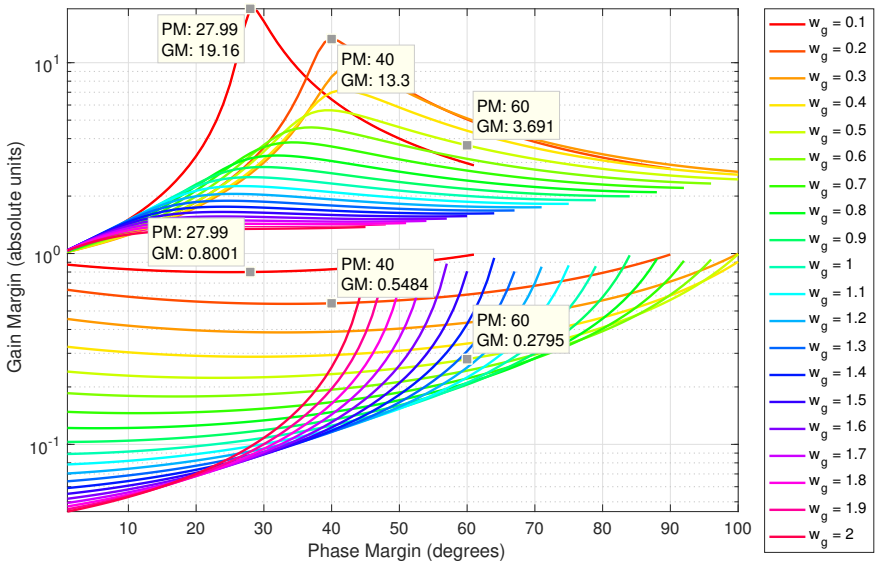


Figure 4.4: Achievable Performance in Terms of GM, PM, and $\omega_g$ for First Order Controller Design in Example 1a

for this value, we get a lower GM of 0.5484. We notice that for a bigger GM from the achievable Gain-Phase margin set, we get lower PM. At the end, the designer has the liberty to choose values for GM, PM, and $\omega_g$ that best suits his design needs.

Now, for illustration purposes, suppose that our desired phase margin specification is $PM = 60^o$, gain margin of $GM = 3.691$ with a gain crossover frequency of $\omega_g^* = 0.5\ rad/s$ from Fig 4.4 a fixed $x_3 = 8$. Then, taking these values for the constant gain and constant phase loci presented in section 3.3.1, we can find the intersection of an ellipse and straight line to get the controller gains, see Fig 4.5. Using (3.34) and (3.35), we have

$$\frac{L_0^2}{(14.3667)^2} + \frac{L_1^2}{(14.3667)^2} = 1 \tag{4.8}$$

and

$$L_1 = 0.6603L_0. \tag{4.9}$$

Using (3.39) we can find the values $x_1 = -2.158$ and $x_2 = -1.431$ for the controller gains.

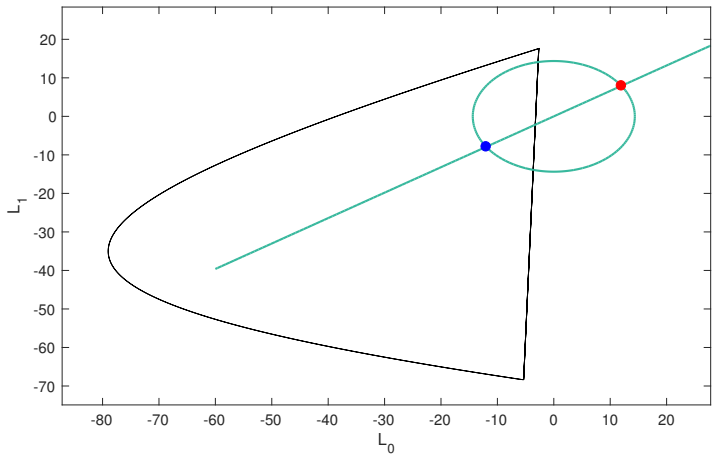


Figure 4.5: Intersection of the Ellipse and Straight Line Superimposed in the Stabilizing Set Corresponding to the GM, PM, and $\omega_g$ Specified in Example 1a.

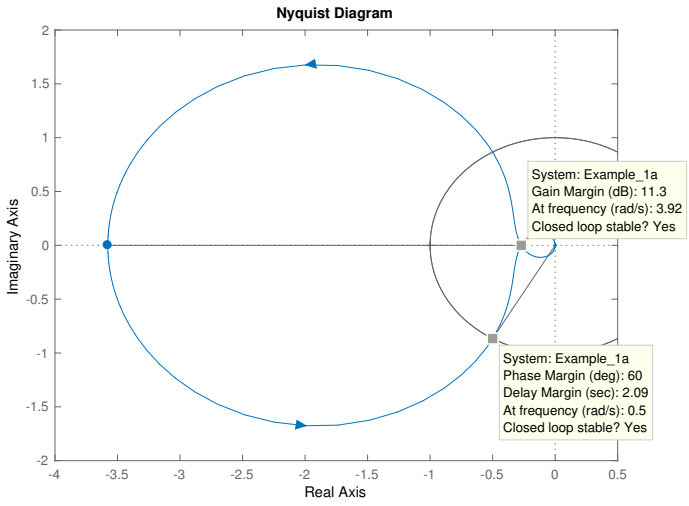


Figure 4.6: Nyquist Plot for $x_1 = -2.158$, $x_2 = -1.431$, and $x_3 = 8$ in the First Order Controller Design in Example 1a.

Then, our desired controller $C^*(s)$ to satisfy the specified phase margin, gain margin, and gain crossover frequency is

$$C^*(s)\frac{-2.158s - 1.431}{s + 8}. \tag{4.10}$$

In Fig 4.6, we can see the Nyquist plot for the controller gains selected. Here, we can see that those controller gains satisfy the desired performance specifications, $PM = 60^o$, $GM = 3.691$ (11.3 dB).

We can also compute the time-delay tolerance design curves. Following equation (4.2) and taking the values from Fig 4.4, we get Fig 4.7.

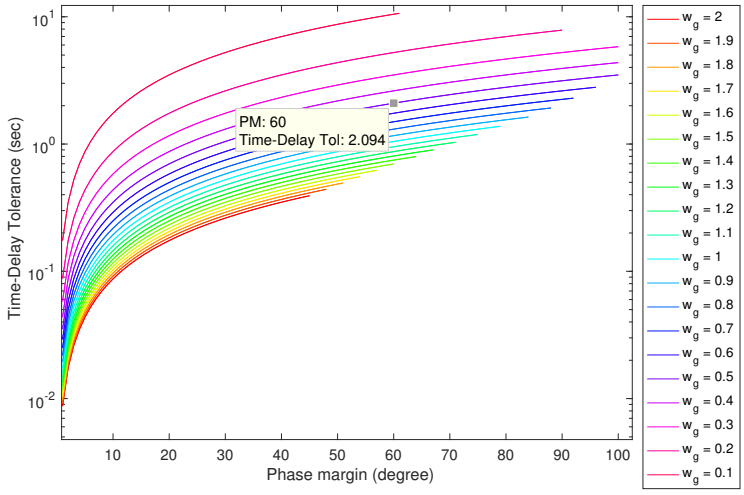


Figure 4.7: Time-Delay Tolerance Design Curves for Example 1a.

In Fig 4.7, we can see the achievable time-delay tolerance for the system using the proposed controller. We can select any point from the curves and retrieve the controller gains following the same procedure as taking a point from the gain-phase margin design curves. In this case, we selected the same $PM = 60^o$ and $\omega_g = 0.5$ rad/s. The time-delay tolerance is

$$\tau_{max} = 2.094 \ \ \text{sec} \tag{4.11}$$

For verification purposes, if we take this time-delay of $\tau_{max} = 2.094$ sec with the plant and the controller (4.10), we can show the Nyquist plot in Fig 4.8.

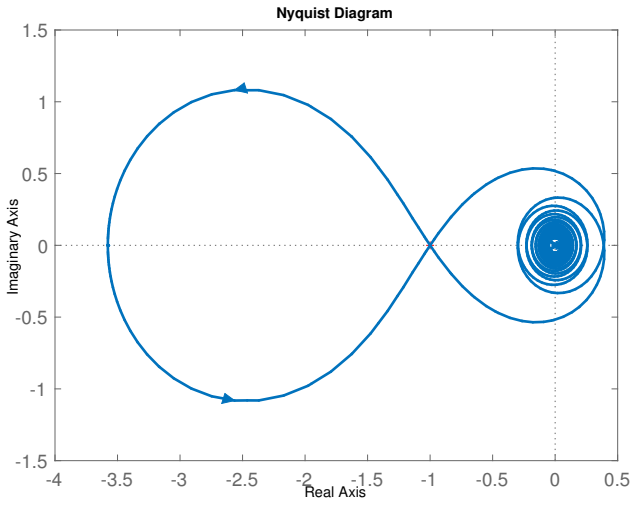


Figure 4.8: Nyquist Plot of the Controller and the Plant with $\tau_{max}$ for Example 1a.

We can see in Fig 4.8 that the Nyquist plot touches the -1 point, so encirclement cannot be done. The closed-loop system is unstable.

## 4.7 Example 2a. Continuous-Time PI Controller Design

Let us consider the continuous-time system represented in Fig 4.1 using the plant

$$P(s) = \frac{s-5}{s^2+1.6s+0.2} \tag{4.12}$$

and the controller

$$C(s) = \frac{K_P s + K_I}{s} \tag{4.13}$$

### *4.7.1 Computation of the Stabilizing Set*

The first step in the controller design is to obtain the stabilizing set of PI controllers for the given plant. Then, the closed-loop characteristic polynomial is

$$\delta(s, K_P, K_I) = s^3 + (K_P + 1.6)s^2 + (K_I - 5K_P + 0.2)s - 5K_I \tag{4.14}$$

Here $n = 2$, $m = 1$, and $N(-s) = -5 - s$. Therefore, we obtain

$$\begin{aligned} v(s) &= \delta(s, K_P, K_I)N(-s) \\ &= -s^4 - (6.6 + K_P)s^3 - (8.2 + K_I)s^2 + (25K_P - 1)s + 25K_I \end{aligned} \tag{4.15}$$

so that

$$\begin{aligned} v(j\omega, K_P, K_I) &= (-\omega^4 + (K_I + 8.2)\omega^2 + 25K_I) + j[(K_P + 6.6)\omega^3 + (25K_P - 1)\omega] \\ &= p(\omega) + jq(\omega) \end{aligned} \tag{4.16}$$

We find that $z^+ = 1$ so that the signature requirement on $v(s)$ for stability is,

$$n - m + 1 + 2z^+ = 4 \tag{4.17}$$

Since the degree of $v(s)$ is even (see (2.49)), we see from the signature formulas that $q(\omega)$ must have at least one positive real root of odd multiplicity. The range of $K_P$ such that $q(\omega, K_P)$ has at least one real, positive, distinct, finite zero with odd multiplicity was determined to be $K_P \in (-1.6, 0.04)$ which is the allowable range for $K_P$. By sweeping over different $K_P$ values within the interval $(-1.6, 0.04)$ and following the procedure summarized in the design methodology section, we can generate the

set of stabilizing $(K_P, K_I)$ values. This set is shown in Fig 4.9.

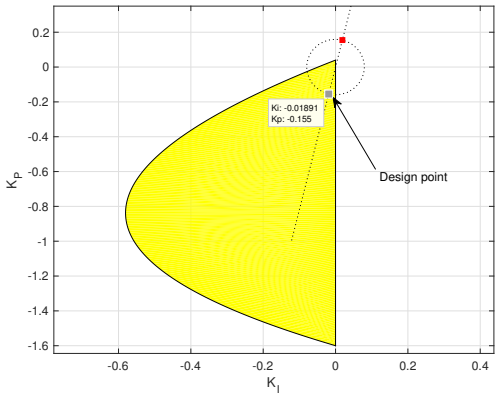


Figure 4.9: PI Stabilizing Set for Example 2a and Intersection of Ellipse and Straight Line for the Final Design Point [3]

### *4.7.2 Construction of the Achievable Gain-Phase Margin Design Curves*

Following the description in the Design Methodology, for a range of phase margins and gain crossover frequencies, we superimpose ellipses and straight lines on the stabilizing set (see Fig. 4.10).

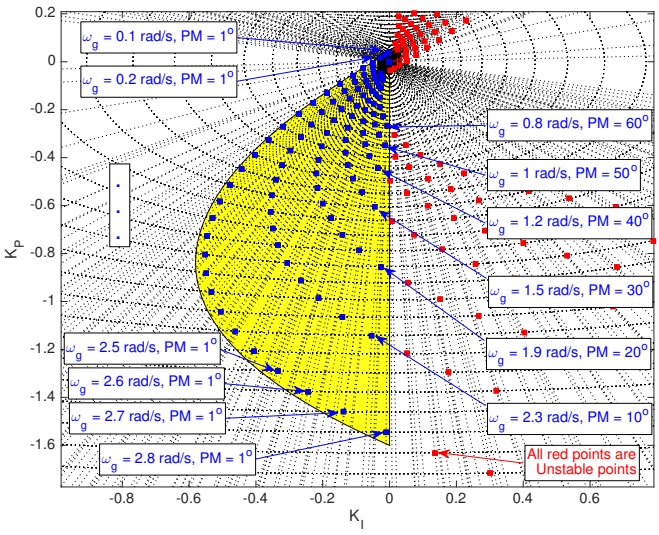


Figure 4.10: Construction of the Gain-Phase Margin Design Curves for PI controller Design in Example 2a by Intersection Points of Ellipses and Straight Lines [3]

We can see in Fig. 4.10 the intersection points of ellipses and straight lines for different values of phase margin and gain crossover frequency. We notice how for different values of phase margin, the gain crossover frequency limit is different. In this way, we obtain the maximum achievable values for the gain crossover frequency. For example, the maximum value of gain crossover frequency is 2.3 rad/s when considering a $PM = 10^o$ and a maximum gain crossover frequency of 0.8 rad/s when considering $PM = 60^o$. All the intersection points, contained in the stabilizing set, determine the PI controller gains and are used to construct the Gain-Phase design curves shown in Fig. 4.11. For this example, the evaluated range for phase margin is from $1^o$ to $90^o$ and the range for the gain crossover frequency is from 0.1 to 3 rad/s.

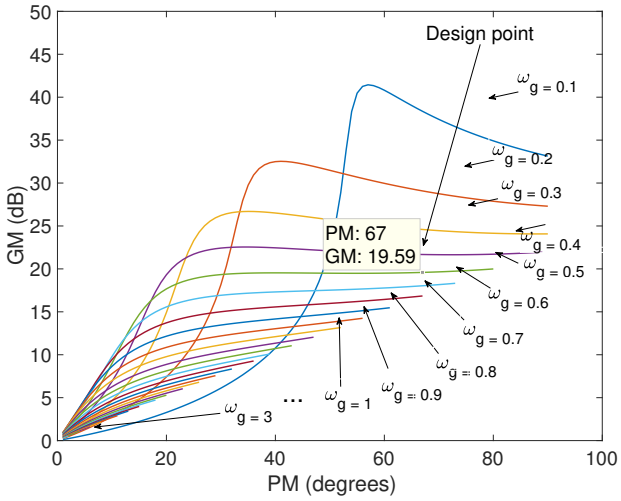


Figure 4.11: Achievable Gain-Phase Margin Design Curves in the Gain-Phase Plane for PI Controller Design in Example 2a [3]

### *4.7.3 Simultaneous Specifications and Retrieval of Controller Gains*

As shown in Fig 4.11, we can clearly see the achievable performance for example 1. In this case, the maximum gain margin that we can get is 41.44 dB. The phase margin, corresponding to this maximum gain margin, is of $57^o$ with a gain crossover frequency of 0.1 rad/s. We can see how increasing the gain crossover frequency leads to decrease in our values for gain and phase margins. For example, for a gain crossover frequency of 0.4 rad/s, the corresponding maximum gain margin we can get is 22.55 dB and the corresponding phase margin is $34^o$. In Fig 4.11, we have chosen a candidate design (called design point). The controller corresponding to this design specifications can be recovered by constructing the straight line and ellipse corresponding to these specifications (see Fig 4.9). The PI controller gains for these

specifications are

$$K_P^* = -0.1556 \tag{4.18}$$

$$K_I^* = -0.0189 \tag{4.19}$$

The step response for this controller is given in Fig 4.12. These controller gains correspond to the point of $\omega_g = 0.5$, $PM = 67^o$, and $GM = 19.6$ dB in the Gain-Phase Margin design plane (see the design point in Fig 4.11).

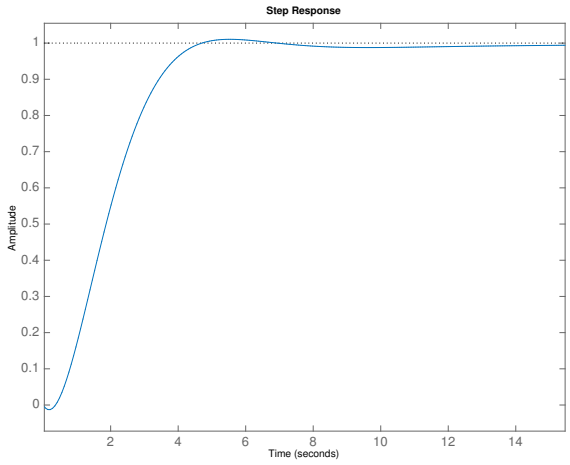


Figure 4.12: Step Response for the System in Example 2a Using the PI Controller Design $C(s)^* = \frac{K_P^* s + K_I^*}{s}$ [3]

In Fig 4.13, we can see the Nyquist plot for the controller gains selected. Here, we can see that those controller gains satisfy the desired performance specifications, $PM = 67^o$, $GM = 19.6dB$.

We can also compute the time-delay tolerance design curves. Following equation

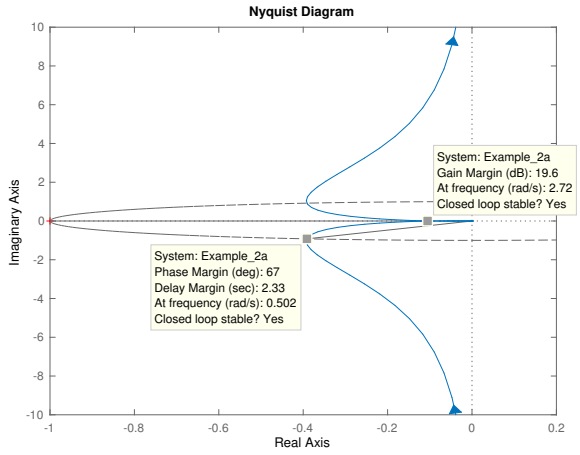


Figure 4.13: Nyquist Plot for $K_P = -0.1556$, $K_I = -0.0189$ in the PI Controller Design in Example 2a

(4.2) and taking the values from Fig 4.11, we get Fig 4.14.

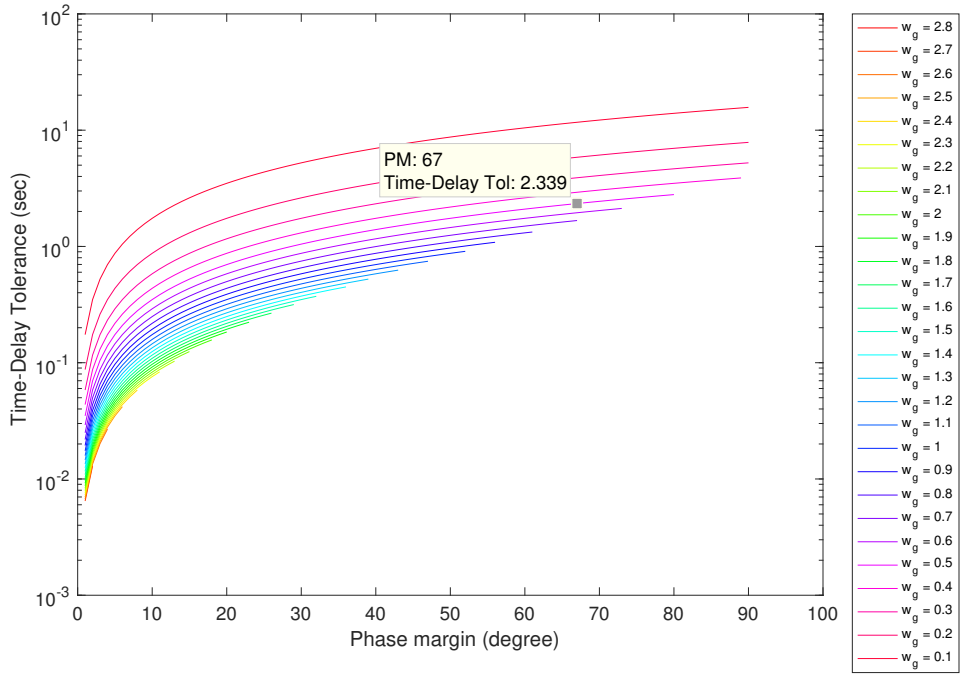


Figure 4.14: Time-Delay Tolerance Design Curves for Example 2a

In Fig 4.14, we can see the achievable time-delay tolerance for the system using the proposed controller. We can select any point from the curves and retrieve the controller gains following the same procedure as taking a point from the gain-phase margin design curves. In this case, we selected the same $PM = 67^o$ and $\omega_g = 0.5$ rad/s. The time-delay tolerance is

$$\tau_{max} = 2.339 \quad \text{sec} \tag{4.20}$$

For verification purposes, if we take this time-delay of $\tau_{max} = 2.339$ sec with the plant and the controller gains in (4.18) and (4.19), we can show the Nyquist plot in Fig 4.15.

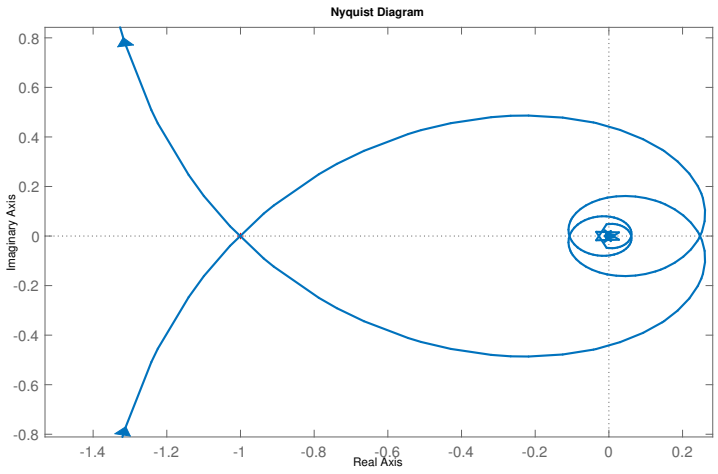


Figure 4.15: Nyquist Plot of the Controller and the Plant with $\tau_{max}$ for Example 2a

We can see in Fig 4.15 that the Nyquist plot touches the -1 point, so encirclement cannot be done. The closed-loop system is unstable.

## 4.8 Example 2b. Continuous-Time PI Controller Design

Let us consider the continuous-time LTI system represented in Fig 4.1 using the plant

$$P(s) = \frac{s^3 - 4s^2 + s + 2}{s^5 + 8s^4 + 32s^3 + 46s^2 + 46s + 17} \tag{4.21}$$

and the controller

$$C(s) = \frac{K_P s + K_I}{s} \tag{4.22}$$

#### *4.8.0.1 Computation of the Stabilizing Set*

We follow the procedure summarized in the Design Methodology section to compute the stabilizing set of PI controllers for the given plant. The closed-loop characteristic polynomial is

$$\begin{aligned}\delta(s, K_P, K_I) = {} & s^6 + 8s^5 + (K_P + 32)s^4 + (K_I - 4K_P + 46)s^3 \\ & + (K_P - 4K_I + 46)s^2 + (K_I + 2K_P + 17)s + 2K_I\end{aligned} \tag{4.23}$$

Here $n = 5$, $m = 3$, and $N(-s) = -s^3 - 4s^2 - s + 2$. Therefore, we obtain

$$
\begin{aligned}
v(s) &= \delta(s, K_P, K_I)N(-s) \\
&= -s^9 - 12s^8 + (-K_P - 65)s^7 + (-K_I - 180)s^6 \\
&+ (14K_P - 246)s^5 + (14K_I - 183)s^4 + (-17K_P - 22)s^3 \\
&+ (75 - 17K_I)s^2 + (4K_P + 34)s + 4K_I
\end{aligned} \tag{4.24}
$$

so that

$$
\begin{aligned}
v(j\omega, K_P, K_I) &= -12\omega^8 + (K_I + 180)\omega^6 + (14K_I - 183)\omega^4 + (17K_I - 75)\omega^2 \\
&+ 4K_I \\
&+ j[-\omega^9 + (K_P + 65)\omega^7 + (14K_P - 246)\omega^5 + (17K_P + 22)\omega^3 \\
&+ (4K_P + 34)\omega] \\
&= p(\omega) + jq(\omega)
\end{aligned} \tag{4.25}
$$

We find that $z^+ = 2$ so that the signature requirement on $v(s)$ for stability is,

$$
n - m + 1 + 2z^+ = 7 \tag{4.26}
$$

Since the degree of $v(s)$ is odd, we see from the signature formulas (see (2.50)) that $q(\omega)$ must have at least three positive real root of odd multiplicity. The range of $K_P$ such that $q(\omega, K_P)$ has at least one real, positive, distinct, finite zero with odd multiplicity was determined to be $K_P \in (-8.5, 4.2)$ which is the allowable range for $K_P$. By sweeping over different $K_P$ values within the interval $(-8.5, 4.2)$ and following the procedure summarized in the design methodology section, we can generate the

set of stabilizing $(K_P, K_I)$ values. This set is shown in Fig 4.16.

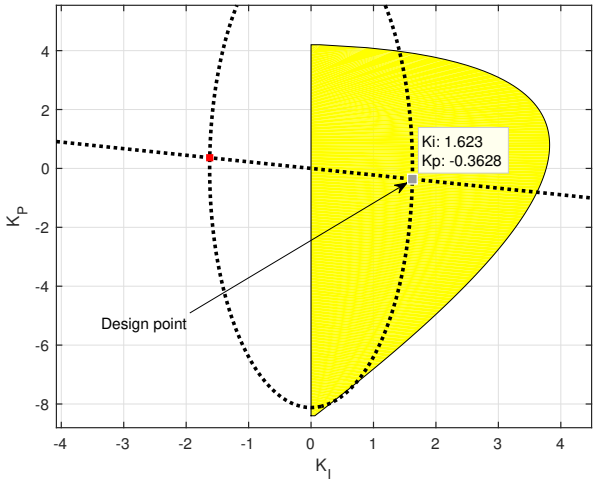


Figure 4.16: PI Stabilizing Set for Example 2b and Intersection of Ellipse and Straight Line for the Final Design Point [3]

### *4.8.1 Construction of the Achievable Gain-Phase Margin Design Curves*

As mentioned in Example 2a, for a range of phase margins and gain crossover frequencies, we superimpose ellipses and straight lines on the stabilizing set. All the intersection points, contained in the stabilizing set, determine the PI controller gains to construct the Gain-Phase design curves shown in 4.17. For this example, the evaluated range for phase margin is from $1^o$ to $90^o$ and the range for the gain crossover frequency is from 0.1 to 1 rad/s.

### *4.8.2 Simultaneous Specifications and Retrieval of Controller Gains*

As shown in Fig 4.17, we notice the achievable performance for example 2. In this case, the maximum gain margin that we can get is 13.13 dB. The phase margin,

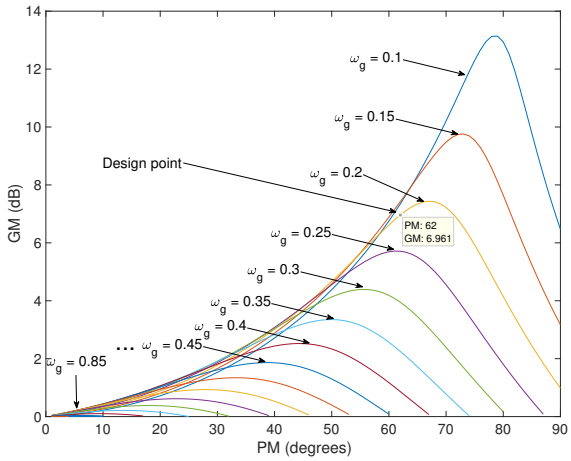


Figure 4.17: Achievable Gain-Phase Margin Design Curves in the Gain-Phase Plane for Example 2b [3]

corresponding to this maximum gain margin, is $79^o$ with a gain crossover frequency of 0.1 rad/s. We can see how when increasing the gain crossover frequency, our values for gain and phase margins decrease. For example, for a gain crossover frequency of 0.4 rad/s, the maximum gain margin we can get is 2.522 dB and the corresponding phase margin is $44^o$. In Fig 4.17, we have chosen a candidate design (called design point). The controller corresponding to this design specification can be recovered by constructing the straight line and ellipse corresponding to these specifications (see Fig. 4.16). The PI controller gains for these specifications are

$$K_P^* = -0.36283 \tag{4.27}$$

$$K_I^* = 1.6228 \tag{4.28}$$

The step response for this controller is given in Fig 4.18. These controller gains correspond to the point $\omega_g = 0.2$, $PM = 62^o$, and $GM = 6.96$ dB in the Gain-Phase Margin design plane (see the design point in Fig 4.17).

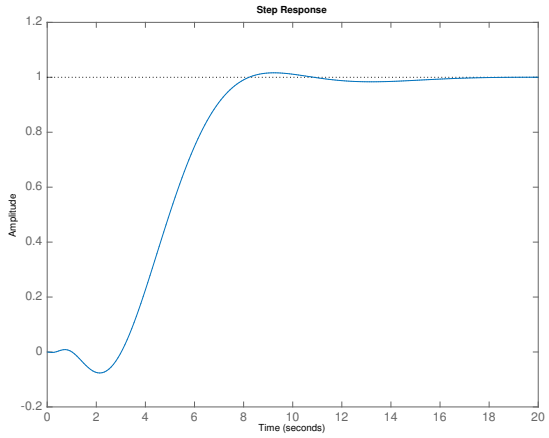


Figure 4.18: Step Response for the System in Example 2b Using $C(s)^* = \frac{K_P^* s + K_I^*}{s}$ [3]

In Fig 4.19, we can see the Nyquist plot for the controller gains selected. Here, we can see that those controller gains satisfy the desired performance specifications, $PM = 62^o$, $GM = 6.96dB$.

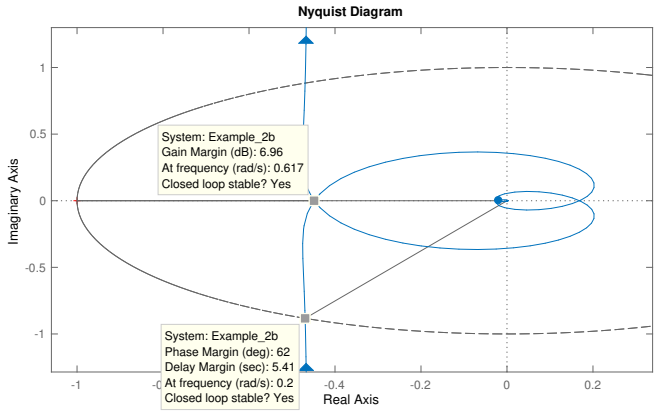


Figure 4.19: Nyquist Plot for $K_P = -0.36283$, $K_I = 1.6228$ in the PI Controller Design in Example 2b

We can also compute the time-delay tolerance design curves. Following equation (4.2) and taking the values from Fig 4.17, we get Fig 4.20.

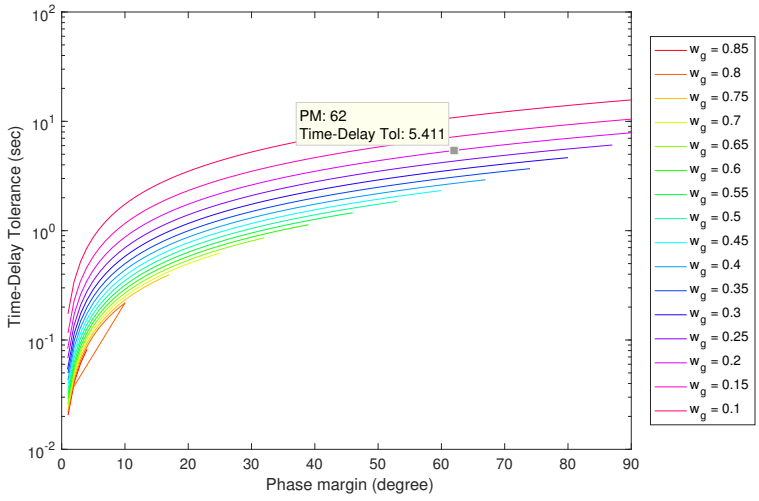


Figure 4.20: Time-Delay Tolerance Design Curves for Example 2b

In Fig 4.20, we can see the achievable time-delay tolerance for the system using the proposed controller. We can select any point from the curves and retrieve the controller gains following the same procedure as taking a point from the gain-phase margin design curves. In this case, we selected the same $PM = 62^o$ and $\omega_g = 0.2$ rad/s. The time-delay tolerance is

$$\tau_{max} = 5.411 \quad \text{sec} \tag{4.29}$$

For verification purposes, if we take this time-delay of $\tau_{max} = 5.411$ sec with the plant and the controller gains in (4.27) and (4.28), we can show the Nyquist plot in Fig 4.21.

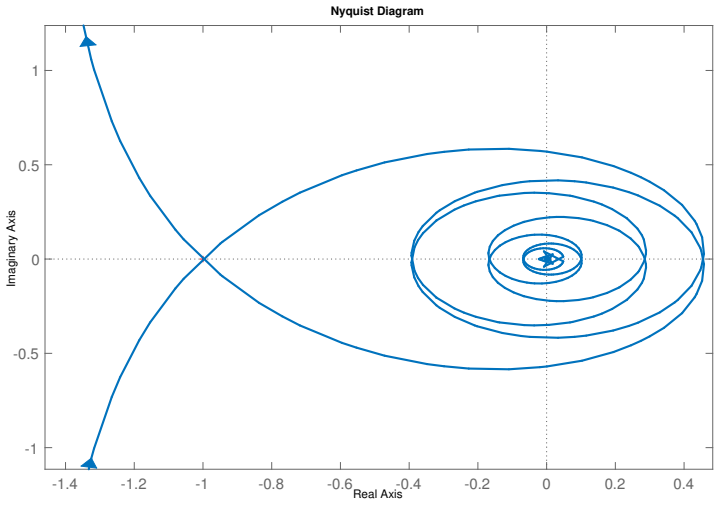


Figure 4.21: Nyquist Plot of the Controller and the Plant with $\tau_{max}$ for Example 2b.

We can see in Fig 4.21 that the Nyquist plot touches the -1 point, so encirclement cannot be done. The closed-loop system is unstable.

## 4.9 Example 2c. Discrete-Time PI Controller Design

Consider the discrete-time system represented in Fig. 4.22, with

$$P(z) = \frac{z - 0.1}{z^3 + 0.1z - 0.25} \quad \text{and} \quad C(z) = \frac{K_0 + K_1 z}{z - 1} \tag{4.30}$$

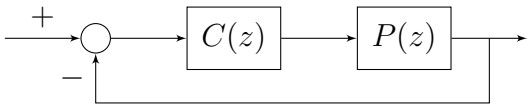


Figure 4.22: Unity Feedback Block Diagram

### *4.9.1 Computation of the Stabilizing Set*

Using the Tchebyshev representation with $\rho = 1$, we have

$$\begin{aligned}
T_N(\nu) &= -\nu - 0.1, \\
U_N(\nu) &= 1, \\
T_D(\nu) &= -4\nu^3 + 2.9\nu - 0.25, \\
U_D(\nu) &= 4\nu^2 - 0.9, \\
P_1(\nu) &= 0.4\nu^3 + 2\nu^2 - 0.04\nu - 0.875, \\
P_2(\nu) &= 0.34 - 0.4\nu^2 - 2\nu, \\
P_3(\nu) &= 0.2\nu + 1.01
\end{aligned} \tag{4.31}$$

Then, we have

$$T(\nu, K_0, K_1) = -0.8\nu^4 - 4.4\nu^3 - (1.22 + 0.2K_1)\nu^2 + (2.915 - 1.01K_1 + 0.2K_0)\nu + (0.535 + 1.01K_0),$$

$$U(\nu, K_1) = 0.8\nu^3 + 4.4\nu^2 + (1.62 + 0.5K_1)\nu + (-1.215 + 1.01K_1) \tag{4.32}$$

Since $P(z)$ is of order 3 and $C(z)$, the PI controller, is of order 1, the number of roots of $\delta(z)$ inside the unit circle is required to be 4 for stability. Then

$$i_1 - i_2 = \underbrace{(i_\delta + i_{N_r})}_{i_1} - \underbrace{l}_{i_2} = 3 \tag{4.33}$$

where $i_\delta$ and $i_{N_r}$ are the number of roots of $\delta(z)$ and the reverse polynomial of $N(z)$, respectively, and $l$ is the order of $N(z)$. Since the required $i_\delta$ is 4, $i_{N_r} = 0$, and $l = 1$, $i_1 - i_2$ is required to be 3. Therefore, we require two real roots from $U(\nu, K_1)$ to satisfy the stability condition. We can find the feasible range for $K_1$, so we can find these two required roots. For this example, the range taken in consideration is $K_1 \in [-0.94, 1.415]$. Following the stabilizing set procedure for the range of $K_1$, we obtain the stability region shown in Fig. 4.23 in $(K_0, K_1)$ space. To illustrate the example in detail, we fix $K_1 = 1$.Then, the real roots of $U(\nu, K_1)$ in $(-1, +1)$ are $-0.5535$ and $0.0919$. Furthermore, $Sgn[U(-1)] = +1$, and $i_1 - i_2 = 3$ requires that

$$\frac{1}{2}Sgn[U(-1)] \quad (Sgn[T(-1)] - 2Sgn[T(-0.5535)] + 2Sgn[T(0.0919)] - Sgn[T(1)]) = 3 \tag{4.34}$$

Here, the only valid sequence satisfying the last equations is

$$\begin{aligned} Sgn[T(-1)] = +1, \quad Sgn[T(-0.5535)] = -1 \\ Sgn[T(0.0919)] = +1, \qquad\qquad Sgn[T(1)] = -1 \end{aligned} \tag{4.35}$$

Corresponding to this sequence, we have the following set of linear inequalities:

$$\begin{aligned} K_0 > -1, \qquad\qquad & K_0 < 0.3151 \\ K_0 > -0.6754 \qquad\qquad & K_0 < 3.4545 \end{aligned} \tag{4.36}$$

This set of inequalities characterizes the stability region in $K_0$ space for a fixed $K_1 = 1$. By repeating this procedure for the range of $K_1$, we obtain the stability region shown in Fig. 5.4 in $(K_0, K_1)$ space.

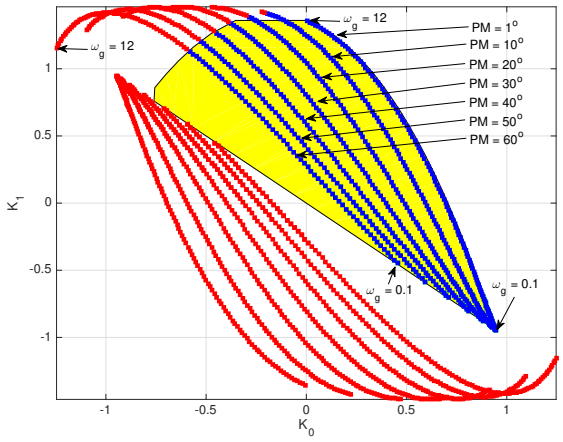


Figure 4.23: Stabilizing Set in Yellow and Intersection Points of Ellipses and Straight Lines in $(K_0, K_1)$ Plane for $PM \in [1, 60]$ Degree and $\omega_g \in [0.1, 12]$ rad/s for the Discrete-Time PI Controller in Example 2c

### *4.9.2 Construction of the Achievable Gain-Phase Margin Design Curves*

In Fig 4.24 we can see an example of selecting a specific phase margin ($PM = 60^o$) for a range of gain crossover frequencies. In Fig 4.23, we can see the intersection points of ellipses and straight lines superimposed in the stabilizing set. In this case, the range of gain crossover frequency is from 0 to 12 rad/s and for phase margins of $PM$ from 1 to 60 degree.

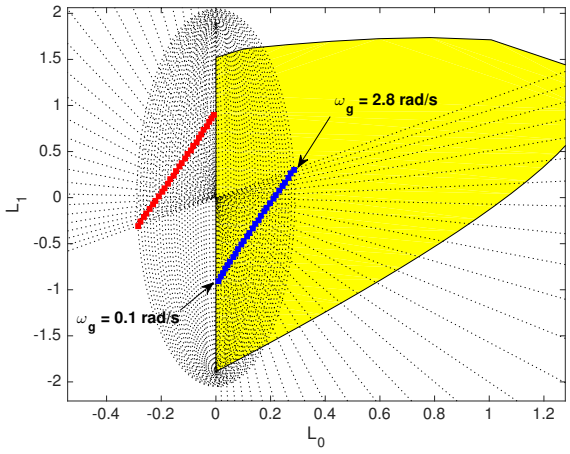


Figure 4.24: Stabilizing Set in Yellow and Intersection Points of Ellipses and Straight Lines in $(L_0, L_1)$ Plane for $PM = 60^o$ and $\omega_g \in [0.1, 2.8]$ rad/s. for the Discrete-Time PI Controller in Example 2c

### *4.9.3 Simultaneous Specifications and Retrieval of Controller Gains*

In Fig 4.25, we can see the achievable performance for the example. In this case, the maximum gain margin that we can get is 35 dB with a phase margin of $88^o$ with a gain crossover frequency of 0.1 rad/s. The Gain-Phase plane contains information

about the capabilities of the system achieving gain margin, phase margins and gain crossover frequency simultaneously. Also, it shows the limitations of the system associated with the use of a PI controller.

We can select a Design point from Fig 4.25. After selecting the point, this Design point is found by the intersection of the ellipse and straight line contained in the stabilizing set shown in Fig 4.24. In this case, we selected a Design point having $PM = 68^o$, $GM = 13.56$ dB, and $\omega_g = 2.3$ rad/s. The PI controller gains for these specifications are

$$K_0^* = -0.06349, \qquad K_1^* = 0.2912 \tag{4.37}$$

These controller gains correspond to the point of $\omega_g = 2.3$, $PM = 68^o$, and $GM = 13.56$ dB in the Gain-Phase Margin design plane. The step response for these controller gains is given in Fig 4.26.

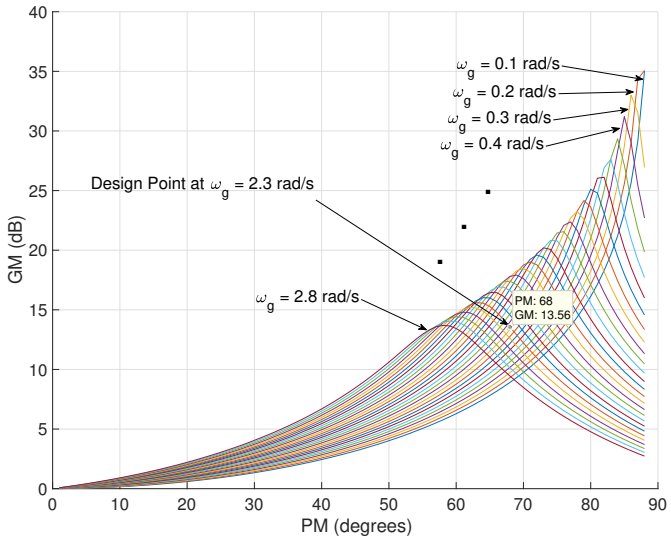


Figure 4.25: Achievable Gain-Phase Margin Design Curves in the Gain-Phase Plane for $\omega_g \in [0.1, 2.8]$ rad/s and $PM \in [0, 90]$ Degrees for the Discrete-Time PI Controller in Example 2c

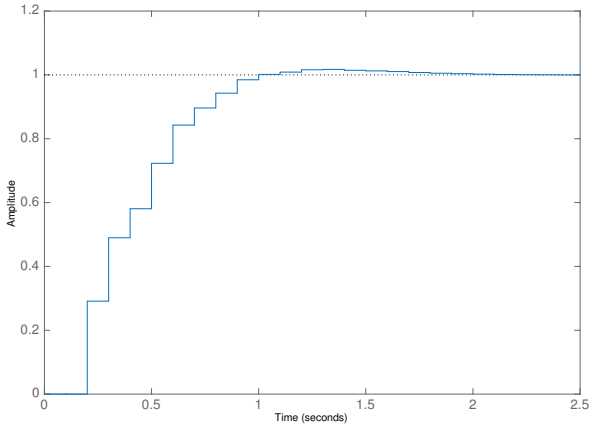


Figure 4.26: Step Response with $C^*(z) = \frac{K_1^* z + K_0^*}{z-1}$ in the Example 2c

In Fig 4.27, we can see the Nyquist plot for the controller gains selected. Here, we can see that those controller gains satisfy the desired performance specifications, $PM = 68^o$, $GM = 13.56$.

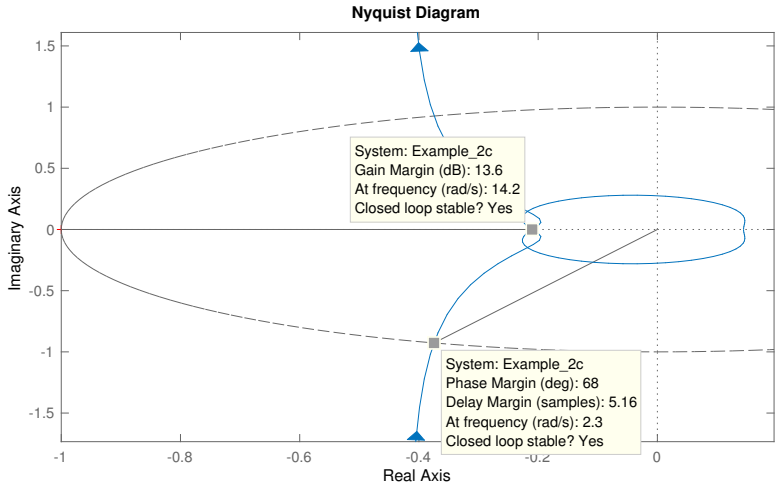


Figure 4.27: Nyquist Plot for $K_0 = -0.06349$, $K_1 = 0.2912$ in the PI Controller Design in Example 2c

## 4.10 Example 2d. Continuous-Time PI Controller Design Power Electronics Application

In this section we apply the special case of the first order controller $C(s) = (x_1 s + x_2)/(s + x_3)$ when $x_3 = 0$ (PI controller) design approach to a single-phase voltage source inverter application provided in Section 2 of the book [4]. Fig. 4.28 shows the half-bridge voltage source inverter. In this application, an ideal voltage source $V_{DC}$ is considered. Also, the power switches plus diode couple are assumed to behave like an ideal switch, i.e., one whose voltage is zero in the "on" state and

whose current is zero in the "off" state. Moreover, it is assumed that the change from the "on" state to the "off" state and vice versa takes place in zero time. The load will be described as the series connection of a resistor $R_S$, an inductor $L_S$, and a voltage source $E_S$, which can be either dc or ac. The control problem considered in

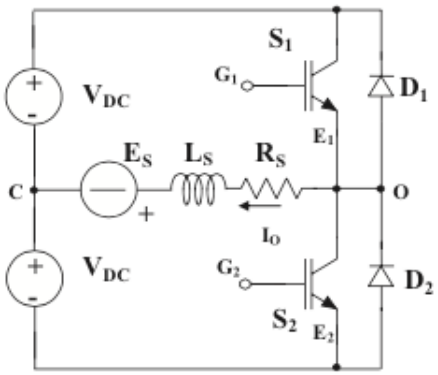


Figure 4.28: Half-Bridge Source Inverter for Example 2d [4]

this application is the linear regulation of the output current $I_O$ of the voltage source inverter. In Fig. 4.29 we have a block diagram of the system to be considered. In this example the purpose of the voltage source inverter is to deliver a given amount of output power $P_O$ the load and of the inverter inductor. This can be difficult in typical ac motor drive applications, where a sinusoidal current of suitable amplitude and given frequency, $f_O$, must be generated on each motor phase. Consequently, it has been taken into account the presence of a current transducer, whose gain, $G_{TI}$, is given. In the block diagram, the controller to be considered is a Proportional-Integral control. The output of the regulator represents the modulating signal that drives the pulse width modulator. In this PWM block, a time delay has been considered, this has been replaced with a Pade approximation. Then we have the inverter and

load models and a typical implementation of a transducer gain.

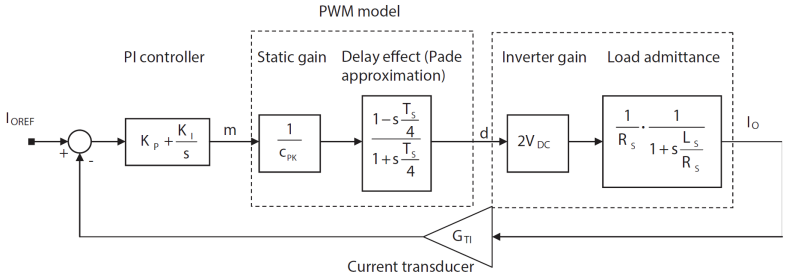


Figure 4.29: Control Block Diagram for Example 2d [4]

### *4.10.1 Stabilizing Set Based Design of PI Current Controller*

First, the open loop transfer function to be considered is the following:

$$\begin{aligned} G_{OL}(s) &= C(s)P(s) \\ G_{OL}(s) &= \left(K_P + \frac{K_I}{s}\right) \frac{2V_{DC}}{C_{PK}} \frac{1 - s\frac{T_S}{4}}{1 + s\frac{T_S}{4}} \frac{G_{TI}}{R_S} \frac{1}{1 + s\frac{L_S}{R_S}} \end{aligned} \tag{4.38}$$

where $V_{DC} = 250\ (V)$, $C_{PK} = 4\ (V)$, $Ts = 0.00002\ (sec)$, $G_{TI} = 0.1\ (V/A)$, $R_S = 1\ (\Omega)$, $L_S = 1.5\ (mH)$. We will consider the notation of the PI controller in (4.38) to be $x_1 := K_P$, $x_2 := K_I$, and $x_3 = 0$ for our special case of first order controller. We have

$$G_{OL}(s) = \left(\frac{x_1 s + x_2}{s}\right) \frac{-6.25 \times 10^{-5} s + 12.5}{7.5 \times 10^{-9} s^2 + 0.0015 s + 1} \tag{4.39}$$

The closed-loop characteristic polynomial is

$$\begin{aligned}\delta(s, x_1, x_2) =& 7.5 \times 10^{-9} s^3 + (0.0015 - 6.25 \times 10^{-5} x_1) s^2 \\ &+ (12.5 x_1 - 6.25 \times 10^{-5} x_2 + 1) s + 12.5 x_2 \end{aligned} \tag{4.40}$$

Here $n = 2$, $m = 1$, and $N(-s) = 12.5 + 6.25 \times 10^{-5} s$. Therefore, we obtain

$$\begin{aligned} v(s) &= \delta(s, x_1, x_2) N(-s) \\ &= 4.69 \times 10^{-13} s^4 + (1.87 \times 10^{-7} - 3.91 \times 10^{-9} x_1) s^3 \\ &+ (0.0188 - 3.91 \times 10^{-9} x_2) s^2 + (156 x_1 + 12.5) s + 156 x_2 \end{aligned} \tag{4.41}$$

so that

$$\begin{aligned} v(j\omega, x_1, x_2) &= 4.69 \times 10^{-13} \omega^4 + (3.91 \times 10^{-9} x_2 - 0.0188) \omega^2 + 156 x_2 \\ &+ j[(3.91 \times 10^{-9} x_1 - 1.87 \times 10^{-7}) \omega^3 + (156 x_1 + 12.5) \omega] \\ &= p(\omega) + j q(\omega) \end{aligned} \tag{4.42}$$

We find that $z^+ = 1$ so that the signature requirement on $v(s)$ for stability is,

$$n - m + 1 + 2z^+ = 4 \tag{4.43}$$

Since the degree of $v(s)$ is even, we see from the signature formulas that $q(\omega)$ must have at least one positive real root of odd multiplicity. The range of $x_1$ such that $q(\omega, x_1)$ has at least one real, positive, distinct, finite zero with odd multiplicities was determined to be $x_1 \in (-0.08, \infty)$. However, the range for which we can get a region is given by $x_1 \in (-0.08, 24)$ the allowable range for $x_1$. By sweeping over different $x_1$

values within the interval $(-0.08, 24)$, we can generate the set of stabilizing $(x_1, x_2)$ values. This set is shown in Fig 4.30.

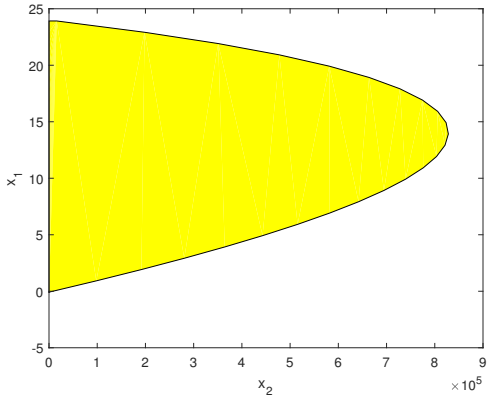


Figure 4.30: Stability Region for $-0.08 \leq x_1 \leq 24$ in Example 2d

### *4.10.2 Construction of the Achievable Gain-Phase Margin Design Curves*

For the construction of the achievable Gain-Phase margin set for the PI controller design case, the evaluated range of $\omega_g$ is $[1000, 69000]$ and the range for PM is from $1^o$ to $120^o$. For the PI case, using the constant gain and constant phase loci equations, (3.44) and (3.45) we now get an ellipse and a straight line in the $(x_1, x_2)$ space, respectively. The intersection $(x_1, x_2)$ superimposed in the stabilizing set represents the PI controller gains that satisfy the PM and $\omega_g$. Evaluating the range of PM and $\omega_g$, we can construct the achievable Gain-Phase margin set represented in Fig. 4.31.

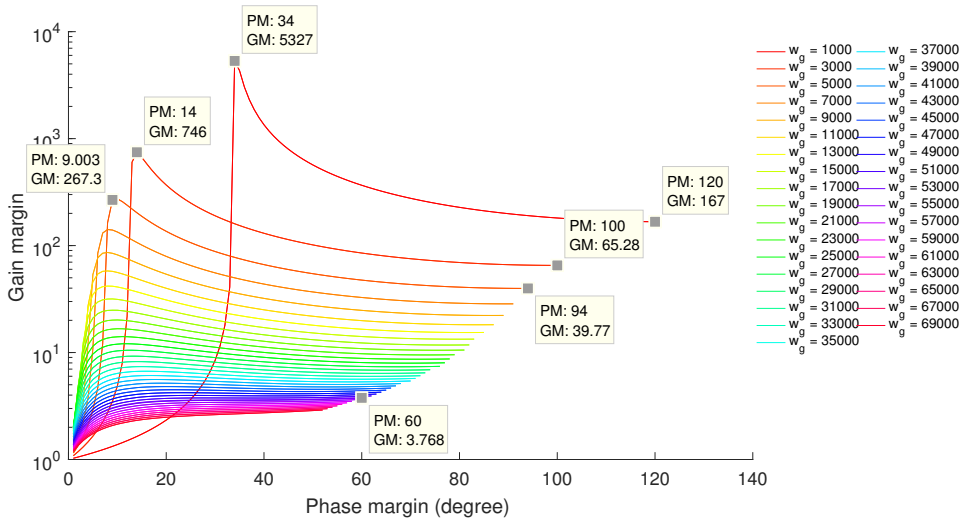


Figure 4.31: Achievable Performance in Terms of GM, PM, and $\omega_g$ for PI controller Design in Example 2d

### *4.10.3 Simultaneous Specifications and Retrieval of the Controller Gains*

In Fig. 4.31, we can see the achievable Gain-Phase margin set of curves indexed by fixed $\omega_g$ in different colors. Notice that we can get more GM and PM for lower values of $\omega_g$. For example, for $\omega_g = 1000$ rad/sec, the maximum GM that we can get is 5327 with a PM of $34^o$. For $\omega_g = 3000$ rad/sec, the maximum GM is 746 with a $PM = 14^o$. The designer has the liberty to choose values for GM, PM, and $\omega_g$ that best suits his design needs.

After the selection of simultaneous GM, PM, and $\omega_g$ from the achievable gain-phase margin set, the designer can retrieve the controller gains corresponding to the point. For illustration purposes, let us say that the desired performance values chosen for this example are a PM of $60^o$, GM of 3.768, and a $\omega_g$ of 53000 rad/s (see Fig 4.31). Then, taking these values and the constant gain and constant phase loci for PI controllers presented in the methodology, we can find the intersection of the

ellipse and the straight line in the $(x_1, x_2)$ space shown in Fig 4.32. The controller gains are

$$x_1^* = 6.34 \tag{4.44}$$

$$x_2^* = 5812 \tag{4.45}$$

In Fig 4.33 we can see the Nyquist plot for the controller gains selected. Here, we can see that those controller gains satisfy the desired performance specifications, $PM = 60^o$, $GM = 3.7681$ (11.5 dB).

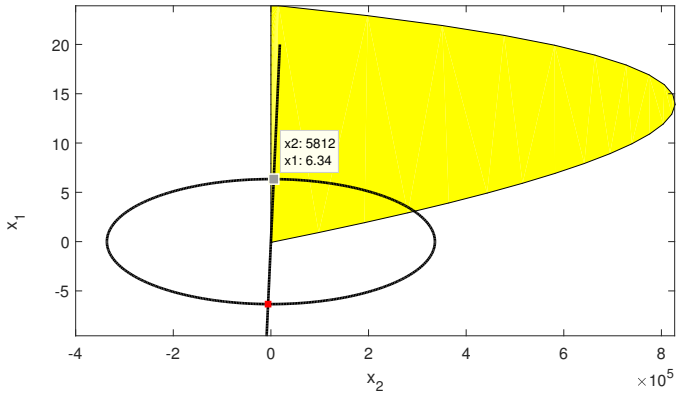


Figure 4.32: Ellipse and Straight Line Superimposed in the PI Controller Stabilizing Set in Example 2d

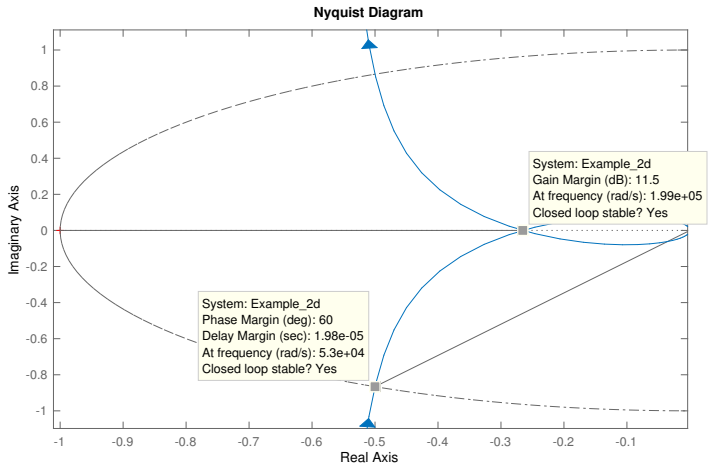


Figure 4.33: Nyquist Plot for $x_1^* = 6.34$, $x_2^* = 5812$ in the PI Controller Design in Example 2d

We can also compute the time-delay tolerance design curves. Following equation (4.2) and taking the values from Fig 4.31, we get Fig 4.34.

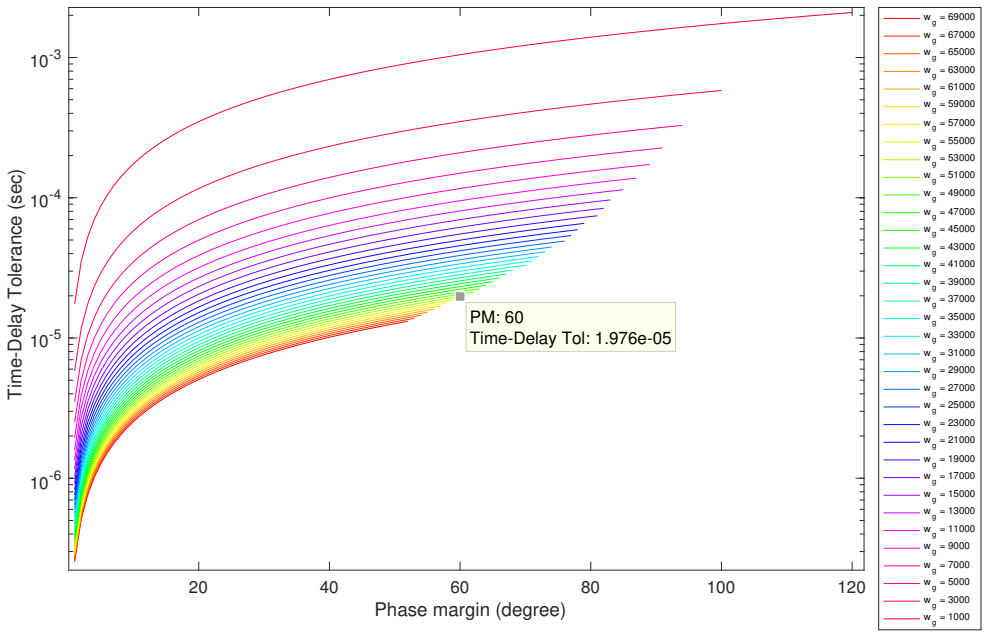


Figure 4.34: Achievable Performance in Terms of Time-Delay Tolerance, PM, and $\omega_g$ for PI Controller Design in Example 2d

In Fig 4.34, we can see the achievable time-delay tolerance for the system using the proposed controller. We can select any point from the curves and retrieve the controller gains following the same procedure as taking a point from the gain-phase margin design curves. In this case, we selected the same $PM = 60^o$ and $\omega_g = 53000$ rad/s. The time-delay tolerance is

$$\tau_{max} = 1.976 \text{ x } 10^{-5} \text{ sec} \tag{4.46}$$

For verification purposes, if we take this time-delay of $\tau_{max} = 1.976$ x $10^{-5}$ sec with the plant and the controller gains in (4.44) and (4.45), we can show the Nyquist plot in Fig 4.35.

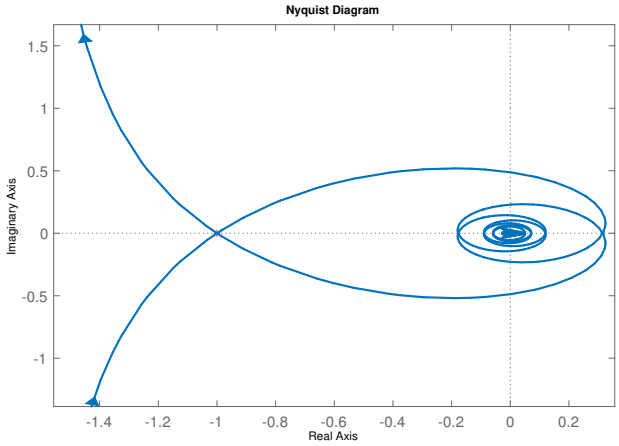


Figure 4.35: Nyquist Plot of the Controller and the Plant with $\tau_{max}$ for Example 2d

We can see in Fig 4.35 that the Nyquist plot touches the -1 point, so encirclement cannot be done. The closed-loop system is unstable.

## 4.11 Example 3a. Continuous-Time PID Controller Design

Let us consider the continuous-time LTI system represented in Fig 4.1 using the plant

$$P(s) = \frac{s-3}{s^3+4s^2+5s+2} \tag{4.47}$$

and the controller

$$C(s) = \frac{K_D s^2 + K_P s + K_I}{s} \tag{4.48}$$

### *4.11.1 Computation of the Stabilizing Set*

We follow the procedure summarized in the Design Methodology section to compute the stabilizing set of PID controllers for the given plant. The closed-loop characteristic polynomial is

$$\delta(s, K_P,K_I) = s^4 + (K_D + 4)s^3 + (K_P - 3K_D + 5)s^2 + (K_I - 3K_P + 2)s - 3K_I \tag{4.49}$$

Here $n = 3$, $m = 1$, and $N(-s) = -s - 3$. Therefore, we obtain

$$\begin{aligned} v(s) &= \delta(s, K_P, K_I)N(-s) \\ &= -s^5 + (-K_D - 7)s^4 + (-K_P - 17)s^3 + (9K_D - K_I - 17)s^2 + (9K_P - 6)s \\ &\quad + 9K_I \end{aligned} \tag{4.50}$$

so that

$$\begin{aligned} v(j\omega, K_P, K_I) &= (-K_D - 7)\omega^4 + (K_I - 9K_D + 17)\omega^2 + 9K_I \\ &\quad + j[\omega^5 + (K_P + 17)\omega^3 + (9K_P - 6)\omega] \\ &= p(\omega) + jq(\omega) \end{aligned} \tag{4.51}$$

We find that $z^+ = 1$ so that the signature requirement on $v(s)$ for stability is,

$$n - m + 1 + 2z^+ = 5 \tag{4.52}$$

Since the degree of $v(s)$ is odd, we see from the signature formulas (see (2.50)) that $q(\omega)$ must have at least two positive real root of odd multiplicity. The range of $K_P$ such that $q(\omega, K_P)$ has at least two real, positive, distinct, finite zero with odd multiplicity was determined to be $K_P \in (-4, 0.65)$ which is the allowable range for $K_P$. By sweeping over different $K_P$ values within the interval $(-4, 0.65)$ and following the procedure summarized in the design methodology section, we can generate the set of stabilizing $(K_P, K_I)$ values. This set is shown in Fig 4.36.

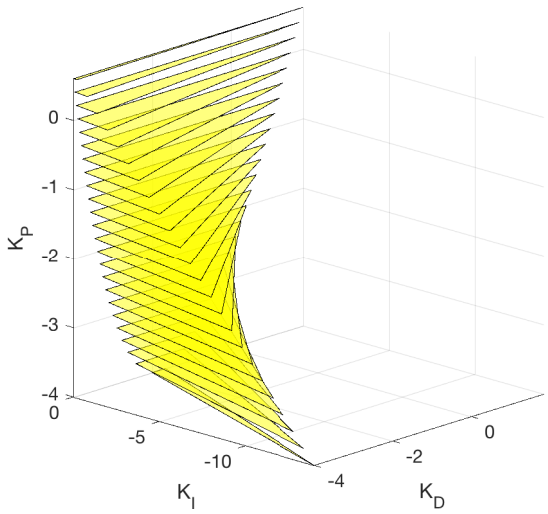


Figure 4.36: PID Stabilizing Set for Example 3a

### *4.11.2 Construction of the Achievable Gain-Phase Margin Design Curves*

For the construction of the achievable Gain-Phase margin set for the PID controller design case, the evaluated range of $\omega_g$ is $[0.1, 1.2]$ and the range for PM is from $1^o$ to $100^o$. For the PID case, using the constant gain and constant phase loci

equations, (3.51) and (3.52) we now get a cylinder and a plane in the $(K_P, K_I, K_D)$ 3D space, respectively. The cylinder and the plane, superimposed in the stabilizing set (see Fig. 4.50) will have two intersection line segments in the $(K_I, K_D)$ plane. The specific value where the intersection occurs can be obtained using (3.55). Equation (3.55) will give us two values for $K_P$, but only one is contained in the stabilizing set. The intersection line segment in the $(K_P, K_I, K_D)$ represents the PID controller gains that satisfy the PM and $\omega_g$. Evaluating the range of PM and $\omega_g$, we can construct the achievable Gain-Phase margin set represented in 3D in Fig. 4.37. If we take a fixed value of $\omega_g = 0.8$ rad/sec, we can see the achievable performance in 2D in Fig 4.38. Here we can see that the maximum GM we can get is 6.269 with a PM of $9^o$ and for a PM of $60^o$ the GM is 3.548.

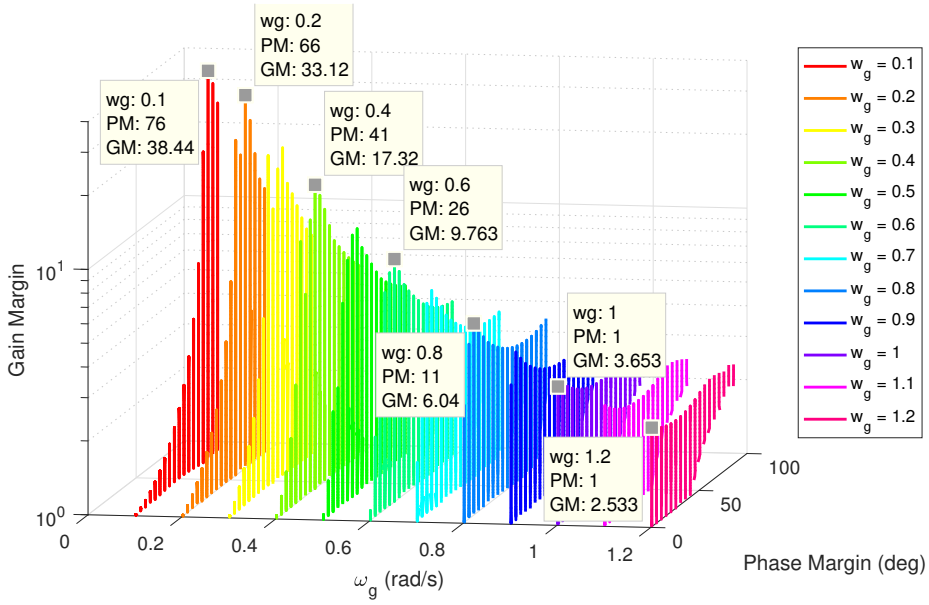


Figure 4.37: Achievable Performance in Terms of GM, PM, and $\omega_g$ for PID Controller Design in Example 3a

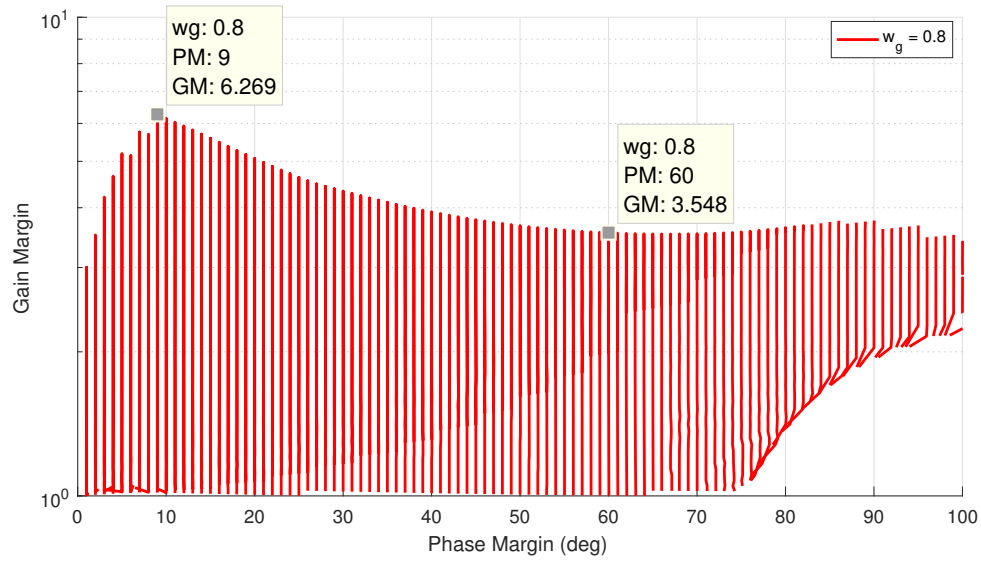


Figure 4.38: Achievable Gain-Phase Margin Set for $\omega_g = 0.8$ rad/sec for PID Controller Design in Example 3a

### *4.11.3 Simultaneous Specifications and Retrieval of the Controller Gains*

In Fig. 4.37, we can see the achievable Gain-Phase margin set of curves indexed by fixed $\omega_g$ in different colors. Notice that we can get more GM and PM for lower values of $\omega_g$. For example, for $\omega_g = 0.1$ rad/sec, the maximum GM that we can get is 38.44 with a PM of $76^o$. For $\omega_g = 0.2$ rad/sec, the maximum GM is 33.12 with a $PM = 66^o$. For a bigger value of $\omega_g$, we get lower values for GM and PM. For example, for $\omega_g = 1.2$ rad/sec we get a maximum $GM = 2.533$ and $PM = 1^o$. The designer has the liberty to choose values for GM, PM, and $\omega_g$ that best suits his design needs.

After the selection of simultaneous GM, PM, and $\omega_g$ from the achievable gain-phase margin set, the designer can retrieve the controller gains corresponding to the point. For illustration purposes, let us say that the desired performance values chosen

for this example are a PM of $60^o$, GM of 3.548, and a $\omega_g$ of 0.8 rad/s (see Fig 4.38.) Then, taking these values and the constant gain and constant phase loci for PID controllers presented in the methodology, we can find the intersection of the cylinder and the plane in the $(K_P, K_I, K_D)$ 3D space shown in Fig 4.39. The controller gains are $K_P^* = -1.1317$, $K_I^* = -0.4783$, and $K_D^* = -0.6$. In Fig 4.40 we can see the Nyquist plot for the controller gains selected. Here, we can see that those controller gains satisfy the desired performance specifications, $PM = 60^o$, $GM = 3.5482$ (11 dB).

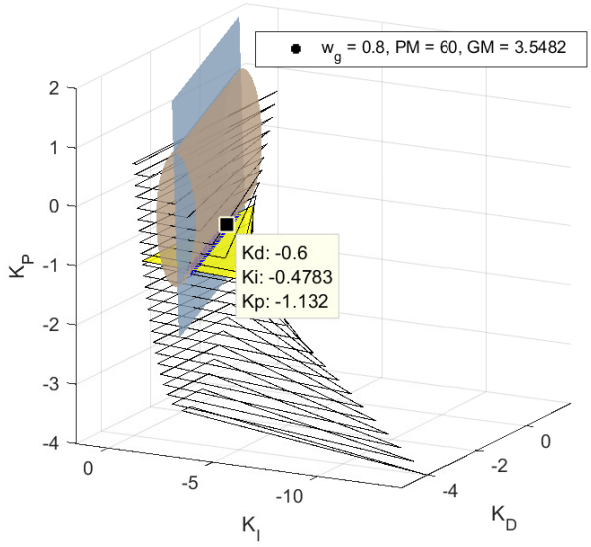


Figure 4.39: Intersection of Cylinder and Plane in the PID Controller Design in Example 3a

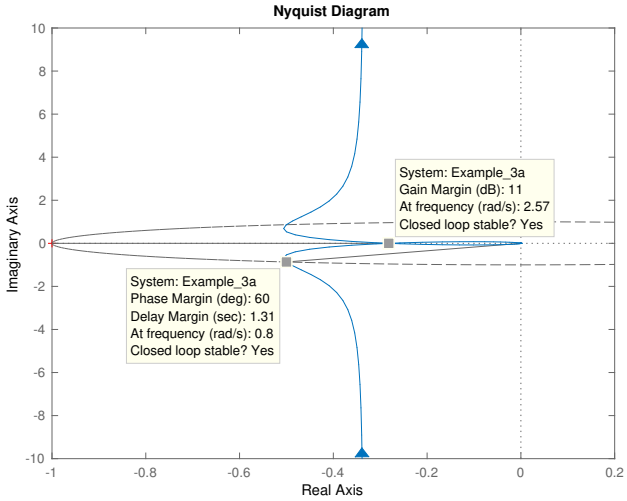


Figure 4.40: Nyquist Plot for $K_P^* = -1.1317$, $K_I^* = -0.4783$, and $K_D^* = -0.6$ in the PID Controller Design in Example 3a

## 4.12 Example 3b. Discrete-Time PID Controller Design

Consider the unity feedback discrete time system with

$$P(z) = \frac{1}{z^2 - 0.25} \quad \text{and} \quad C(z) = \frac{K_0 + K_1 z + K_2 z^2}{z(z-1)} \tag{4.53}$$

### *4.12.1 Computation of the Stabilizing Set*

Then, using the Tchebyshev representation with $\rho = 1$, we have

$$\begin{aligned} T_N(\nu) &= 1, \\ U_N(\nu) &= 0, \\ T_D(\nu) &= 2\nu^2 - 1.25, \\ U_D(\nu) &= -2\nu, \\ P_1(\nu) &= 2\nu^2 - 1.25, \\ P_2(\nu) &= -2\nu \\ P_3(\nu) &= 1 \end{aligned} \tag{4.54}$$

Then, by (2.26) we have

$$\begin{aligned} T(\nu, L_0, K_1) &= -4\nu^3 - 2\nu^2 + (3.25 - L_0)\nu + K_1 + 1.25, \\ U(\nu, L_1) &= 4\nu^2 + 2\nu + L_1 - 1.25 \end{aligned} \tag{4.55}$$

Since $P(z)$ is of order 2 and $C(z)$, the PID controller, is of order 2, the number of roots of $\delta(z)$ inside the unit circle is required to be 4 for stability. Then,

$$i_1 - i_2 = \underbrace{(i_\delta + i_{N_r})}_{i_1} - \underbrace{(l+1)}_{i_2} \tag{4.56}$$

where $i_\delta$ and $i_{N_r}$ are the number of roots of $\delta(z)$ and the reverse polynomial of $N(z)$, respectively, and $l$ is the order of $N(z)$. Since the required $i_\delta$ is 4, $i_{N_r} = 0$, and $l = 0$, $i_1 - i_2$ is required to be 3. Therefore, we require two real roots from $U(\nu, L_1)$ to satisfy the stability condition. We can find the feasible range for $L_1$, so we can

find these two required roots. For this example, the range taken in consideration is $L_1 \in [-1, 1.4]$. To illustrate the example in detail, we fix $L_1 = 1$.Then, the real roots of $U(\nu, L_1)$ in $(-1, +1)$ are $-0.6036$ and $0.1036$. Furthermore, $Sgn[U(-1)] = +1$, and $i_1 - i_2 = 3$ requires that

$$\frac{1}{2}Sgn[U(-1)](Sgn[T(-1)] - 2Sgn[T(-0.6036)] + 2Sgn[T(0.1036)] - Sgn[T(1)]) = 3 \tag{4.57}$$

Here, the only valid sequence satisfying the last equations is

$$\begin{aligned} Sgn[T(-1)] = +1, \quad Sgn[T(-0.6036)] = -1 \\ Sgn[T(0.1036)] = +1, \qquad Sgn[T(1)] = -1 \end{aligned} \tag{4.58}$$

Corresponding to this sequence, we have the following set of linear inequalities:

$$\begin{aligned} -0.5607 + 0.6036L_0 + K_1 < 0, \qquad L_0 + K_1 > 0 \\ +1.5607 + 0.1036L_0 + K_1 > 0, \quad -1.5 - L_0 + K_1 < 0 \end{aligned} \tag{4.59}$$

This set of inequalities characterize the stability region in $(L_0, K_1)$ space for a fixed $L_1 = 1$. By repeating this procedure for the considered range of $L_1$, we obtain the stability region shown in Fig. 5.8.

### *4.12.2 Construction of the Achievable Gain-Phase Margin Design Curves*

Suppose our desired phase margin specification to be $\phi_g^* = 60^o$ with a gain crossover frequency of $\omega_g^* = 2.23\ rad/s$ and a fixed value $K_1 = 0.1$. Then, using

(3.20) and (3.23) we have that

$$|C(e^{j\theta_g})|^2 = \frac{\left(L_0 + \frac{K_1}{\cos\theta_g}\right)^2}{\left(\frac{\sqrt{\mu}}{\cos\theta_g}\right)^2} + \frac{L_1^2}{\left(\frac{\sqrt{\mu}}{\sin\theta_g}\right)^2} = \frac{1}{|P(e^{j\theta_g})|^2} \tag{4.60}$$

which implies that

$$\frac{(L_0 + K_1 1.0254)^2}{(0.1784)^2} + \frac{L_1^2}{(0.7868)^2} = 1 \tag{4.61}$$

$$\begin{aligned} \angle C(e^{j\theta_g}) &= \tan^{-1}\left(\frac{\sin\theta_g\left(L_1(\cos\theta_g - 1) - (L_0\cos\theta_g + K_1)\right)}{(L_0\cos\theta_g + K_1)(\cos\theta_g - 1) + L_1\sin^2\theta_g}\right) \\ &= \pi + \phi_g^* - \angle P(e^{j\theta_g}) \end{aligned} \tag{4.62}$$

which implies that $L_1 = (0.7672)L_0 + 0.0787$.

We can consider a range of $K_1$ and desired phase margins so we have a set of ellipses and straight lines. For each ellipse there is a corresponding straight line with the intersection points. For $K_1 \in [-1.4, 0.8]$ we can see in Fig 4.41 all the ellipses and straight lines for the different values. We choose the intersection point with $K_1 = 0.1$. Thus

$$K_0 = -0.0308, \quad K_1 = 0.1, \quad K_2 = 0.1041 \tag{4.63}$$

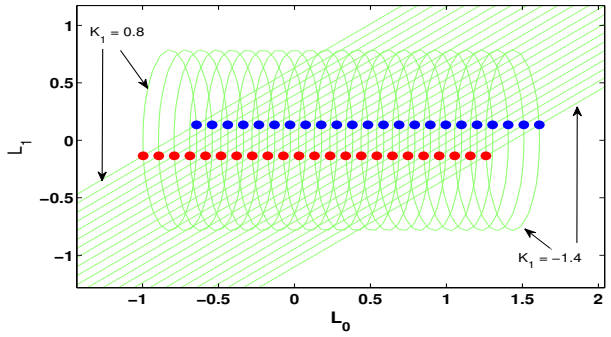


Figure 4.41: Gain and Phase Loci for Values of $K_1 \in [-1.4, 0.8]$ in Example 3b [5]

Then, our desired controller $C^*(z)$ to satisfy the specified phase margin is

$$C^*(z) = \frac{-0.0308 + 0.1z + 0.1041z^2}{z(z-1)} \tag{4.64}$$

In Fig. 4.42 we can see the step response of the system. In classical control it is known empirically that good phase margin leads to reduced overshoot; we observe that in this example. In Fig. 4.43 we can see that the controller is found to be contained in the stabilizing set shown previously.

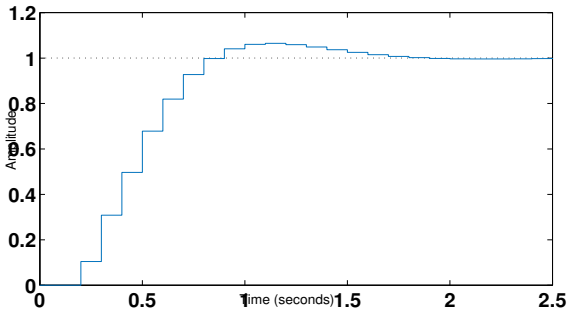


Figure 4.42: Step Response of the Discrete-Time System with $C^*(z)$ in Example 3b [5]

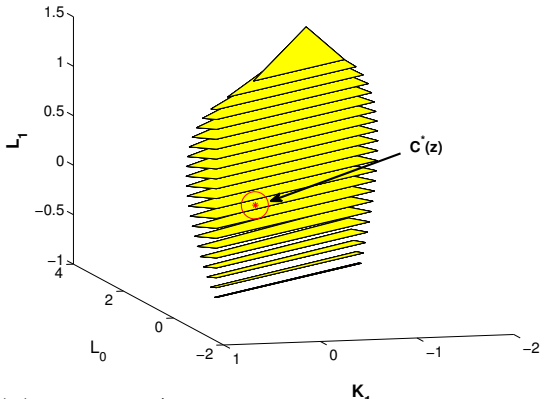


Figure 4.43: $C^*(z)$ in Red '*' Contained in the Stabilizing Set in Example 3b [5]

## 4.13 Example 4a. Continuous-Time PI Controller Design for Stable FOPTD Systems

Let us consider an stable continuous-time FOPTD system

$$P(s) = \frac{1}{2s+1}e^{-0.3s} \tag{4.65}$$

and the PI controller, $C_{PI}$. We proceed to apply the procedure presented in the methodology.

### *4.13.1 Computation of the Stabilizing Set.*

The characteristic equation is given by

$$\delta(s) = (2s+1)s + (K_P s + K_I)e^{-0.3s}. \tag{4.66}$$

By (2.72),

$$\delta^*(s) = e^{0.3s}(2s+1)s + (K_P s + K_I). \tag{4.67}$$

For $L = 0$, we have

$$\delta(s) = 2s^2 + (K_P + 1)s + K_I. \tag{4.68}$$

For stability, it is required $K_P > -1$, $K_I > 0$. For $L > 0$ and by (2.74) and (2.75),

$$\delta^*(j\omega) = \delta_r(\omega) + j\delta_i(j\omega) \tag{4.69}$$

where

$$\delta_r(\omega) = K_I - \omega \sin(0.3\omega) - 2\omega^2 \cos(0.5\omega) \tag{4.70}$$

$$\delta_i(\omega) = \omega \left[5K_P + \cos(0.5\omega) + 12\omega \sin(0.5\omega)\right]. \tag{4.71}$$

By (2.78), we can calculate the range fo $K_P$ for stability

$$-1 < K_P < 6.6667\sqrt{\alpha_1^2 + 0.0225} \tag{4.72}$$

Following all the steps we get the stabilizing set in Fig. 4.44.

### *4.13.2 Construction of the Achievable Gain-Phase Margin Design Curves.*

For the construction of the achievable Gain-Phase margin set in this example, the evaluated range of $\omega_g$ is $[0.1, 2.8]$ and the range for PM is from $1^o$ to $110^o$. The calculation of the GM for each case is done by (4.1). Using the ellipse and straight line intersection points, we can construct the achievable Gain-Phase margin set presented in Fig 4.45.

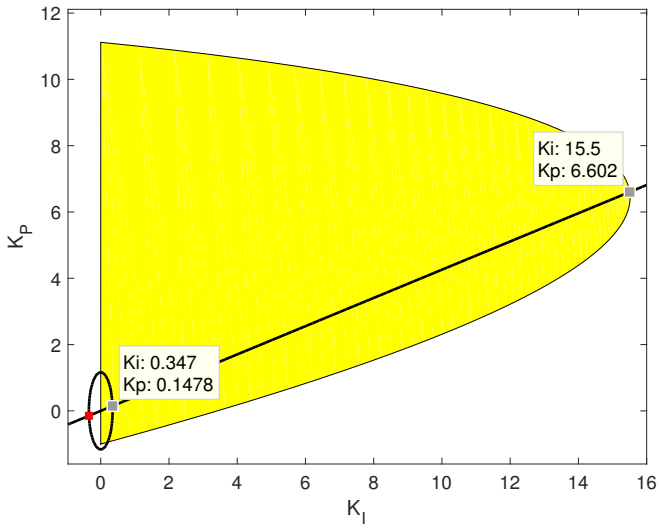


Figure 4.44: Stabilizing Set in Yellow for PI Controller Design in Example 4a

### *4.13.3 Selection of Simultaneous Desired GM, PM, and $\omega_g$ Specifications From the Achievable Gain-Phase Margin Design Curves.*

In Fig 4.45, we can see the achievable Gain-Phase margin set of curves indexed by fixed $\omega_g^*$ in different colors. We notice that the maximum PM that we can get is $103.8^o$ for a $\omega_g = 0.8$ rad/sec with a value of GM of 5.872. Another example of the values of GM and PM that we can get is the point with a PM of $79.72^o$ with a GM of 149 and a $\omega_g = 0.1$ rad/sec. The designer has the liberty to choose values for GM, PM, and $\omega_g$ that best suits his design needs.

### *4.13.4 Retrieval of the PI Controller Gains Corresponding to a Selected Desired Point in the Achievable Performance Set.*

After the selection of simultaneous GM, PM, and $\omega_g$ from the achievable Gain-Phase margin set, the designer can retrieve the controller gains corresponding to the point. For illustration purposes, let us say that the desired performance values chosen

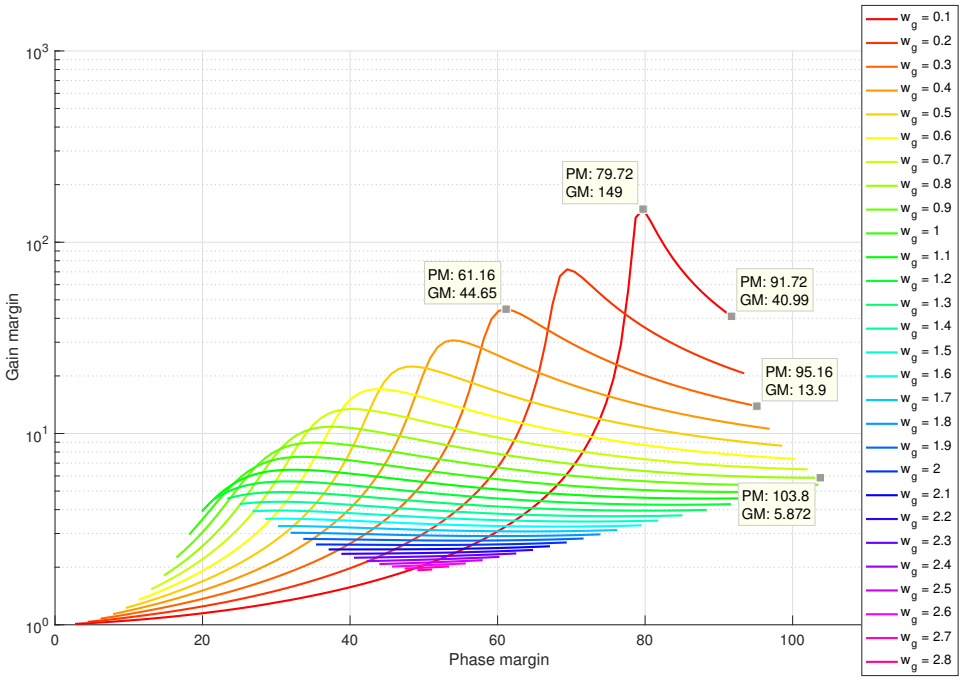


Figure 4.45: Achievable Performance in Terms of GM, PM, and $\omega_g$ for PI Controller Design in Example 4a, Intersection of an Ellipse and a Straight Line (dot in black), and the Controller Gains $(K_P^{ub}, K_I^{ub})$ at the Upper Boundary Points in the Stabilizing Set.

for this example are a PM of $61.16^o$, $GM = 44.6$ (33 dB), and a $\omega_g = 0.3$ rad/s from Fig 4.45. Then, taking these values for the constant gain and constant phase loci presented in the methodology, we can find the intersection of an ellipse and a straight line shown in Fig 4.45. The controller gains are $K_P^* = 0.1478$ and $K_I^* = 0.347$. In Fig 4.46 we can see the Nyquist plot for the controller gains selected. Here, we can see that those controller gains satisfy the desired performance specifications, $PM = 61.2^o$, $GM = 44.6$ (33 dB).

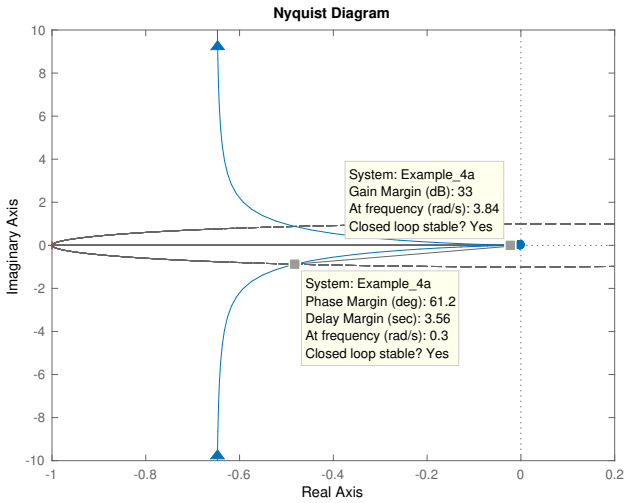


Figure 4.46: Nyquist Plot for $K_P^* = 0.1478$ and $K_I^* = 0.347$ in the PI controller Design in Example 4a

## 4.14 Example 4b. Continuous-Time PI Controller Design for Unstable FOPTD Systems

Let us consider an unstable continuous-time FOPTD system

$$P(s) = \frac{5}{-12s+1}e^{-0.5s} \tag{4.73}$$

and the PI controller, $C_{PI}$. We proceed to apply the procedure presented in the methodology.

### *4.14.1 Computation of the Stabilizing Set.*

The characteristic equation is given by

$$\delta(s) = (-12s+1)s + 5(K_P s + K_I)e^{-0.5s}. \tag{4.74}$$

By (2.86),

$$\delta^*(s) = e^{0.5s}(-12s+1)s + (K_P s + K_I)5. \tag{4.75}$$

For $L = 0$, we have

$$\delta(s) = -12s^2 + (5K_P + 1)s + 5K_I. \tag{4.76}$$

For stability, it is required $K_P < -\frac{1}{5}$, $K_I < 0$. For $L > 0$ and by (2.88) and (2.89),

$$\delta^*(j\omega) = \delta_r(\omega) + j\delta_i(j\omega) \tag{4.77}$$

where

$$\delta_r(\omega) = 5K_I - \omega\sin(0.5\omega) + 12\omega^2\cos(0.5\omega) \tag{4.78}$$

$$\delta_i(\omega) = \omega\left[5K_P + \cos(0.5\omega) + 12\omega\sin(0.5\omega)\right]. \tag{4.79}$$

By (2.93), we can calculate the range fo $K_P$ for stability

$$-4.8\sqrt{\alpha_1^2 + 0.0017} < K_P < -\frac{1}{5} \tag{4.80}$$

Following all the steps we get the stabilizing set in Fig. 4.47

### *4.14.2 Construction of the Achievable Gain-Phase Margin Design Curves.*

For the construction of the achievable Gain-Phase margin set in this example, the evaluated range of $\omega_g$ is $[0.1, 3]$ and the range for PM is from $0^o$ to $70^o$. The calculation of the GM for each case is done by (4.1). Using the ellipse and straight line intersection points, we can construct the achievable Gain-Phase margin set pre-

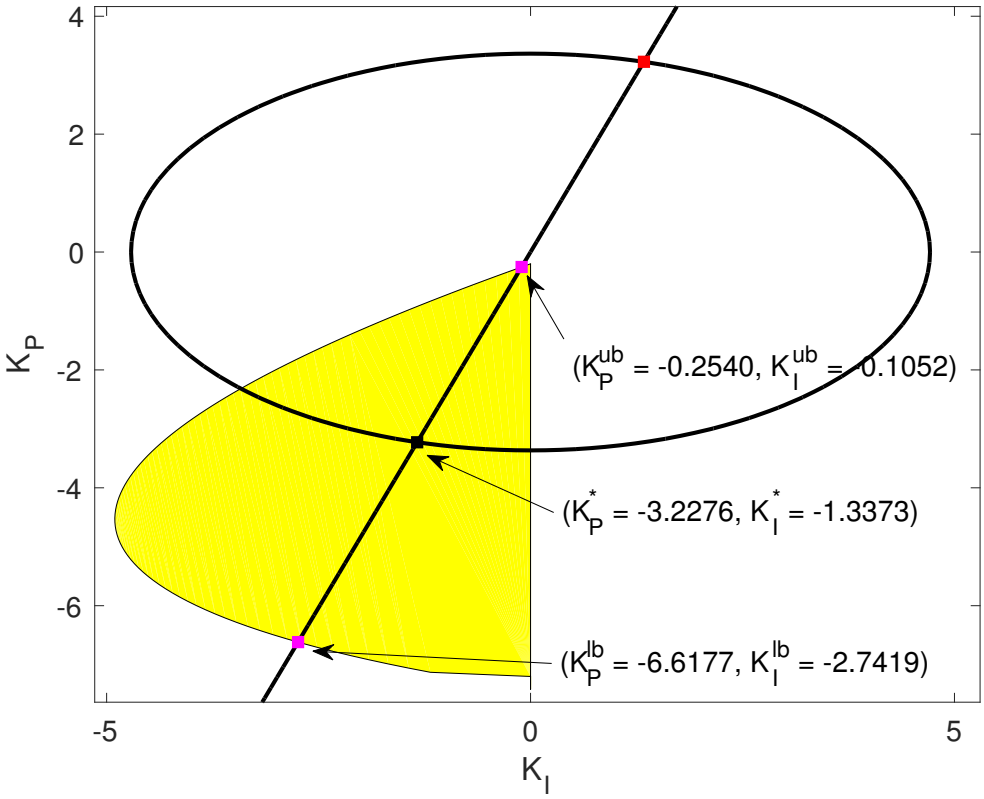


Figure 4.47: Stabilizing Set in Yellow for PI controller Design in Example 4b, Intersection of an Ellipse and a Straight Line (dot in black), and the Controller Gains $(K_P^{lb}, K_I^{lb})$ and $(K_P^{ub}, K_I^{ub})$ at the Lower and Upper Boundary Points in the Stabilizing Set (Dots in Magenta) [6]

sented in Fig 4.48.

#### *4.14.2.1 Selection of Simultaneous Desired GM, PM, and $\omega_g$ Specifications From the Achievable Gain-Phase Margin Design Curves.*

In Fig 4.48, we can see the achievable Gain-Phase margin set of curves indexed by fixed $\omega_g^*$ in different colors. Notice that the curves above the $10^0$ GM represent the upper GM and the curves below $10^0$ GM represent the lower GM. We notice that the maximum PM that we can get is $66^o$ for a $\omega_g = 0.4$ rad/sec with a value

of upper GM of 7.547 and lower GM of 0.2045. Another example of the values of GM and PM that we can get is the point with a PM of $47^o$ with an upper GM of 23.72 and a $\omega_g = 0.1$ rad/sec. However, for this value, we get a lower GM of 0.6404. We notice that for a bigger GM from the achievable Gain-Phase margin set, we get lower PM. The blue dots represent the specification points corresponding to a PM of $30^o$. The designer has the liberty to choose values for GM, PM, and $\omega_g$ that best suits his design needs.

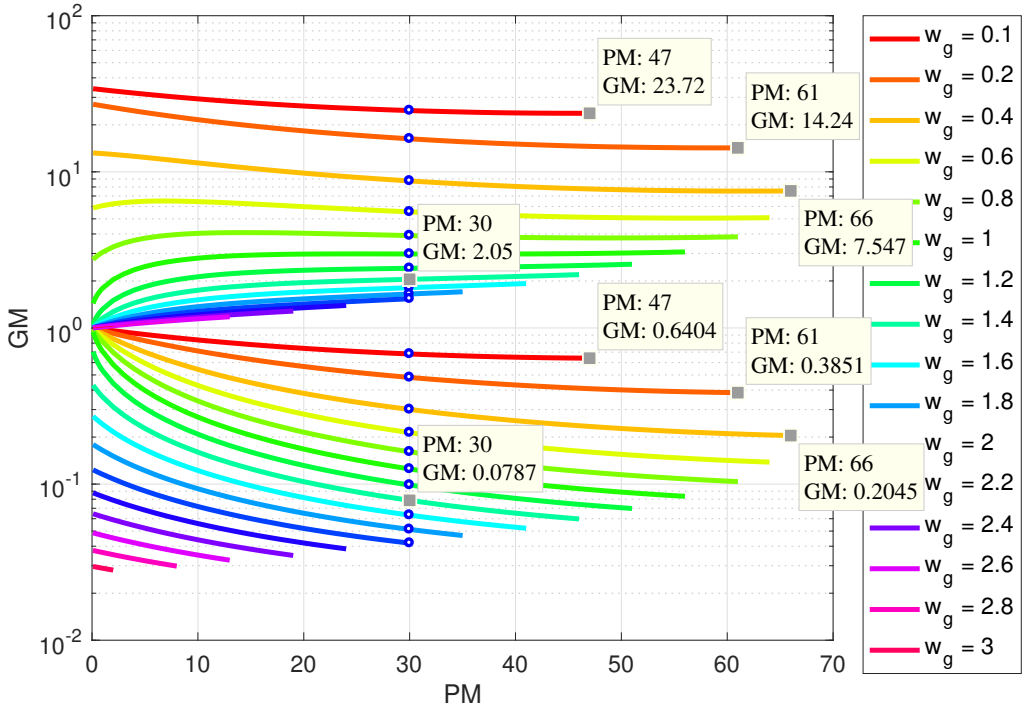


Figure 4.48: Achievable Performance in Terms of GM, PM, and $\omega_g$ for PI Controller Design in Example 4b. The Blue Dots Represent the Intersections of Ellipses and Straight Lines with a PM of $30^o$ [6]

### *4.14.3 Retrieval of the PI Controller Gains Corresponding to a Selected Desired Point in the Achievable Performance Set.*

After the selection of simultaneous GM, PM, and $\omega_g$ from the achievable Gain-Phase margin set, the designer can retrieve the controller gains corresponding to the point. For illustration purposes, let us say that the desired performance values chosen for this example are a PM of $30^o$, $GM = 2.05$, and a $\omega_g = 1.4$ rad/s from Fig 4.48. Then, taking these values for the constant gain and constant phase loci presented in the methodology, we can find the intersection of an ellipse and a straight line shown in Fig 4.47. The controller gains are $K_P^* = -3.2276$ and $K_I^* = -1.3373$. In Fig 4.49 we can see the Nyquist plot for the controller gains selected. Here, we can see that those controller gains satisfy the desired performance specifications, $PM = 30^o$, $GM = 2.05$ (6.23 dB).

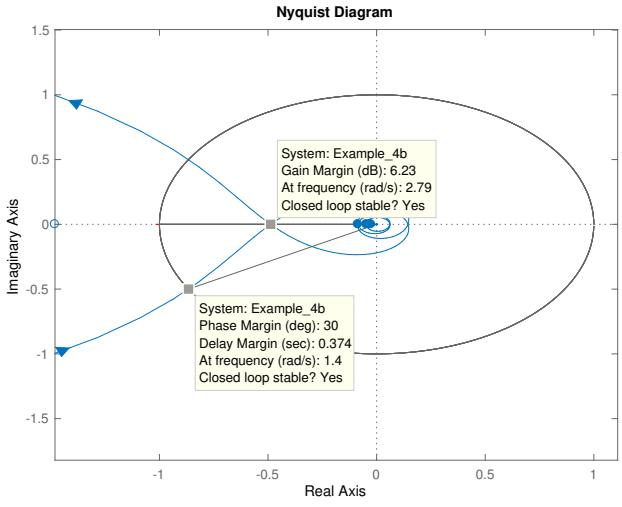


Figure 4.49: Nyquist Plot for $K_P^* = -3.2276$ and $K_I^* = -1.3373$ in the PI Controller Design in Example 4b [6]

## 4.15 Example 5a. Continuous-Time PID Controller Design for Stable FOPTD Systems

Let us consider an stable continuous-time FOPTD system

$$P(s) = \frac{1}{2s+1}e^{-2s} \tag{4.81}$$

and the PID controller $C_{PID}(s)$. We proceed to apply the procedure presented in the methodology.

### *4.15.1 Computation of the Stabilizing Set.*

The characteristic equation (2.99) is given by

$$\delta_{PID}(s) = (2s+1)s + (K_D s^2 + K_P s + K_I)e^{-2s} \tag{4.82}$$

and by (2.102)

$$\delta^*(s) = e^{2s}(2s+1)s + (K_D s^2 + K_P s + K_I) \tag{4.83}$$

For $L = 0$ we have

$$\delta(s) = (K_D + 2)s^2 + (K_P + 1)s + K_I \tag{4.84}$$

For stability, it is required

$$K_P > -1, \quad K_I > 0, \quad K_D > -2 \tag{4.85}$$

For $L > 0$

$$\delta^*(j\omega) = \delta_r(\omega) + j\delta_i(j\omega) \tag{4.86}$$

where

$$\delta_r(\omega) = K_I - K_D\omega^2 - \omega\sin(2\omega) - 2\omega^2\cos(2\omega) \tag{4.87}$$

$$\delta_i(\omega) = \omega\left[K_P + \cos(2\omega) - 2\omega\sin(2\omega)\right] \tag{4.88}$$

By (2.108), we can calculate the range fo $K_P$ for stability

$$-1 < K_P < \left[\alpha_1\sin(\alpha_1) - \cos(\alpha_1)\right] \tag{4.89}$$

Following all the steps, we get the stabilizing set in Fig. 4.29.

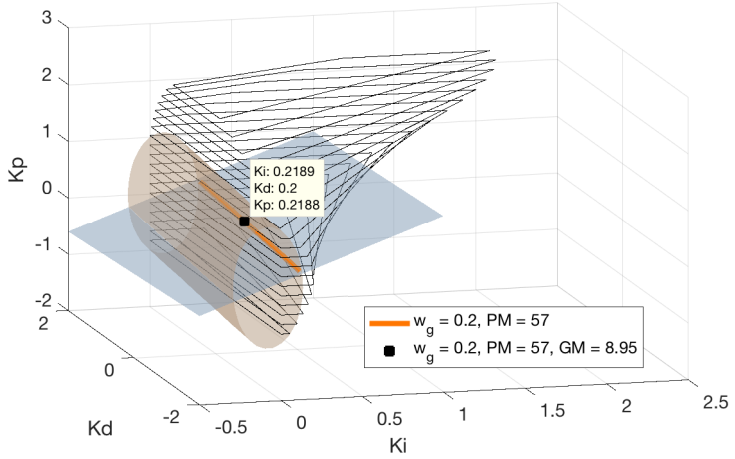


Figure 4.50: Intersection of a Cylinder and a Plane Superimposed in the PID Stabilizing Set and a PID Design Point for Example 5a [6]

### *4.15.2 Construction of the Achievable Gain-Phase Margin Design Curves.*

For the construction of the achievable Gain-Phase margin set for the PID controller design case, the evaluated range of $\omega_g$ is $[0.1, 1.3]$ and the range for PM is from $1^o$ to $120^o$. For the PID case, using the constant gain and constant phase loci equations, (3.51) and (3.52) we now get a cylinder and a plane in the $(K_P, K_I, K_D)$ 3D space, respectively. The cylinder and the plane, superimposed in the stabilizing set (see Fig. 4.50) will have two intersection line segments in the $(K_I, K_D)$ plane. The specific value where the intersection occurs can be obtained using (3.53). Equation (3.55) will give us two values for $K_P$, but only one is contained in the stabilizing set. The intersection line segment in the $(K_P, K_I, K_D)$ represents the PID controller gains that satisfy the PM and $\omega_g$. Evaluating the range of PM and $\omega_g$, we can construct the achievable Gain-Phase margin set represented in 3D in Fig. 4.51. If we take a fixed value of $\omega_g = 0.2$ rad/sec, we can see the achievable performance in 2D in Fig 4.52. Here we can see that the maximum GM we can get is 8.95 with a PM of $57^o$.

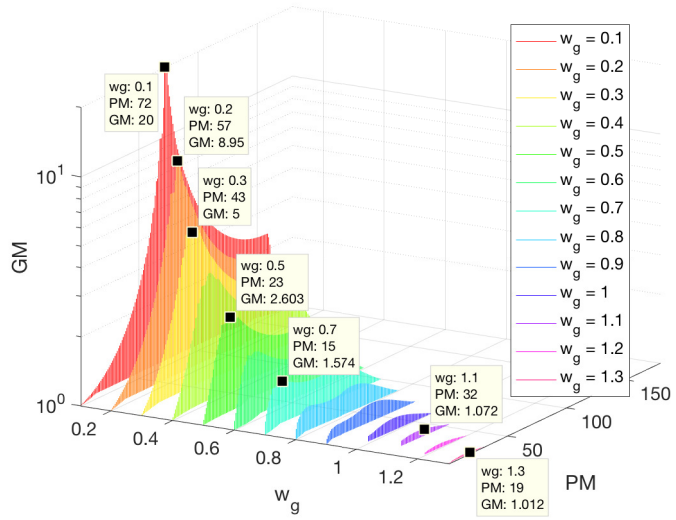


Figure 4.51: Achievable Performance in Terms of GM, PM, and $\omega_g$ for PID Controller Design in Example 5a [6]

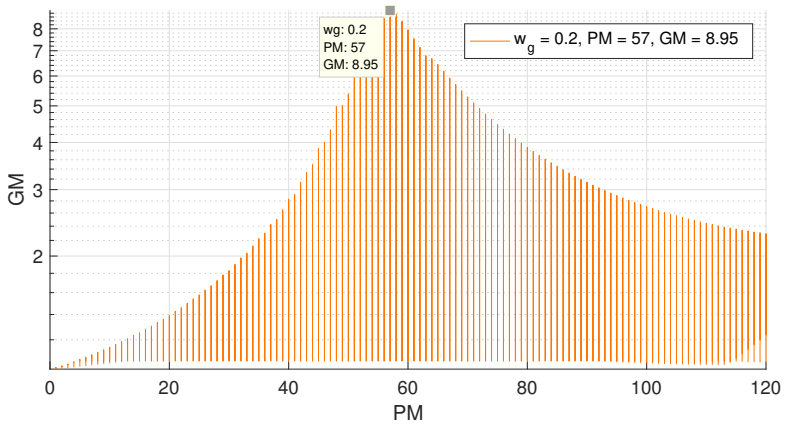


Figure 4.52: Achievable Gain-Phase Margin Set for $\omega_g = 0.2$ rad/sec for PID Controller Design in Example 5a [6]

### *4.15.3 Simultaneous Specifications and Retrieval of the Controller Gains*

In Fig. 4.51, we can see the achievable Gain-Phase margin set of curves indexed by fixed $\omega_g$ in different colors. Notice that we can get more GM and PM for lower values of $\omega_g$. For example, for $\omega_g = 0.1$ rad/sec, the maximum GM that we can get is 20 with a PM of $72^o$. For $\omega_g = 0.2$ rad/sec, the maximum GM is 8.95 with a $PM = 57^o$. For a bigger value of $\omega_g$, we get lower values for GM and PM. For example, for $\omega_g = 1.3$ rad/sec we get a maximum $GM = 1.012$ and $PM = 19^o$. The designer has the liberty to choose values for GM, PM, and $\omega_g$ that best suits his design needs.

After the selection of simultaneous GM, PM, and $\omega_g$ from the achievable gain-phase margin set, the designer can retrieve the controller gains corresponding to the point. For illustration purposes, let us say that the desired performance values chosen for this example are a PM of $57^o$, GM of 8.95, and a $\omega_g$ of 0.2 rad/s (see Fig 4.51.) Then, taking these values and the constant gain and constant phase loci for PID controllers presented in the methodology, we can find the intersection of the cylinder and the plane in the $(K_P, K_I, K_D)$ 3D space shown in Fig 4.50. The controller gains are $K_P^* = 0.2188$, $K_I^* = 0.2189$, and $K_D^* = 0.2$. In Fig 4.53 we can see the Nyquist plot for the controller gains selected. Here, we can see that those controller gains satisfy the desired performance specifications, $PM = 57^o$, $GM = 8.95$ (19 dB).

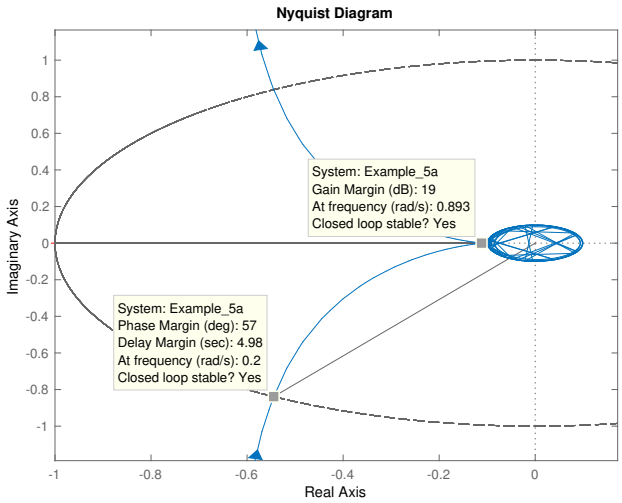


Figure 4.53: Nyquist Plot for $K_P^* = 0.2188$, $K_I^* = 0.2189$, and $K_D^* = 0.2$ in the PID Controller Design in Example 5a [6]

## 4.16 Example 5b. Continuous-Time PID Controller Design for Unstable FOPTD Systems

Let us consider an unstable continuous-time FOPTD system

$$P(s) = \frac{2}{-3s+1}e^{-0.5s} \tag{4.90}$$

and the PID controller $C_{PID}(s)$. We proceed to apply the procedure presented in the methodology.

### *4.16.1 Computation of the Stabilizing Set.*

The characteristic equation, for $L = 0$ (2.113), is given by

$$\delta(s) = (-3 + 2K_D)s^2 + (2K_P + 1)s + 2K_I \tag{4.91}$$

For stability, it is required

$$K_P < -\frac{1}{2}, \quad K_I < 0, \quad K_D < \frac{3}{2} \tag{4.92}$$

For $L > 0$

$$\delta^*(j\omega) = \delta_r(\omega) + j\delta_i(j\omega) \tag{4.93}$$

where

$$\delta_r(\omega) = 2K_I - 2K_D\omega^2 - \omega\sin(0.5\omega) + 3\omega^2\cos(0.5\omega) \tag{4.94}$$

$$\delta_i(\omega) = \omega\left[2K_P + \cos(0.5\omega) + 3\omega\sin(0.5\omega)\right] \tag{4.95}$$

By (2.122), we can calculate the range fo $K_P$ for stability

$$\frac{1}{2}\left[-\frac{3}{2}\alpha_1\sin(\alpha_1) - \cos(\alpha_1)\right] < K_P < -\frac{1}{2} \tag{4.96}$$

Following all the steps, we get the stabilizing set in Fig. 4.54.

### *4.16.2 Construction of the Achievable Gain-Phase Margin Design Curves.*

For the construction of the achievable Gain-Phase margin set for the PID controller design case, the evaluated range of $\omega_g$ is $[0.3, 1.5]$ and the range for PM is from $1^o$ to $90^o$. For the PID case, using the constant gain and constant phase loci equations, (3.51) and (3.52) we now get a cylinder and a plane in the $(K_P, K_I, K_D)$ 3D space, respectively. The cylinder and the plane, superimposed in the stabilizing set (see Fig. 4.50) will have two intersection line segments in the $(K_I, K_D)$ plane.

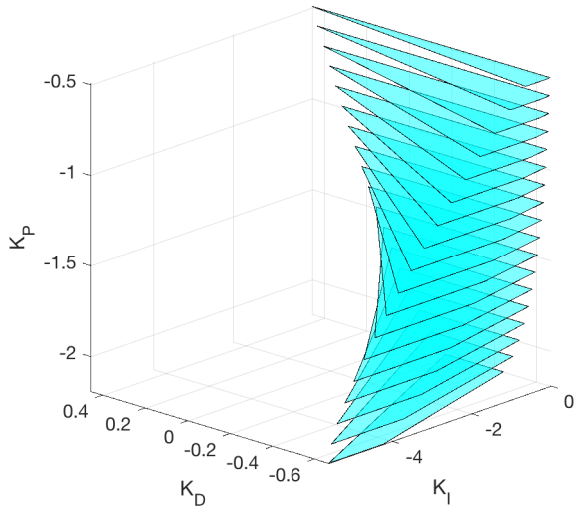


Figure 4.54: PID Stabilizing Set for Example 5b

The specific value where the intersection occurs can be obtained using (3.55). Equation (3.55) will give us two values for $K_P$, but only one is contained in the stabilizing set. The intersection line segment in the $(K_P, K_I, K_D)$ represents the PID controller gains that satisfy the PM and $\omega_g$. Evaluating the range of PM and $\omega_g$, we can construct the achievable Gain-Phase margin set represented in 3D in Fig. 4.55. If we take a fixed value of $\omega_g = 0.7$ rad/sec, we can see the achievable performance in 2D in Fig 4.56.

### *4.16.3 Simultaneous Specifications and Retrieval of the Controller Gains*

In Fig. 4.55, we can see the achievable Gain-Phase margin set of curves indexed by fixed $\omega_g$ in different colors. Notice that we can get more GM and PM for lower values of $\omega_g$. For example, for $\omega_g = 0.1$ rad/sec, the maximum GM that we can get is 20 with a PM of $72^o$. For $\omega_g = 0.2$ rad/sec, the maximum GM is 8.95 with a $PM = 57^o$. For a bigger value of $\omega_g$, we get lower values for GM and PM. For example, for $\omega_g = 1.3$ rad/sec we get a maximum $GM = 1.012$ and $PM = 19^o$. The

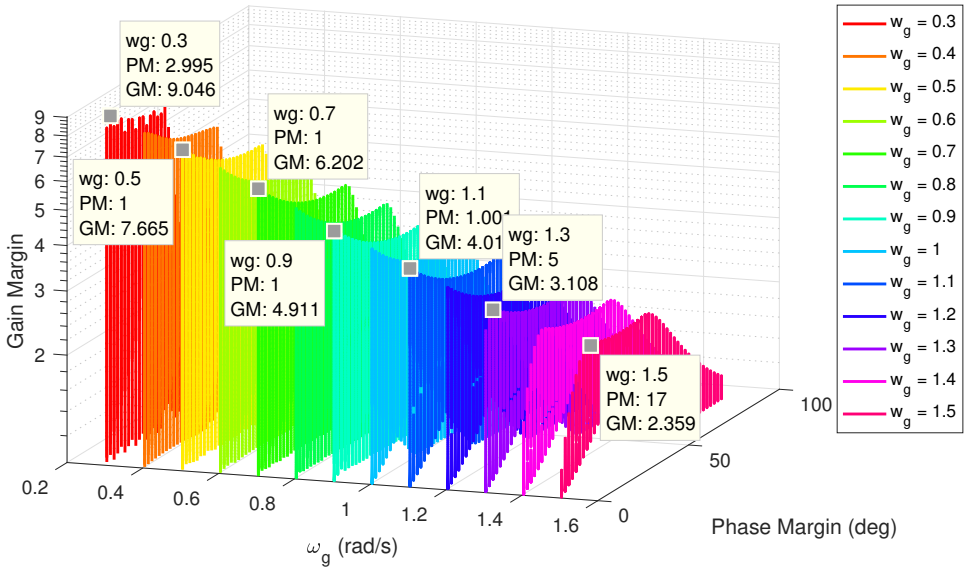


Figure 4.55: Achievable Performance in Terms of GM, PM, and $\omega_g$ for PID Controller Design in Example 5b

designer has the liberty to choose values for GM, PM, and $\omega_g$ that best suits his design needs.

After the selection of simultaneous GM, PM, and $\omega_g$ from the achievable gain-phase margin set, the designer can retrieve the controller gains corresponding to the point. For illustration purposes, let us say that the desired performance values chosen for this example are a PM of $49^o$, GM of 4.5285, and a $\omega_g$ of 0.7 rad/s (see Fig 4.51.) Then, taking these values and the constant gain and constant phase loci for PID controllers presented in the methodology, we can find the intersection of the cylinder and the plane in the $(K_P, K_I, K_D)$ 3D space shown in Fig 4.57. The controller gains are $K_P^* = -1.1594$, $K_I^* = -0.01$, and $K_D^* = -0.1512$. In Fig 4.58 we can see the Nyquist plot for the controller gains selected. Here, we can see that those controller gains satisfy the desired performance specifications, $PM = 49^o$, $GM = 4.5285$ (13.1

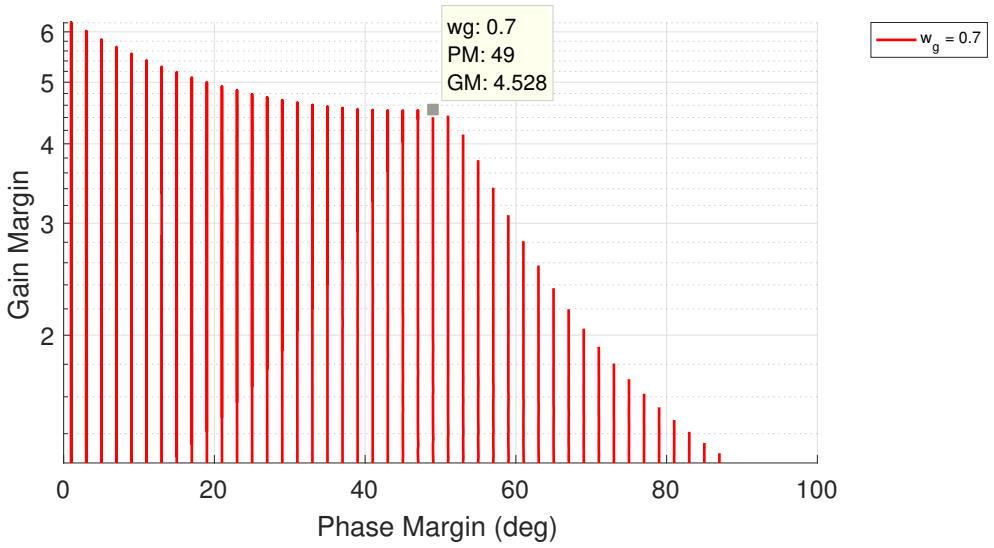


Figure 4.56: Achievable Gain-Phase Margin Set for $\omega_g = 0.7$ rad/sec for PID Controller Design in Example 5b

dB).

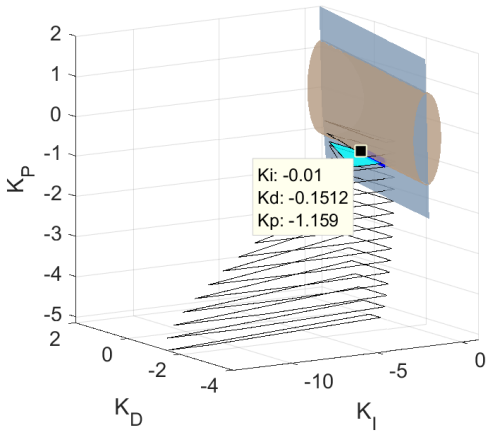


Figure 4.57: Intersection of Cylinder and Plane in the PID Controller Design in Example 5b

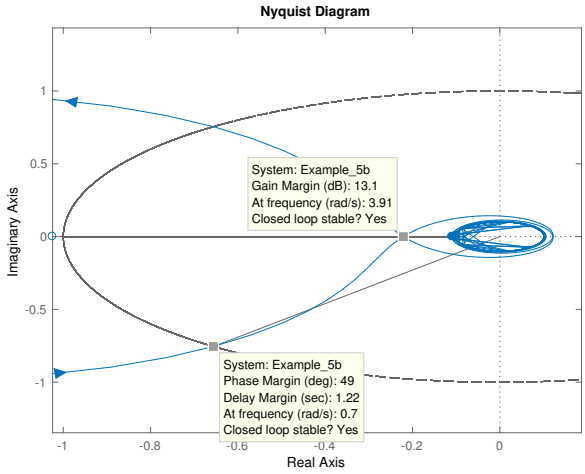


Figure 4.58: Nyquist Plot for $K_P^* = -1.1594$, $K_I^* = -0.01$, and $K_D^* = -0.1512$ in the PID Controller Design in Example 5b

## 4.17 References

Some examples presented in this section have been published in [5] and [83].

# 5. MULTIVARIABLE CONTROLLER DESIGN AND GAIN-PHASE MARGIN ACHIEVABLE PERFORMANCE

## 5.1 Introduction

The study of MIMO systems is more challenging compared to SISO systems. The problem arises from the fact that, in MIMO systems, there is an interaction between the manipulated and the controlled variables, which is not present in SISO systems. Therefore, because there is an interaction in the control loop, it is not possible to control one loop independently without affecting the others. In recent years, there has been an interest in studying MIMO systems. One of the most common approaches is to transform the MIMO system into an equivalent representation, also called equivalent transfer function parametrization or effective open-loop representation. For example, in [84], [85], [86], [87], an equivalent representation is presented to design Multi-loop PI or PID controllers mainly using Internal Model Control methods. In [88], [89], and [90] a design of MIMO systems is presented as individual channel design where SISO design is exploited for MIMO systems. In this section, we present an advanced tuning approach to design a controller for MIMO systems by taking advantage of the simplicity of SISO system's design tools. First, a transformation of the MIMO system into a Multiple SISO system is performed. Then, novel PI controller design methods are used to find the achievable performance regarding gain margin, phase margin, and gain crossover frequency for the independent SISO subsystems. After the PI controller is selected, based on a desired achievable performance, a transformation to the original system is performed. Finally, the MIMO controller with the original system in unity feedback configuration, will satisfy a gain margin, phase margin, and gain crossover frequency that is minimum achieved by

one of the Multiple SISO subsystems.

## 5.2 Problem Formulation

Consider a multivariable continuous-time Linear Time Invariant (LTI) plant with an $n \times n$ transfer function matrix $P(s)$. An $n \times n$ controller $C(s)$ in a unity feedback configuration with $P(s)$ as shown in Fig 5.1. The design problem is to find $C(s)$ such that the control system achieves a predesigned gain and phase margins.

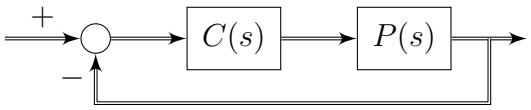


Figure 5.1: MIMO Unity Feedback Block Diagram

## 5.3 Design Methodology

The general approach developed here to solve this problem can be summarized as following steps.

(i) Transform the multivariable system $P(s)$ into a diagonal transfer function matrix and call each diagonal element $P_i(s)$ a Smith-McMillan plant.

(ii) Introduce a diagonal controller transfer function matrix where each diagonal element $C_i(S)$ is the proposed controller for the Smith-McMillan plant $P_i(s)$.

(iii) Design each diagonal controller to obtain predesigned gain margin, phase margin, and gain crossover frequency for Smith-McMillan plants.

(iv) Transform the diagonal controller matrix into the MIMO controller $C(s)$ for the original plant $P(s)$.

(v) Verify that the gain and phase margins of this multivariable system is the minimum gain margin and the minimum phase margin of the Smith-McMillan plants.

### *5.3.1 Transformation of the Multivariable Plant Into a Diagonal Transfer Function Matrix*

Multivariable system can be transformed into a diagonal transfer function matrix by using the Smith-McMillan form. The transfer function matrix $P(s)$ can be expressed as

$$P(s) = \frac{1}{d(s)} N(s) \tag{5.1}$$

where $d(s)$ is the least common multiple of denominators of elements of $P(s)$ and $N(s)$ is a polynomial matrix. The Smith form of $N(s)$ is given by

$$S(s) = Y(s)N(s)U(s) \tag{5.2}$$

where $S(s)$ is a diagonal matrix and $Y(s)$, $U(s)$ are unimodular matrices. Let

$$P_d(s) = \frac{S(s)}{d(s)}. \tag{5.3}$$

Then $P_d(s)$ is the Smith-McMillan form of $P(s)$ and $P_i(s)$ is the Smith-McMillan plant for $i = 1, 2, ...n$. Since $P_d(s)$ is of diagonal form we can introduce a diagonal controller matrix $C_d(s)$ where each controller $C_i(s)$ is designed for each $P_i(s)$. Consider the multiple SISO loops as in Fig 5.2 below.

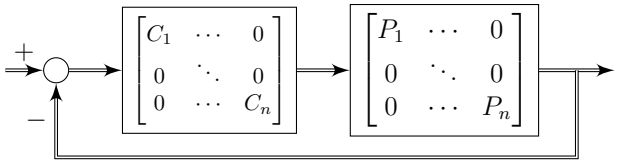


Figure 5.2: Multiple SISO Unity Feedback Block Diagram

### *5.3.2 Design of the Controller to Obtain Predesigned Gain Margin, Phase Margin, and Gain Crossover Frequency for the Smith-McMillan Plants.*

The controller $C_i(s)$ can be designed to achieve specific gain margin, phase margin, and gain crossover frequency for the Smith-McMillan plant $P_i(s)$. It is important to consider the relative degree of $P_i(s)$ when designing $C_i(s)$.

**Lemma 1** *Let $r_k$ be the relative degree of the controller $C_k(s)$ for the Smith-McMillan plant $P_k(s)$. If $r_k$ for $k = 1, 2, ..., n$ satisfies*

$$\min_{k=1,2,...,n} \left\{ r_k - d^U_{ik} - d^Y_{kj} \right\} \geq 0, \quad \forall i, j = 1, 2, ..., n \tag{5.4}$$

*where $d^U_{ik}$ and $d^Y_{kj}$ are the degree of $(i,k)^{th}$ and $(k,j)^{th}$ polynomials of the unimodular matrices $U(s)$ and $Y(s)$, respectively, then the MIMO controller $C(s)$ will be proper.*

*Proof.* See [91]. □

Lemma 1 is necessary for the MIMO controller $C(s)$ to be proper. In section 5.3.3, we describe the transformation from the diagonal controller $C_d(s)$ into the MIMO controller $C(s)$.

### 5.3.3 Transformation of the Diagonal Controller Matrix Into the Corresponding MIMO Controller

After designing the controller $C_i(s)$ for each Smith-McMillan plant $P_i(s)$, we can transform the diagonal controller matrix $C_d(s)$ into the MIMO controller matrix $C(s)$ via

$$C(s) = U(s)C_d(s)Y(s) \tag{5.5}$$

where $U(s)$ and $Y(s)$ are the unimodular matrices in (5.2). $C(s)$ is the MIMO controller that stabilizes the MIMO plant $P(s)$.

### 5.3.4 Gain and Phase Margin Design for MIMO Plants

In order to design the controller $C_i(s)$ for each Smith-McMillan plant $P_i(s)$ one can specify gain and phase margins for the corresponding SISO loop. Let $g_i$ and $\phi_i$ be the gain margin and phase margin for the $i^{th}$ SISO loop for $i = 1, 2, ..., n$.

Define $\Delta$ as

$$\Delta := \begin{bmatrix} \delta & & 0 \\ & \ddots & \\ 0 & & \delta \end{bmatrix}. \tag{5.6}$$

Consider $G(s) = P(s)C(s)$ in Fig 5.3. The multivariable stability margins can be defined as follows: For gain margins replace $\delta$ by $K$ in (5.6) and find the smallest $K$, called $K^*$, such that the loop in Fig. 5.3 becomes marginally unstable. A similar definition applies to phase margin where $\delta$ is replace by $e^{-j\theta}$.

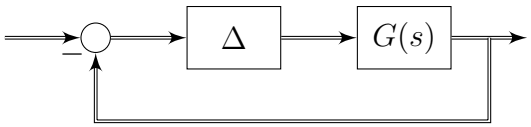


Figure 5.3: Unity Feedback MIMO System with a Perturbation Matrix $\Delta$

We need a preliminary lemma to prove the main result.

**Lemma 2** *$det(I + P(s)C(s)) = \Pi_{i=1}^{n} \left(1 + P_i(s)C_i(s)\right)$.*

*Proof.*

$$
\begin{aligned}
&det(I+P(s)C(s)) = \\
&\qquad det\left(Y^{-1}(s)Y(s) + Y^{-1}(s)P_d(s)C_d(s)Y(s)\right) \\
&\qquad = det\left(Y^{-1}(s)\right) det\left(I + P_d(s)C_d(s)\right) det\left(Y(s)\right) \\
&\qquad = det\left(I + P_d(s)C_d(s)\right) \\
&\qquad = \Pi_{i=1}^{n} \left(1 + P_i(s)C_i(s)\right).
\end{aligned}
$$

□

**Theorem 1** *Suppose $C(s)$ in (5.5) is a proper controller such that $C_i(s)$ stabilizes the corresponding Smith-McMillan plant $P_i(s)$. Then $C(s)$ stabilizes $P(s)$ with a gain margin $G$, phase margin $\Phi$, and time-delay tolerance $T$ where*

$$G = \min_{i=1,2,\ldots,n} \{g_i\}, \tag{5.7}$$

$$\Phi = \min_{i=1,2,\ldots,n} \{\phi_i\}, \tag{5.8}$$

$$T = \min_{i=1,2,\ldots,n} \{\tau_i\}, \tag{5.9}$$

*and $g_i$, $\phi_i$, and $\tau_i$ are the gain margin, phase margin, and time-delay tolerance of the SISO loops $C_i(s)P_i(s)$ for $i = 1, 2, ...n$.*

*Proof.* The proof of this theorem follows from the following observations. If

$$\Delta := \begin{bmatrix} K & & 0 \\ & \ddots & \\ 0 & & K \end{bmatrix}. \tag{5.10}$$

Then from Lemma 2,

$$det\left(I + \Delta P(s)C(s))\right) = \Pi_{i=1}^{n}\left(1 + KP_i(s)C_i\right). \tag{5.11}$$

If

$$\Delta := \begin{bmatrix} e^{j\theta} & & 0 \\ & \ddots & \\ 0 & & e^{j\theta} \end{bmatrix}, \tag{5.12}$$

then

$$det\left(I + \Delta P(s)C(s)\right) = \Pi_{i=1}^{n}\left(1 + e^{j\theta}P_i(s)C_i\right). \tag{5.13}$$

If

$$\Delta := \begin{bmatrix} e^{-sT} & & 0 \\ & \ddots & \\ 0 & & e^{-sT} \end{bmatrix}, \tag{5.14}$$

then

$$det\left(I + \Delta P(s)C(s)\right) = \Pi_{i=1}^{n}\left(1 + e^{-sT}P_i(s)C_i\right). \tag{5.15}$$

Combining (5.11), (5.13), and (5.15) evaluated at $s = j\omega$ we obtain (5.7), (5.8), and (5.9). □

This theorem shows that the gain margin, phase margin, and time-delay tolerance for the multivariable system are the minimum of the gain margins, the minimum of the phase margins, and the minimum of the time-delay tolerance of the multiple SISO loops.

## 5.4 PI Controller Design

For the step (iii) in the summary of the methodology the following sub-steps are explained in greater detail.

(a) Compute the stabilizing set

(b) Parametrize constant gain and constant phase loci for PI controllers

(c) Construct the achievable Gain-Phase margin design curves

(d) Select achievable gain margin, phase margin, and gain crossover frequency and retrieve the PI controller gains.

### *5.4.1 Computation of the Stabilizing Set*

Consider a continuous-time LTI SISO system

$$P(s) = \frac{N(s)}{D(s)} \tag{5.16}$$

and a PI controller

$$C(s) = \frac{K_P s + K_I}{s}. \tag{5.17}$$

The computation of the stabilizing set can be calculated following the steps described in subsection 2.3.2.

### *5.4.2 Constant Gain and Constant Phase Loci for PI Controllers*

Let $P(s)$ and $C(s)$ be the plant and controller transfer functions in LTI SISO system. The frequency response of the plant and controller are $P_i(j\omega)$, $C_i(j\omega)$, respectively, where $\omega \in [0, \infty]$. For the PI controller

$$C(j\omega) = \frac{jK_P\omega + K_I}{j\omega}. \tag{5.18}$$

Then, we have

$$|C(j\omega)|^2 = K_P^2 + \frac{K_I^2}{\omega^2} =: m^2 \tag{5.19}$$

$$\angle C(j\omega) = \arctan\left(\frac{-K_I}{K_P\omega}\right) =: \phi \tag{5.20}$$

Equations (5.19) and (5.20) can be written as

$$\frac{(K_P)^2}{a^2} + \frac{(K_I)^2}{b^2} = 1 \quad \text{and} \quad K_I = cK_P \tag{5.21}$$

where

$$a^2 = m^2, \quad b^2 = m^2\omega^2, \quad c = -\omega\tan\phi \tag{5.22}$$

Thus constant gain loci are **ellipses** and constant phase loci are **straight lines** in $K_P$, $K_I$ space. The major and minor axes of the ellipse are given by $a$ and $b$. The slope of the straight line (5.21) is $c$. Suppose $\omega_g^*$ is the prescribed closed-loop gain

crossover frequency. Then

$$|C(j\omega_g^*)| = \frac{1}{|P(j\omega_g^*)|} =: m_g \tag{5.23}$$

If $\phi_g^*$ is the desired phase margin in radians,

$$\angle C(j\omega_g^*) = \pi + \phi_g^* - \angle P(j\omega_g^*) =: \phi_g \tag{5.24}$$

Combining (5.21), (5.23), and (5.24) we obtain the ellipse and straight line corresponding to $m = m_g$ and $\phi = \phi_g$, giving the design point ($K_P^*$, $K_I^*$). If these intersection points lie in the stabilizing set $S$, the design is feasible, otherwise the specifications have to be altered. The graphical procedure (intersection of ellipse and straight line in the stabilizing set) makes it a convenient tool for computer-aided design.

### *5.4.3 Computation of the Achievable Performance Gain-Phase Margin Design Curves*

The Gain-Phase margin design curves represent the actual performance in terms of gain margin (GM), phase margin (PM), and gain crossover frequency ($\omega_g$) for a plant $P(s)$ achievable with a PI controller. The procedure to construct these design curves is the following:

1. Set a test range of $\phi_g^* \in [\phi_g^{\min}, \phi_g^{\max}]$ and $\omega_g \in [\omega_g^{\min}, \omega_g^{\max}]$.

2. For fixed values of $\phi_g^*$ and $\omega_g$, plot an ellipse and a straight line.

3. If an intersection point of the ellipse and the straight line lies outside of the stabilizing set, then this point is rejected and go to step 2).

4. If an intersection point of the ellipse and straight line is contained in the stabilizing set, it represents the design point with the PI controller gains $(K_P^*, K_I^*)$ that satisfies the $\phi_g^*$ and $\omega_g$.

5. Given the selected PI controller gains $(K_{P_i}^*, K_{I_i}^*)$, the upper and lower GM of the system are given by

$$GM_{upper} = \frac{K_P^{ub}}{K_P^*} \quad \text{and} \quad GM_{lower} = \frac{K_P^{lb}}{K_P^*} \tag{5.25}$$

   where $K_P^{ub}$ and $K_P^{lb}$ are the $K_P$ values at the upper and lower boundary respectively of the stabilizing set following the straight line intersecting the ellipse.

6. Go to step 2 and repeat for all values of $\phi_g^*$ and $\omega_g$ in the ranges.

### *5.4.4 Selecting an Achievable GM, PM, and $\omega_g$ and Retrieving the PI Controller Gains*

The designer can select a desired point from the achievable performance Gain-Phase margin set and retrieve the controller gains corresponding to that simultaneous specification of desired GM, PM, and $\omega_g$. The controller gain retrieval process is the following.

(1) Select desired GM, PM, and $\omega_g$ from the achievable gain-margin set.

(2) For the specified point, construct the ellipse and straight line by using the selected PM and $\omega_g$ in the constant gain and constant phase loci.

(3) Take the intersection of the ellipse and straight line contained in the stabilizing set. This will provide the gains $(K_P^*, K_I^*)$.

(4) The controller that satisfies the prescribed margin specifications is $C(s) = \frac{K_P^* s + K_I^*}{s}$.

## 5.5 Example 6a. Multivariable PI Controller Design

Let us consider a Two-Input Two-Output system as in Fig 5.1 with $P(s)$ as

$$P(s) = \begin{bmatrix} \frac{4}{(s+1)(s+2)} & \frac{-1}{s+1} \\ \frac{2}{s+1} & -\frac{6s+7}{2(s^2+3s+2)} \end{bmatrix}. \tag{5.26}$$

The objective is to find the controller $C(s)$ such that it satisfies the predesigned gain margin, phase margin, and gain crossover frequency.

### *5.5.1 Transformation of the Multivariable System Into Multiple SISO Systems.*

The least common multiple of the denominator of $P(s)$ is

$$d(s) = (s+1)(s+2) \tag{5.27}$$

Then, we can rewrite $P(s)$ as

$$P(s) = \frac{1}{(s+1)(s+2)} \underbrace{\begin{bmatrix} 4 & -1(s+2) \\ 2(s+2) & -(3s+3.5) \end{bmatrix}}_{N(s)} \tag{5.28}$$

The Smith form of $N(s)$ is expressed as

$$S(s) = \underbrace{\begin{bmatrix} \frac{1}{4} & 0 \\ -(s+2) & 2 \end{bmatrix}}_{Y(s)} \underbrace{\begin{bmatrix} 4 & -1(s+2) \\ 2(s+2) & -(3s+3.5) \end{bmatrix}}_{N(s)} \underbrace{\begin{bmatrix} 1 & \frac{1}{4}(s+2) \\ 0 & 1 \end{bmatrix}}_{U(s)}$$
$$= \begin{bmatrix} 1 & 0 \\ 0 & s^2 - 2s - 3 \end{bmatrix} \tag{5.29}$$

Dividing every element of $S(s)$ by $d(s)$ we get the Smith-McMillan form

$$P_d(s) = \begin{bmatrix} \frac{1}{(s+1)(s+2)} & 0 \\ 0 & -\frac{s-3}{s+2} \end{bmatrix} \tag{5.30}$$

Considering Fig 5.2 with a diagonal controller $C_d(s)$, we have multiple SISO loops where we can apply the SISO controller design method discussed in the previous section. Let us consider $C_d(s)$ as

$$C_d(s) = \begin{bmatrix} \frac{K_{P_1}s + K_{I_1}}{s} & 0 \\ 0 & \frac{K_{P_2}s + K_{I_2}}{s(s+2)^2} \end{bmatrix} \tag{5.31}$$

Note that there are two additional poles included in $C_2(s)$. The relative degree must be $r_2 = 2$ for the controller $C(s)$ to be proper. This addition of poles can be considered as another design variable since they will affect the achievable performance of the system.

### 5.5.2 Computation of the PI Stabilizing Sets for the Multiple SISO Loops

Considering the SISO loops $C_1(s)P_1(s)$ and $C_2(s)P_2(s)$, we can find the stabilizing set and the achievable performance in terms of GM, PM, and $\omega_g$ for each case. For $C_1(s)P_1(s)$ the range of $K_{P_1}$ for stability was determined to be $K_{P_1} \in (-2, \infty)$. For $C_2(s)P_2(s)$ the range of $K_{P_2}$ for stability was determined to be $K_{P_2} \in (-9.2702, 2.6667)$. By sweeping $K_{P_1}$ and $K_{P_2}$ within the intervals we can generate the set of stabilizing $(K_{P_1}, K_{I_1})$ and $(K_{P_2}, K_{I_2})$ sets. These sets are shown in Fig 5.4 and Fig 5.5, respectively.

### 5.5.3 Construction of the Gain-Phase Margin Design Curves for the Multiple SISO Loops

For the construction of the achievable Gain-Phase margin set for each of the SISO systems, we specified the following. For the system $C_1(s)P_1(s)$, the evaluated range of $\omega_g$ is $[0.1, 2.1]$ and the range for PM is from $0^o$ to $90^o$. For the system $C_2(s)P_2(s)$, the evaluated range of $\omega_g$ is $[0.1, 2.1]$ and the range for PM is from $0^o$ to $120^o$. The calculation of the GM for each case is done by (5.25). Using the ellipse and straight line intersection points, we can construct the achievable Gain-Phase margin set as shown in Fig 5.6.

### 5.5.4 Selection of Simultaneous Design Specifications and Retrieval of the PI Controller Gains

In Fig 5.6 and Fig 5.8, we can see the achievable Gain-Phase margin set of curves indexed by fixed $\omega_g^*$ in different colors for $C_1(s)P_1(s)$ and $C_2(s)P_2(s)$. For $C_1(s)P_1(s)$, we notice that all the curves are going up. This means that the GM is

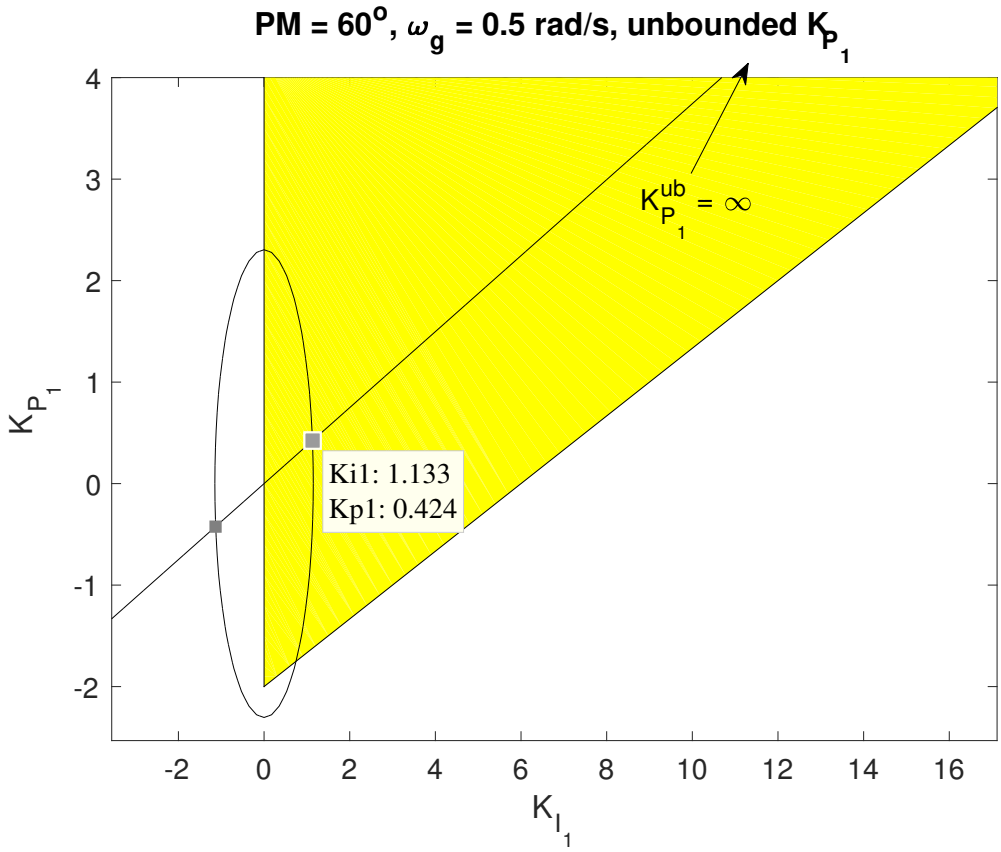


Figure 5.4: Stabilizing Set in Yellow for PI Controller Design in Example 6a for $C_1(s)P_1(s)$, Intersection of an Ellipse and a Straight Line, and the Controller Gain $(K_{P_1}^{ub})$ at the Upper Boundary Point in the Stabilizing Set.

going to infinity for the first SISO system. However, the maximum PM that we can get is $83^o$ for a $\omega_g = 0.1$ rad/sec. For $C_2(s)P_2(s)$, we have limited GM compared to $C_1(s)P_1(s)$. In this case, the maximum GM that we can achieve is 17.69 with a PM of $83^o$. In Fig 5.8, there are several points indicating the possible maximum values of GM for specific $\omega_g$. The designer has the liberty to choose values for GM, PM, and $\omega_g$ that best suits his design needs. For this MIMO example, we want to show that selecting GM and PM from the achievable performance from the SISO loops we can get a MIMO controller $C(s)$ that will achieve the margin which is

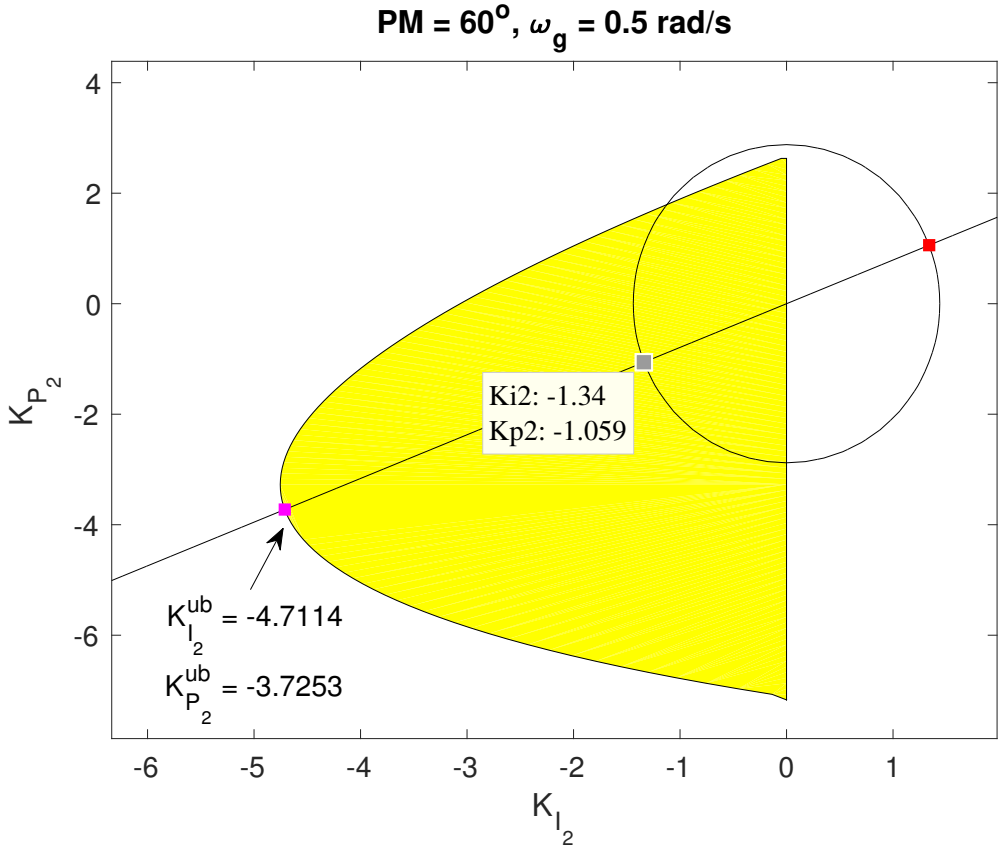


Figure 5.5: Stabilizing Set in Yellow for PI controller Design in Example 6a for $C_2(s)P_2(s)$, Intersection of an Ellipse and a Straight Line (dot in black), and the Controller Gains $(K_{P_2}^{ub}, K_{I_2}^{ub})$ at the Upper Boundary Points in the Stabilizing Set.

equal to the minimum of the margins of the SISO loops. Therefore, for illustration purposes, we are going to select a $GM = \infty$, $PM = 60^o$, and $\omega_g = 0.5$ rad/sec for $C_1(s)P_1(s)$ and $GM = 3.518$, $PM = 60^o$, and $\omega_g = 0.5$ rad/sec for $C_2(s)P_2(s)$. These values represent $\tau_1 = 2.094$ and $\tau_2 = 2.094$. After the selection of simultaneous GM, PM, and $\omega_g$ from the achievable Gain-Phase margin set, the designer can retrieve the controller gains corresponding to the point. Then, taking these values for the constant gain and constant phase loci presented in the methodology, we can find the intersection of an ellipse and a straight line shown in Fig 5.4 and Fig 5.5. The

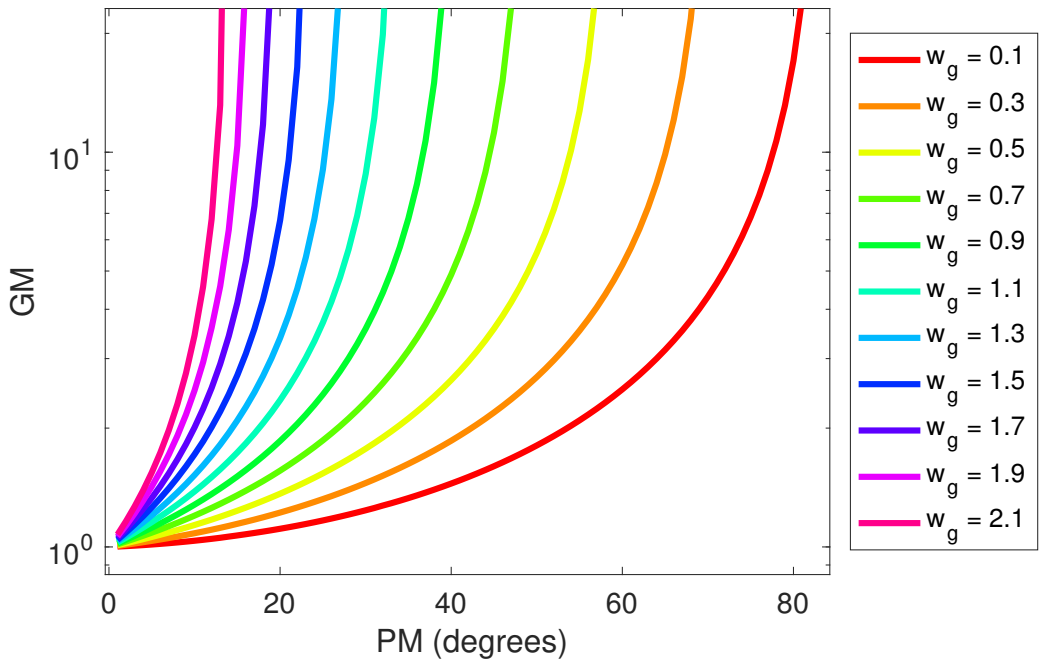


Figure 5.6: Achievable Performance in Terms of GM, PM, and $\omega_g$ for PI Controller Design in Example 6a for $C_1(s)P_1(s)$

controller gains for both loops are $K^*_{P_1} = 0.424$ and $K^*_{I_1} = 1.133$ for $C_1(s)P_1(s)$ and $K^*_{P_2} = -1.059$ and $K^*_{I_2} = -1.34$ for $C_2(s)P_2(s)$.

### *5.5.5 Transformation of the Diagonal Controller $C_d(s)$ Into the MIMO Controller $C(s)$*

The final design step is to take the diagonal controller $C_d(s)$ and transform it into the MIMO controller $C(s)$ in (5.5) by substituting the unimodular matrices $Y(s)$ and $U(s)$ in (5.29). Then, using the assigned values of $(K^*_{P_1}, K^*_{I_1})$ and $(K^*_{P_2}, K^*_{I_2})$ we have

$$C(s) = \begin{bmatrix} \frac{0.371s+0.618}{s} & \frac{-0.53s-0.67}{s(s+2)} \\ \frac{1.061s+1.34}{s(s+2)} & \frac{-2.12s-2.68}{s(s+2)^2} \end{bmatrix} \tag{5.32}$$

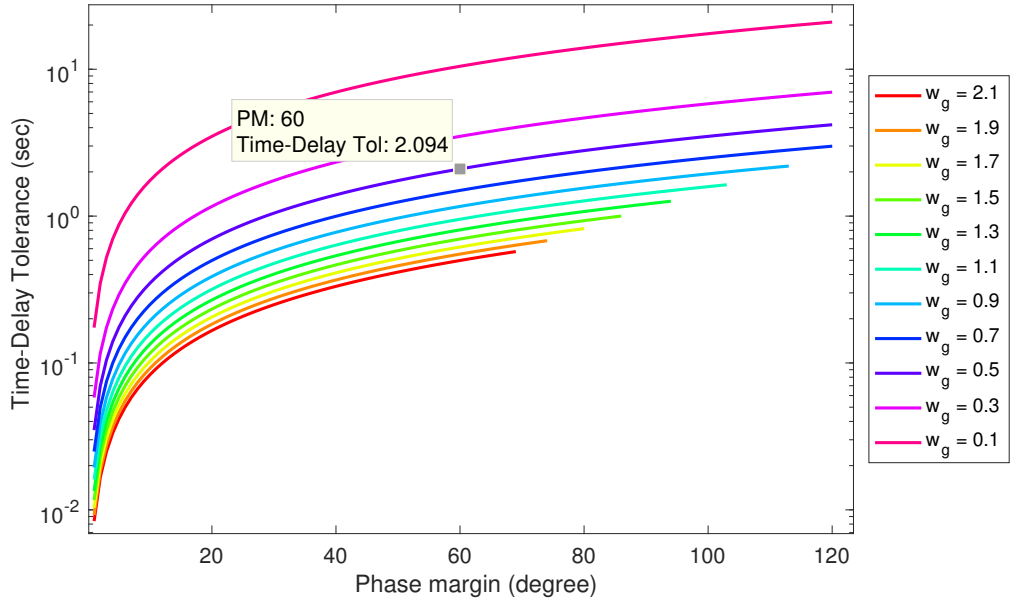


Figure 5.7: Achievable Performance in Terms of $\tau_{max}$, PM, and $\omega_g$ for PI Controller Design in Example 6a for $C_1(s)P_1(s)$

We can verify the results by computing the gain margin and phase margin of the multivariable system using the controller $C(s)$. In Fig 5.3, the characteristic equation of the multivariable system is given by

$$det[I + \Delta G(s)] \tag{5.33}$$

where $G(s) = P(s)C(s)$ and $\Delta$ is defined as in (5.6). Let $\delta = k$. Then

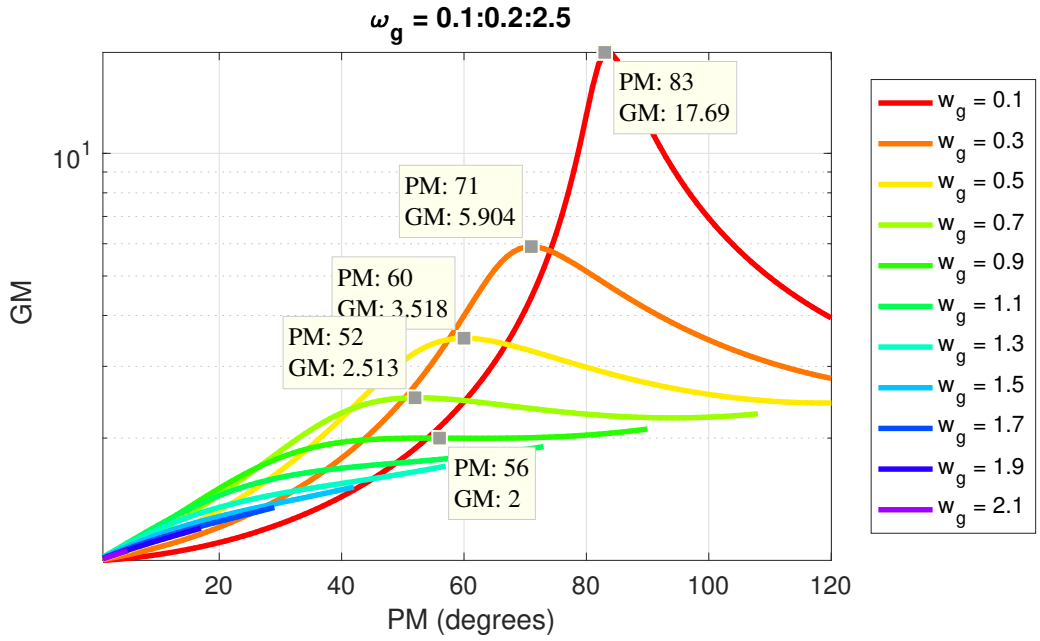


Figure 5.8: Achievable Performance in Terms of GM, PM, and $\omega_g$ for PI Controller Design in Example 6a for $C_2(s)P_2(s)$

$$\begin{aligned} det[I + \Delta G(s)] = {} & s^7 + 9s^6 + (32 - 0.637k)s^5 \\ & + (56 + 2.33k)s^4 \\ & + (48 - 0.4484k^2 + 19.288k)s^3 \\ & + (16 - 0.4216k^2 + 32.708k)s^2 \\ & + (3.7833k^2 + 17.096k)s + 4.5506k^2. \end{aligned} \tag{5.34}$$

We found that the minimum range of $k$ for the closed-loop system in Fig 5.3 to be stable is

$$0 < k < 3.518 \tag{5.35}$$

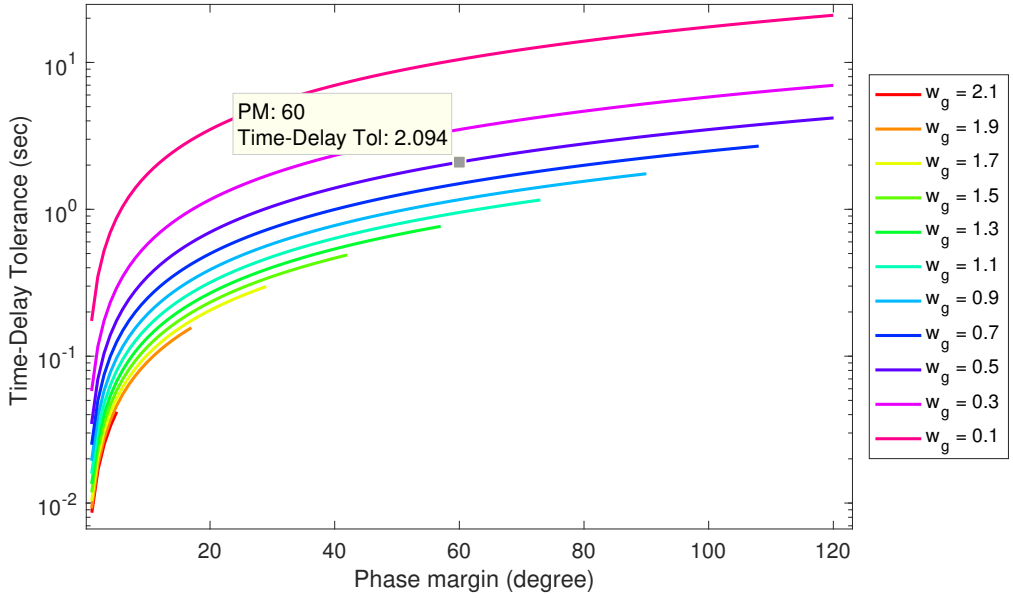


Figure 5.9: Achievable Performance in Terms of $\tau_{max}$, PM, and $\omega_g$ for PI Controller Design in Example 6a for $C_2(s)P_2(s)$

the roots of (5.34) with $k = 3.518$ are

$$\begin{cases} 0.00030784192 - j1.5532363 \\ 0.00030784192 + j1.5532363 \\ -0.38174169 + j1.2786136 \\ -0.38174169 - j1.2786136 \\ -1.2283752 \\ -2.2365012 \\ -4.7722559 \end{cases} \tag{5.36}$$

We can see that the real part of two of the roots just crossed the imaginary axis. Thus the gain margin is $k^* = 3.518$ for the MIMO system. This is the same value

that we selected in the desired specifications for $C_2(s)P_2(s)$.

Now, let $\delta = e^{j\theta}$. (5.33) is

$$\begin{aligned} det[I + \Delta G(s)] = {} & s^7 + 9s^6 + (32 - 0.637e^{j\theta})s^5 \\ & + (2.33e^{j\theta} + 56.0)s^4 \\ & + (19.29e^{j\theta} - 0.4484e^{j2\theta} + 48.0)s^3 \\ & + (32.7e^{j\theta} - 0.4218e^{j2\theta} + 16.0)s^2 \\ & + (e^{j\theta} + 3.784e^{j2\theta} + 17.1)s + 4.551e^{j2\theta} \end{aligned} \tag{5.37}$$

The range for $\theta$ to keep the multivariable system stable is

$$0 < \theta < 60^o. \tag{5.38}$$

The roots of (5.37) for $\theta = 60^o$ are

$$\begin{cases} -3.5159631 - j0.67153706 \\ -2.0790212 - j0.081079624 \\ -1.2506782 - j0.1211673 \\ -1.2333837 + j1.2928996 \\ -0.92099468 + j0.58077106 \\ 0.000015906289 - j0.49969144 \\ 0.000025099732 - j0.50019525 \end{cases} \tag{5.39}$$

Likewise, the real part of two of the roots just crossed the imaginary axis. So, the phase margin is $\theta^* = 60^o$ for the MIMO system. This is the same value that we

selected in the desired specifications for the SISO system $C_2(s)P_2(s)$.

Now, let $\delta = e^{-sT}$. (5.33) is

$$\begin{aligned} det[I + \Delta G(s)] = {} & s^7 + 9s^6 + s^5(0.423e^{-Ts} + 32.0) \\ & + s^4(4.45e^{-Ts} + 56.0) + s^3(18.23e^{-Ts} + 48.0) \\ & + s^2(30.59e^{-Ts} + 0.3299e^{-2Ts} + 16.0) + s(17.1e^{-Ts} + 2.583e^{-2Ts}) \\ & + 4.551e^{-2Ts} \end{aligned} \tag{5.40}$$

The range for $T$ to keep the multivariable system stable is

$$0 < T < 2.094 \text{ sec.} \tag{5.41}$$

The time-delay tolerance is $T = 2.094$ for the MIMO system. This is the same value that we selected in the desired specifications for the SISO system $C_2(s)P_2(s)$.

## 5.6 References

For more details about the Smith-McMillan transformation and the computation of the stabilizing set see [91] and [92] respectively. The transformation of a multivariable system into a scalar equivalent system is presented in [93].

# 6. CONCLUSIONS

## 6.1 Summary

In this dissertation, we have presented an advanced tuning approach for First Order, PI and PID controllers for discrete-time, delay-free and First Order plus time-delay continuous-time linear time-invariant Single-input single-output systems. These results were possible to extend to the controller design of multivariable linear time-invariant continuous-time systems. It was shown how First Order, PI, and PID controllers can be designed to satisfy simultaneously desired gain margin, phase margin, gain crossover frequency, and time delay tolerance by selecting the specifications from a constructed achievable performance set in the Gain-Phase margin plane. First, the stabilizing set was computed using recent results for discrete-time and continuous-time systems. Then, we showed a graphical approach for the parametrization of constant gain and constant phase loci respectively by ellipses/cylinders and straight lines/planes. We then constructed an achievable Gain-Phase margin set indexed by gain crossover frequencies. After that, given a selected desired specification from the achievable performance set, retrieval of the controller gains was presented as the intersection of an ellipse/cylinder and a straight line/plane superimposed on the stabilizing set. In the end, different examples were presented for different cases to show the proposed approach.

The results presented in this dissertation provide us with a computational tool for an advanced design of classical controllers for different types of systems. Also, it provides a general perspective to the designer about how much design is possible by constructing the achievable performance set for a specific type of controller (First

Order, PI, or PID). This approach offers the freedom to the designer to select any desired specification that can be achieved by the proposed controller. This result is of great importance because many of these types of controller are currently being used in many industrial applications and new technology developments like in autonomous cars, renewable energies, and drones.

## 6.2 Future research

The results presented in this dissertation represent an important contribution to the classical controller theory by introducing new computer-aided approaches to satisfy different simultaneous design specifications. However, the results in this dissertation are related to the design of classical controllers considering a frequency response analysis. There are time response considerations such as overshoot, undershoot, rise time, and settling time that need to be addressed. Another consideration for future research is to improve the computations involved in the controller design process and construct a toolbox where the designer can manipulate better the information and have an organized representation of the results in one screen. Then, use this computational tool more efficiently for controller design. Finally, a consideration for future research is the application of this controller design approach to real applications where PI or PID controllers are mostly used. For example, some industrial applications in automatic processes, power electronics, autonomous cars, renewable energies, and drones.

# REFERENCES


[1] K. J. Astrom and T. Hagglund. *PID Controllers: Theory, Design, and Tuning, Second Edition - See more at: https://ww2.isa.org/store/products/product-detail/?productId=116103*. International Society of Automation, 1995.

[2] I. D. Díaz-Rodríguez. Modern Design of Classical Controllers: Continuous-Time First Order Controllers. In *Industrial Electronics Society, IECON 2015-41st Annual Conference of the IEEE*, pages 000070–000075. IEEE, 2015.

[3] I. D. Díaz-Rodríguez and S. P. Bhattacharyya. PI Controller Design in the Achievable Gain-Phase Margin Plane. In *IEEE, CDC 55th IEEE Conference on Decision and Control*, pages 000000–000000. IEEE, 2016.

[4] S. Buso and P. Mattavelli. *Digital Control in Power Electronics*. Morgan and Claypool Publishers, 2006.

[5] I. D. Diaz-Rodriguez, V. A. Oliveira, and S. P. Bhattacharyya. Modern Design of Classical Controllers: Digital PID Controllers. In *Industrial Electronics (ISIE), 2015 IEEE 24th International Symposium on*, pages 1010–1015. IEEE, 2015.

[6] I. D. Diaz-Rodriguez, Sangjin Han, L. H. Keel, and S. P. Bhattacharyya. Advanced Tuning for Ziegler-Nichols Plants. In *The 20th World Congress of the International Federation of Automatic Control*, pages –. IFAC, 2017.

[7] L. H. Keel and S. P. Bhattacharyya. Robust, Fragile, or Optimal? *IEEE Transactions on Automatic Control*, 42(8):1098–1105, 1997.

[8] K. Natarajan. Robust PID Controller Design for Hydroturbines. *IEEE Transactions on Energy Conversion*, 20(3):661–667, 2005.

[9] R. A. Krohling, H. Jaschek, and J. P. Rey. Designing PI/PID Controllers for a Motion Control System Based on Genetic Algorithms. In *Intelligent Control, 1997. Proceedings of the 1997 IEEE International Symposium on*, pages 125–130. IEEE, 1997.

[10] L. Dubonjić, N. Nedić, V. Filipović, and D. Pršić. Design of PI Controllers for Hydraulic Control Systems. *Mathematical Problems in Engineering*, 2013:1–10, 2013.

[11] B. Singh, R. P. Payasi, K. S. Verma, V. Kumar, and S. Gangwar. Design of Controllers PD, PI & PID for Speed Control of DC Motor Using IGBT Based Chopper. *German Journal of Renewable and Sustainable Energy Research (GJRSER)*, 1(1):29–49, 2013.

[12] A. Visioli and Q. Zhong. *Control of Integral Processes with Dead Time*. Springer Science & Business Media, 2010.

[13] A. J. Michael and H. M. Mohammad. PID Control New Identification and Design Methods. *Nottingham: Springer*, 2005.

[14] S. P. Bhattacharyya, A. Datta, and L. H. Keel. *Linear Control Theory Structure, Robustness, and Optimization*. CRC Press Taylor & Francis Group, 2009.

[15] K. K. Tan, Q. G. Wang, and C. C. Hang. *Advances in PID Control*. Springer Science & Business Media, 2012.

[16] H. B. Patel and S. N. Chaphekar. Developments in PID Controllers: Literature Survey. *International Journal of Engineering Innovation and Research*, 1(5):425–430, 2012.

[17] Ang, K. H., G. Chong, and Yun L. PID Control System Analysis, Design, and Technology. *IEEE Transactions on Control Systems Technology*, 13(4):559–576,

jul 2005.

[18] K. J. Astrom and T. Hagglund. The Future of PID Control. *Control Engineering Practice*, 9(11):1163–1175, 2001.

[19] J. G. Ziegler and N. B. Nichols. Optimum Settings for Automatic Controllers. *Trans. ASME*, 64(11), 1942.

[20] F. Haugen. *PID Control*. Tapir, 2004.

[21] C. E. Garcia and M. Morari. Internal Model Control. A Unifying Review and Some New Results. *Industrial & Engineering Chemistry Process Design and Development*, 21(2):308–323, 1982.

[22] D. E. Rivera, M. Morari, and S. Skogestad. Internal Model Control: PID Controller Design. *Industrial & Engineering Chemistry Process Design and Development*, 25(1):252–265, 1986.

[23] A. Datta, M. T. Ho, and S. P Bhattacharyya. *Structure and Synthesis of PID Controllers*. Springer Science & Business Media, 2013.

[24] D. E. Rivera, M. Morari, and S. Skogestad. Internal Model Control: PID Controller Design. *Industrial & Engineering Chemistry Process Design and Development*, 25(1):252–265, 1986.

[25] W. K. Ho, T. H. Lee, H. P. Han, and Y. Hong. Self-Tuning IMC-PID Control With Interval Gain and Phase Margins Assignment. *IEEE Transactions on Control Systems Technology*, 9(3):535–541, 2001.

[26] I. Kaya. Tuning PI Controllers for Stable Processes With Specifications on Gain and Phase Margins. *ISA Transactions*, 43(2):297–304, 2004.

[27] I. Kaya. Two-Degree-of-Freedom {IMC} Structure and Controller Design for Integrating Processes Based on Gain and Phase-Margin Specifications. *IEE Proc. \-Control Theory Appl.*, 151(4):481–487, 2004.

[28] W. K. Ho, C. C. Hang, and J. H. Zhon. Performance and Gain and Phase Margins of Well-Known PI Tuning Formulas. *IEEE Transactions on Control Systems Technology*, 3(2):245–248, 1995.

[29] W. K. Ho, O. P. Gan, E. B. Tay, and E. I. Ang. Performance and Gain and Phase Margins of Well-Known PID Tuning Formulas. *IEEE Transactions on Control Systems Technology*, 4(4):473–477, 1996.

[30] Powell J. D. Franklin, G. F. and A. Emami-Naeini. *Feedback Control of Dynamic Systems, Sixth Edition*. Pearson Prentice Hall, 2009.

[31] P. Cominos and N. Munro. PID Controllers: Recent Tuning Methods and Design to Specification. *IEE Proceedings-Control Theory and Applications*, 149(1):46–53, 2002.

[32] Q. G. Wang, Z. Zhang, K. J. Astrom, and L. S. Chek. Guaranteed Dominant Pole Placement with PID Controllers. *Journal of Process Control*, 19(2):349–352, 2009.

[33] E. Dincel and M. T. Söylemez. Guaranteed Dominant Pole Placement with Discrete-PID Controllers: a Modified Nyquist Plot Approach. *IFAC Proceedings Volumes*, 47(3):3122–3127, 2014.

[34] Y. Zhang, Q. G. Wang, and K. J. Astrom. Dominant Pole Placement for Multi-Loop Control Systems. *Automatica*, 38(7):1213–1220, 2002.

[35] S. H. Hwang and S. J. Shiu. A New Autotuning Method with Specifications on Dominant Pole Placement. *International Journal of Control*, 60(2):265–282,

1994.

[36] S. H. Hwang and S. M. Fang. Closed-Loop Tuning Method Based on Dominant Pole Placement. *Chemical Engineering Communications*, 136(1):45–66, 1995.

[37] S. Srivastava and V. S. Pandit. A PI/PID Controller for Time Delay Systems with Desired Closed Loop Time Response and Guaranteed Gain and Phase Margins. *Journal of Process Control*, 37:70–77, 2016.

[38] Y. G. Wang and W. J. Cai. Advanced Proportional-Integral-Derivative Tuning for Integrating and Unstable Processes with Gain and Phase Margin Specifications. *Industrial & Engineering Chemistry Research*, 41(12):2910–2914, 2002.

[39] N. M. Darwish. Design of Robust PID Controllers For First-Order Plus Time Delay Systems Based on Frequency Domain Specifications. *Journal of Engineering Sciences*, 43(4):472–489, 2015.

[40] A. O'Dwyer. PI and PID Controller Tuning Rule Design for Processes with Delay , to Achieve Constant Gain and Phase Margins for all Values of Delay. In *Irish Signals and Systems Conference*, pages 96–101, 2001.

[41] P.N. Paraskevopoulos, G.D. Pasgianos, and K.G. Arvanitis. PID-Type Controller Tuning for Unstable First Order Plus Dead Time Processes Based on Gain and Phase Margin Specifications. *IEEE Transactions on Control Systems Technology*, 14(5):926–936, sep 2006.

[42] A Open-loop Frequency Analysis. PID Tuning for Optimal Closed-Loop Performance With Specified Gain and Phase Margins. *IEEE Transactions on Control Systems Technology*, 21(3):1024–1030, 2013.

[43] W. K. Ho, C. C. Hang, and J. Zhou. Self-Tuning PID Control of a Plant With Under-Damped Response. *IEEE Transactions on Control Systems Technology*,

5(4):446–452, 1997.

[44] Y. Luo and Y. Q. Chen. Synthesis of Robust PID Controllers Design with Complete Information On. In *American Control Conference*, pages 5013–5018, 2011.

[45] R. Toscano. A Simple Robust PI / PID Controller Design Via Numerical Optimization Approach. *Journal of Process Control*, 15(1):81–88, 2005.

[46] S. E. Hamamci and N. Tan. Design of PI Controllers for Achieving Time and Frequency Domain Specifications Simultaneously. *ISA Transactions*, 45(4):529–543, 2006.

[47] W.K. Ho, K.W. Lim, and Wen Xu. Optimal Gain and Phase Margin Tuning for PID Controllers. *Automatica*, 34(8):1009–1014, 1998.

[48] W. K. Ho and W. Xu. PID Tuning for Unstable Processes Based on Gain and Phase-Margin Specifications. *IEE Proceedings - Control Theory and Applications*, 145(5):392, 1998.

[49] C. H. Lee. A Survey of PID Controller Design Based on Gain and Phase Margins. *International Journal of Computational Cognition*, 2(3):63–100, 2004.

[50] C. H. Lee. A Survey of PID Controller Design Based on Gain and Phase Margins. *International Journal of Computational Cognition*, 2(3):63–100, 2004.

[51] B. Lennartson and B. Kristiansson. Robust and Optimal Tuning of PI and PID Controllers. *IEE Proceedings - Control Theory and Applications*, 149(1):17–25, jan 2002.

[52] Y. J. Wang. Determination of All Feasible Robust PID Controllers for Open-Loop Unstable Plus Time Delay Processes with Gain Margin and Phase Margin Specifications. *ISA Transactions*, 53(2):628–646, 2014.

[53] Z. Shafiei and A. T. Shenton. Frequency-Domain Design of PID Controllers for Stable and Unstable Systems with Time Delay. *Automatica*, 33(12):2223–2232, 1997.

[54] J. Crowe and M.a. Johnson. Towards Autonomous PI Control Satisfying Classical Robustness Specifications, 2002.

[55] Y. G. Wang and H. H. Shao. PID Autotuner Based on Gain- and Phase-Margin Specifications. *Industrial & Engineering Chemistry Research*, 38(8):3007–3012, aug 1999.

[56] W. Ho, C. Hang, and L. Cao. Tuning of PI Controllers Based on Gain and Phase Margin Specifications. *Industrial Electronics*, 2:879–882, 1992.

[57] W. K. Ho, C. C. Hang, and L. S. Cao. Tuning of PID Controllers Based on Gain and Phase Margin Specifications. *Automatica*, 31(3):497–502, 1995.

[58] G.H.M. de Arruda and P.R. Barros. Relay-Based Gain and Phase Margins PI Controller Design. *IEEE Transactions on Instrumentation and Measurement*, 52(5):1548–1553, oct 2003.

[59] M. Senthilkumar and S. A Lincon. Multiloop PI Controller For Achieving Simultaneous Time and Frequency Domain Specifications. *Journal of Engineering Science and Technology*, 10(8):1103–1115, 2015.

[60] H. W. Fung, Q. G. Wang, and T. H. Lee. PI Tuning in Terms of Gain and Phase Margins. *Automatica*, 34(9):1145–1149, 1998.

[61] M. T. Ho and H. S. Wang. PID Controller Design with Guaranteed Gain and Phase Margins. *Asian Journal of Control*, 5(3):374–381, 2003.

[62] M. Nagurka and O. Yaniv. Robust PI controller Design Satisfying Gain and Phase Margin Constraints. *Proceedings of the 2003 American Control Conference, 2003.*, 5:3931–3936, 2003.

[63] J. Crowe and M. A. Johnson. Automated PI Control Tuning to Meet Classical Performance Specifications Using a Phase Locked Loop Identifier. In *American Control Conference*, pages 2186–2191, 2001.

[64] Q. G. Wang, H. W. Fung, and Y. Zhang. PID Tuning with Exact Gain and Phase Margins. *ISA Transactions*, 38(3):243–249, jul 1999.

[65] K. J. Åström, U. Borisson, L. Ljung, and B. Wittenmark. Theory and Applications of Self-Tuning Regulators. *Automatica*, 13(5):457–476, 1977.

[66] K. J. Åström and B. Wittenmark. *Adaptive Control*. Courier Corporation, 2013.

[67] K. J. Åström. Theory and Applications of Adaptive Control a Survey. *Automatica*, 19(5):471–486, 1983.

[68] P. A. Ioannou and B. Fidan. *Adaptive Control Tutorial. Petros Ioannou, Bari Fidan.* Advances in Design and Control. Philadelphia, PA : Society for Industrial and Applied Mathematics, [2006], 2006.

[69] K. J. Åström and T. Hägglund. Automatic Tuning of Simple Regulators with Specifications on Phase and Amplitude Margins. *Automatica*, 20(5):645–651, 1984.

[70] S. Z. He, S. Tan, F. L. Xu, and P. Z. Wang. Fuzzy Self-Tuning of PID Controllers. *Fuzzy Sets and Systems*, 56(1):37–46, 1993.

[71] W. D. Chang and J. J. Yan. Adaptive Robust PID Controller Design Based on a Sliding Mode for Uncertain Chaotic Systems. *Chaos, Solitons & Fractals*, 26(1):167–175, 2005.

[72] Q. G. Wang, B. Zou, T. H. Lee, and Q. Bi. Auto-Tuning of Multivariable PID Controllers From Decentralized Relay Feedback. *Automatica*, 33(3):319–330, 1997.

[73] K. J. Åström, T. Hägglund, C. C. Hang, and W. K. Ho. Automatic Tuning and Adaptation for PID Controllers- a Survey. *Control Engineering Practice*, 1(4):699–714, 1993.

[74] D. E. Seborg, T. F. Edgar, and S. L. Shah. Adaptive Control Strategies for Process Control: a Survey. *AIChE Journal*, 32(6):881–913, 1986.

[75] M. T. Ho, A. Datta, and S. P. Bhattacharyya. Linear Programming Characterization of All Stabilizing PID Controllers. In *Proceedings of the American Control Conference*, pages 3922–3928, 1997.

[76] L. H. Keel, J. I. Rego, and S. P. Bhattacharyya. A New Approach to Digital PID Controller Design. *IEEE Transactions on Automatic Control*, 48(4):687–692, 2003.

[77] H. Xu, A. Datta, and S. P. Bhattacharyya. Computation of All Stabilizing PID Gains for Digital Control Systems. *IEEE Transactions on Automatic Control*, 46(4):647–652, 2001.

[78] L. H. Keel and S. P. Bhattacharyya. Controller Synthesis Free of Analytical Models: Three Term Controllers. *IEEE Transactions on Automatic Control*, 53(6):1353–1369, 2008.

[79] R. N. Tantaris, L. H. Keel, and S. P Bhattacharyya. Stabilization of Discrete-Time Systems by First-Order Controllers. *Automatic Control, IEEE Transactions on*, 48(5):858–860, 2003.

[80] Handscomb D. C. Mason, J. C. *Chebyshev Polynomials*. Chapman and Hall/CRC, 2002.

[81] Datta A. Bhattacharyya S. P. Silva, G. J. PI Stabilization of First-Order Systems with Time Delay. *Automatica*, 2001:20252031, 2001.

[82] Datta A. Bhattacharyya S. P. Silva, G. J. New Results on the Synthesis of PID Controllers. *IEEE Transactions on Automatic Control*, 47:241 – 252, 2002.

[83] I. D. Diaz-Rodriguez and S. P. Bhattacharyya. Modern Design of Classical Controllers: Digital PI controllers. In *Industrial Technology (ICIT), 2015 IEEE International Conference on*, pages 2112–2119. IEEE, 2015.

[84] T. Nguyen L. Vu and M. Lee. Independent Design of Multi-Loop PI/PID Controllers for Interacting Multivariable Processes. *Journal of Process Control*, 20(8):922–933, 2010.

[85] C. Rajapandiyan and M. Chidambaram. Controller Design for MIMO Processes Based on Simple Decoupled Equivalent Transfer Functions and Simplified Decoupler. *Industrial & Engineering Chemistry Research*, 51(38):12398–12410, 2012.

[86] S. R. Zanwar, S. S. Sankeshwari, and P. G. Scholar. Design of Multi Loop PI/PID Controller for Interacting Multivariable Process with Effective Open Loop Transfer Function. *International Journal of Engineering Science*, 7603, 2016.

[87] Q. Xiong, W. J. Cai, and M. J. He. Equivalent Transfer Function Method for PI/PID Controller Design of MIMO Processes. *Journal of Process Control*, 17(8):665–673, 2007.

[88] J. O'Reilly and W. E. Leithead. Multivariable Control by Individual Channel Design. *International Journal of Control*, 54(1):1–46, 1991.

[89] P. Kallakuri, L. H. Keel, and S. P. Bhattacharyya. Multivariable Controller Design with Integrity. In *2013 American Control Conference*, pages 5159–5164. IEEE, 2013.

[90] L. H. Keel and S. P. Bhattacharyya. Exact Multivariable Control Design Using SISO Methods: Recent Results. In *Control Applications (CCA), 2016 IEEE Conference on*, pages 215–223. IEEE, 2016.

[91] D. N. Mohsenizadeh, L. H. Keel, and S. P. Bhattacharyya. Multivariable Controller Synthesis Using SISO Design Methods. In *2015 54th IEEE Conference on Decision and Control (CDC)*, pages 2680–2685. IEEE, 2015.

[92] S. P. Bhattacharyya, A. Datta, and L. H. Keel. *Linear control theory: Structure, Robustness, and Optimization*, volume 33. CRC Press, 2009.

[93] L. H. Keel and S. P. Bhattacharyya. On The Stability of Multivariable Feedback Systems. In *Decision and Control (CDC), 2015 IEEE 54th Annual Conference on*, pages 4627–4631. IEEE, 2015.